UNIVERSITY OF CAPE TOWN

CALIBRATION OF AN ARCH DAM MODEL BY THE FINITE ELEMENT METHOD USING AMBIENT VIBRATION TESTING

BY: RAMONATE MAKHA

NOVEMBER 2012

SUPERVISOR: A/PROF. P. MOYO

CO-SUPERVISOR: DR. H. BEUSHAUSEN

THIS THESIS IS SUBMITTED TO THE DEPARTMENT OF CIVIL ENGINEERING, FACULTY OF ENGINEERING AND BUILT ENVIRONMENT, UNIVERSITY OF CAPE TOWN, IN PARTIAL FULFILMENT OF THE REQUIREMENTS FOR THE DEGREE OF MASTER OF SCIENCE IN ENGINEERING.

DECLARATION

I know the meaning of plagiarism and declare that all the work in the document, save for that which is properly acknowledged, is my own. I also declare that this work has not been previously submitted in any form for a degree at UCT or any other institution.

……

RAMONATE MAKHA

DATE: ……

ABSTRACT

The finite element model of an arch dam was calibrated for dynamic behaviour using the measured natural frequencies and mode shapes as benchmarks. The properties were extracted from the structure using ambient vibration testing techniques. Besides the geometry and general material properties of the dam wall concrete and foundation rock, the measured frequencies and mode shapes depend on the conditions at the dam site namely water level, temperature and the interactions between the several components of the dam. This study, however investigated the effects of the water level and to some extent, the effect of dissimilar foundation abutment material properties on the natural frequencies of the dam.

A dam is continuously in harmonic motion due to some environmental factors such as wind. Either due to this movement of the dam itself or the internal movement of the reservoir water, a dynamic interaction occurs between the water and the dam wall where the movement of the one medium affects the other. A study conducted in the early twentieth century deduced that it is only part of the reservoir water that can be assumed to interact with the dam. It is from the same study that the Westergaard added mass concept was born which says that the interacting water mass can simply be added to the dam wall mass, a procedure from which the extraction of the dynamic properties can ensue as normal. This added mass formulation was derived on a basis of some assumptions which include a rigid and vertical dam wall and the incompressible water body. The added mass concept was extended to account for flexibility and curvature of the upstream dam wall in more recent studies. The extended version of the Westergaard method is normally referred to as the generalized Westergaard method.

The original Westergaard added mass formulation was used to account for the dam wall-water interaction in the double curved Roode Elsberg dam model. This proved to be problematic as this dam is highly asymmetrical and has diverging reservoir walls, the characteristics of which are not catered for in the original Westergaard added mass method. The combined effect of using the original Westergaard method and these deficiencies in the formulation resulted in the model's natural frequencies being lower than the field ones, for the same ambient conditions. On the basis of literature, a factor of 0.8 on the added masses was applied on all the original Westergaard added masses to account for the effect of the diverging reservoir walls. The remaining masses were then reduced until a good correlation

of the field frequencies and model frequencies was achieved. This was done to account for the effects of the flexibility of the dam and the curved upstream dam wall. All in all, a factor of 0.25 on the masses calculated using the original Westergaard added masses was applied to account for all the above-mentioned effects. This factor compares favourably with literature even though in literature it is rarely mentioned what effects are being accounted for when this factor is introduced.

This work hence raises awareness about the shortcomings of the Westergaard method when used for model calibration and how those shortcomings can be accounted for. In summary, these shortcomings are brought about by assuming a prismatic and infinite reservoir, while in reality this is not always the case. It appears that these shortcomings affect the results of the added mass approach when used as a tool to represent the dam-water dynamic interaction in arch dams.

DEDICATION

Dedicated to my ever so loving friends and family.

ACKNOWLEDGEMENTS

I would like to thank my thesis advisor, A/Prof. P. Moyo for his continuous support and valued advice during the past two and half years. His guidance throughout which led to the completion of this work will always be appreciated.

I would like to thank the Concrete Materials and Structural Integrity Research Unit (CoMSIRU) in the University of Cape Town for giving me the chance to pursue a M.Sc. (Eng.) degree. Special mention of gratitude also to the research group leaders Prof. Mark Alexander and Dr H. Beushausen for their academic advice and support on and off the classroom. A special thanks also goes to Ms. Elly Yelverton for her assistance all the time.

My thanks also go to everyone in the department of Civil Engineering in the University of Cape Town for always striving towards a providing a conducive environment in which us the students can study in. In particular, the concrete laboratory staff and the whole administrative staff.

I would like to thank the Dams Surveillance Division in the Department of Water Affairs in South Africa for always attending to our needs which include but are not limited to providing access to the dams, their data etc. The input of everyone in the division contributed immensely to this work, especially Prof. Chris Oosthuizen and Mr Hans Durieux. The Water Research Commission provided the funding for this work; I therefore would like to thank them for their contribution as well.

TABLE OF CONTENTS

LIST OF FIGURES

LIST OF TABLES

GLOSSARY

Double curvature - Continuously curved in plan and elevation.

Depth of excavation- Depth from the ground surface to sound rock as determined from geological sources.

Arch - refers to a portion of the dam bounded by two horizontal planes

Cantilever -Cantilever is a portion of the dam contained between two vertical radial planes

Foundation - The total mass of sound rock supporting the dam.

Abutment - The rock mass which supports the arches (horizontal elements).

Extrados- Curved upstream surface of horizontal arch elements.

Intrados- Curved downstream surface of horizontal arch elements.

Crest - The top of the dam.

Crown Cantilever - Vertical section positioned about midway between abutments and whose base is generally the lowest elevation of the dam. It is directed radially toward the axis centre. It is maximum height vertical cantilever and is usually located in the streambed.

Thickness- Horizontal distance between upstream and downstream faces of dam on line normal to extrados.

Reference Plane -The reference plane contains the crown cantilever and the loci of the central centres. It is from this plane that the angle to the arch abutment is measured.

CHAPTER 1

INTRODUCTION

1.1 Background to the study

Concrete arch dams are curved in plan and in some cases in elevation as well. It is this feature which distinguishes them from all other kinds of dams. They are economical compared to other types of concrete dams as an arch dam is built of less concrete compared to other types of concrete dams of the same reservoir capacity. The arch action carries the load of the water laterally to the abutments instead of the load being transmitted to the foundation as with other dam types (Kennedy and Hanna, 1931). Hence the abutments on the arch dam site need to be capable of resisting the arch thrust.

Arch dams need to be continually inspected for safety (ICOLD, 2001). Failure to assess the safety of dams can be disastrous as the dam might fail; resulting in economic losses and at times even major loss of life (Sevim at al., 2009). Methods that have been used in the past to inspect dams for safety include water leakage monitoring, overall dam deformations monitoring and visual inspections. The common feature within these methods is that they monitor the static behaviour of dams. Studies in the area of structural dynamics have shown that the dynamic behaviour of a structure can also be used for condition monitoring of structures (Mendes, 2006). The basis of dynamic based structural assessment is that the dynamic properties of a structure change if the mass or stiffness of the structure changes.

Dynamic properties of as built structures are extracted through field dynamic testing. The most common field tests used are forced vibration tests and ambient vibration tests (Huang, 2001). In the forced vibration test, known and controlled mechanical forces are applied to the structure to excite it. On the other hand, ambient vibration tests rely on the environmental forces, such as wind, to excite the structure. This study is based on the results obtained from an ambient vibration testing which was carried out on an arch dam.

Ambient vibration testing has not been widely used in arch dams till recently as it was inconceivable that unknown and normally relatively small environmental forces can be used to excite and successfully extract dynamic properties of such massive structures (Mendes et al., 2004). The resulting vibrations in arch dams due to environmental excitations are of very

low amplitudes however recent studies have proven that it is possible to characterise with good precision the dynamic response of arch dams under such loading conditions. This has been made possible by the technological developments achieved at the level of: i) vibration measurements equipments (namely, accelerometers); ii) signal conditioning, acquisition and storage systems; iii) modal identification under environmental excitations (Mendes et al., 2004).

Severn et al. (1988) postulated that with successful ambient vibration testing on dams have been reported in literature, more robust safety inspection methods based on this technique can be developed which can provide an effective, cheap and reliable monitoring system by which damage can be detected from the change of the main dynamic properties of the structure, namely, natural frequencies and mode shapes.

Examples of successful ambient vibration are reported by Toyota et al. (2004) and Loh and Wu (1996) reported successful measurement of dynamic properties using ambient vibration testing on an undislclosed Japanese dam and Fei-Tsui dam in China respectively. These studies were considered to be successful as the results from the ambient vibration testing were found to be consistent with those from the forced vibration test and earthquake excitation respectively.

The data obtained from ambient vibration testing can be used for computational model calibration as well as for long term monitoring of dams. Finite element programs are nowadays predominantly used for providing computational models. Finite element model calibration seeks to match computational models as closely as possible to as built structural behaviour. This can be achieved by using the the ambient vibration test results to provide a control mechanism to check the finite element model results. If there are differences between the analytical and experimental results, the shortcomings in the analytical method can be identified and the initial finite element model can be corrected. Once the model is calibrated it can then be used as part of long term monitoring of the structure.

In the case of dams, the calibrated model should represent the dam site conditions as accurately as possible in the form of both the static and dynamic conditions. The dynamic characteristics of the structure refer to the natural frequencies, mode shapes and damping ratios. These dynamic characteristics, among others, depend on the material properties of the dam wall concrete, the material properties of the foundation rock and the different interactions between the components of the dam.

1.2 Objectives of the study

This research is based on the results of a series of ambient dynamic tests carried out on Roode Elsberg arch dam located near Worcester, Western Cape in South Africa. The aim is to produce a finite element model that will be used for dynamic characteristics monitoring to complement the static behaviour monitoring system that already exists on site.The dynamic properties which will be used to match the finite element model results with on- site results include the natural frequencies and mode shapes.

However, the actual process of fine-tuning the finite element model to match the measured parameters can be a complicated exercise as many factors need to be taken into account. Given the many factors that one needs to consider for such an exercise, it is important that the factors that this study will concentrate on are identified.

This study will hence focus on the following;

i. Development of a finite element model of Roode Elsberg dam in which all the parameters which are assumed to be of importance to a day-by-day ambient behaviour of the dam can be incorporated and used to predict the behaviour. These parameters include temperature and water level.
ii. The applicability of the widely used Westergaard added mass method to represent the dynamic interaction of the water body and the dam wall will be studied for this specific dam.
iii. To carry out an investigative study in which the characteristics of the foundation rock in the model are altered to determine which combination of characteristics best represents the condition on the actual dam site. The foundation size together with the observed varying geological and deformation properties of the foundation rock in the vicinity of the dam wall will form the bigger part of this investigation.

1.3 Organisation of the thesis

This thesis is structured as follows. Chapter 1 introduces the research topic. This includes a brief background to the study and the objectives of the study.

A discussion is made in Chapter 2 to highlight the importance of the various identified factors to the hydrodynamic behaviour of arch dams. This is done through a review of the previous studies which have been carried out in this field.

Foundation models used to represent the real arch dam foundation models are discussed in Chapter 3. Chapter 3 is then be followed by the discussion of the initial development of the finite element model of the Roode Elsberg dam in Chapter 4.

The results of the analysis on the developed model are presented in Chapter 5 together with the relevant discussions on the results. This chapter also includes the discussion of the calibration methods used in an attempt to correlate the analytical results with the experimental data. Chapter 6 presents the concluding remarks which will be followed by recommendations for any further studies in this area of research.

1.4 Scope and limitations

A lot of literature in dynamic behaviour of dams is biased towards earthquake engineering. This is no surprise as the safety of structures under earthquake loading was the main reason for the comprehensive studies of behaviour of structures under dynamic loading since the early twentieth century. However, this study is based on the dynamic behaviour of structures under normal operation or ambient conditions. One very important difference between seismic conditions and ambient conditions is that the vibrations in the latter are hardly felt by human senses while in the former the induced vibrations can be detected by human senses.

While it might be considered a limitation in terms of availability of literature that most studies are based on seismic analysis, it will also provide a very interesting study to investigate what major differences there are between these two kinds of dynamic behaviour. For example, do the expected natural frequencies and mode shapes depend on what kind of dynamic behaviour is being studied given that the excitation forces are very different in these two kinds of dynamic behaviours?

The ambient dynamic behaviour of Roode Elsberg dam will be used in this case for the purpose of dam monitoring and surveillance. Dam monitoring and surveillance is an essential tool for management of risks and avoidance of safety hazards associated with dams. Finite element models have been used widely in dam engineering to assess the behaviour of dams under extreme load conditions such as earthquakes but modelling of dams' behaviour under cyclic or more recurrent loads has lacked behind especially in a South African perspective. Hence, there are still major challenges concerned with finite element modelling of dams' day-to-day behaviour which include foundation modelling and the various interactions that occur between the several components of the dam-foundation-water body system. This work attempts to shed light on some of these challenges and how they can be resolved, starting with fluid-structure interaction of the dam wall and impounded water.

CHAPTER 2

HYDRODYNAMIC BEHAVIOUR OF ARCH DAMS

2.1 Introduction

The arch dam wall and the water body interact with each other dynamically, with the independent solution of any one system being impossible without simultaneous solution of the other (Zienkiewicz and Taylor, 2000). According to Leung et al. (2008), the inertia effect of the fluid medium on the dynamic characteristics, such as natural frequencies, of immersed structures can be significant. This is especially true of structures having large areas of contact with the surrounding fluid. Leung et al. (2008) states that any movement of the dam wall and foundation will impart motions to the water in the reservoir and in turn the pressure generated in the water will cause forces on the dam wall.

The dynamic problem of a linear multi degree of freedom dam structure subjected to time varying force vectors, $\boldsymbol{F_g}$ and $\boldsymbol{F_p}$ is defined in Equation 2.1:

$$[\boldsymbol{M_s}]\{\ddot{\boldsymbol{u}}\} + [\boldsymbol{C_s}]\{\dot{\boldsymbol{u}}\} + [\boldsymbol{K_S}]\{\boldsymbol{u}\} = \left\{\{\boldsymbol{F_g}(t)\} + \{\boldsymbol{F_p}(t)\}\right\} \quad (2.1)$$

$\mathbf{M_s}$, $\mathbf{C_s}$ and $\mathbf{K_s}$ refer to the mass, damping and stiffness matrices of the dam structure and $\boldsymbol{u}$ is a vector of relative displacements. The overdots denote the derivatives of $\boldsymbol{u}$ with respect to time, *t*. $\boldsymbol{F_g}$ and $\boldsymbol{F_p}$ are the force vectors generated by the ground accelerations vector $\boldsymbol{u_g}$ and by the hydrodynamic pressures $\boldsymbol{P}$ on the upstream side of the dam wall respectively. The two force vectors are further defined as follows;

$$\boldsymbol{F_g} = -\mathbf{M}_s\ddot{\boldsymbol{u}}_g \quad (2.2)$$

$$\boldsymbol{F_p} = Q\boldsymbol{P} \quad (2.3)$$

Q in Equation 2.3 is the transformation matrix which converts nodal pressures into hydrodynamic forces. For ambient vibration of arch dams, the ground accelerations force term $\boldsymbol{F_g}$ can be assumed to be zero as ground motions are negligible. The force vector due to the hydrodynamic pressures is small for ambient vibrations but it is not negligible.

It is important to point out at this stage that, this study is not concerned with the full solution of the dynamic Equation 2.1. The full solution of Equation 2.1 will involve the solution of

both the pressures in the upstream side and the displacements. The study is however about the extraction of the natural frequencies and mode shapes of a system that is described by Equations 2.1 and 2.3.

Alternatively, the free vibration representation of Equation 2.1 can be described in terms of the mode shapes $\boldsymbol{\phi}$ and natural frequencies ω of the dam structure as in Equation 2.4 below. The expression in Equation 2.4 is based on several assumptions, notably the following; linear behaviour, the damped natural frequency is very close to the undamped natural frequency and that after the initial disturbance, the motion of the dam is harmonic and all the points vibrate with the same frequency but different amplitudes.

$$([\boldsymbol{K_s}] - \omega^2[\boldsymbol{M_s}]) = \mathbf{0} \tag{2.4}$$

Normally, for simple dynamic systems, Equation 2.4 would be adequate to allow for the correct extraction of the natural frequencies and mode shapes. In arch dams, the fluid structure interaction generates the hydrodynamic pressures $\boldsymbol{P}$ on the upstream wall which affect the deformations of the dam wall, which in turn influence the pressures (USACE, 2003). Thus there is a coupled pressure-displacement relationship. Chopra (1987) indicated that the complete formulation of the fluid-structure interaction produces frequency-dependent hydrodynamic pressures that can be interpreted as an added force, an added mass and an added damping. In light of this information, Equation 2.4 can be written as follows;

$$([\boldsymbol{K_s}] - \omega^2[\boldsymbol{M_s} + \boldsymbol{M_a}]) = \mathbf{0} \tag{2.5}$$

Where, $\boldsymbol{M_a}$ is the added mass of water due to the hydrodynamic interaction of structure and the water body. The added mass concept is however only valid if the water in the dam is assumed to be incompressible (Chopra, 1967).

The two most common added mass formulations applicable to arch dams are the Westergaard method and the fluid-structure coupled finite element added hydrodynamic mass model. These two formulations estimate the added mass $\boldsymbol{M_a}$ in Equation 2.5 differently. However, of note is that both methods first focus on the hydrodynamic pressure estimation which can then be converted to added mass. The estimation of $\boldsymbol{M_a}$ allows for the solution of the equation for the mode shapes and natural frequencies.

Besides the added mass formulations, there are also Lagrangian and Eulerian approaches which are used to solve the fluid-structure interaction problem in arch dams using finite elements. These two approaches both model the water body using finite elements and in the Eulerian approach, normally the displacements are variables in the dam wall and pressures are variables in the fluid; in the Lagrangian approach; the displacements are both variables in the fluid and the structure. The Westergaard added mass method and some examples of the Lagrangian and Eulerian formulations are reviewed in the sections which follow.

2.2 The Westergaard added mass method

Westergaard (1933) published the added equivalent mass theory which can be used to estimate the dynamic action of the water on the dam. Several assumptions were made in the derivation of this theory, which include the following;

i. a 2-dimensional system is assumed
ii. the reservoir extends to infinity in the upstream direction
iii. the dam is rigid and has a vertical upstream face
iv. deformations are small
v. the effect of the surface waves of the homogenous water body can be neglected
vi. ground motions which excite the dam are harmonic and in the downstream-upstream direction. The ground motion's period is also assumed to be more than the natural period of the reservoir.

The harmonic excitation forces imply that the motion of the dam is also harmonic. It is the responsive movement of the dam that Westergaard (1933) estimated using the added equivalent mass theory. The problem of the dynamic action of the mass of the dam was transformed into an equivalent problem of statics from which it was observed that the generated pressures were the same as if a certain body of water were forced to move back and forth with the dam while the remainder of the reservoir is left inactive.

This approach allows the forces exerted on the upstream surface of the dam to be represented as inertia forces like those due to the moving mass of the dam itself. The shape of the body of water that is considered to move with the dam is determined such that the inertia forces become equal to the pressures actually exerted by the water due to the dynamic loading.

Westergaard (1933) concluded that a body of water enclosed by a dam wall and an upside down parabola which intersects with the horizontal bottom of the reservoir at a distance of seven-eighths of the water depth away from the dam wall base can give a good approximation of the inertia forces which would equal the hydrodynamic pressures. The graphical representation of Westergaard theory is shown in Figure 2.1.

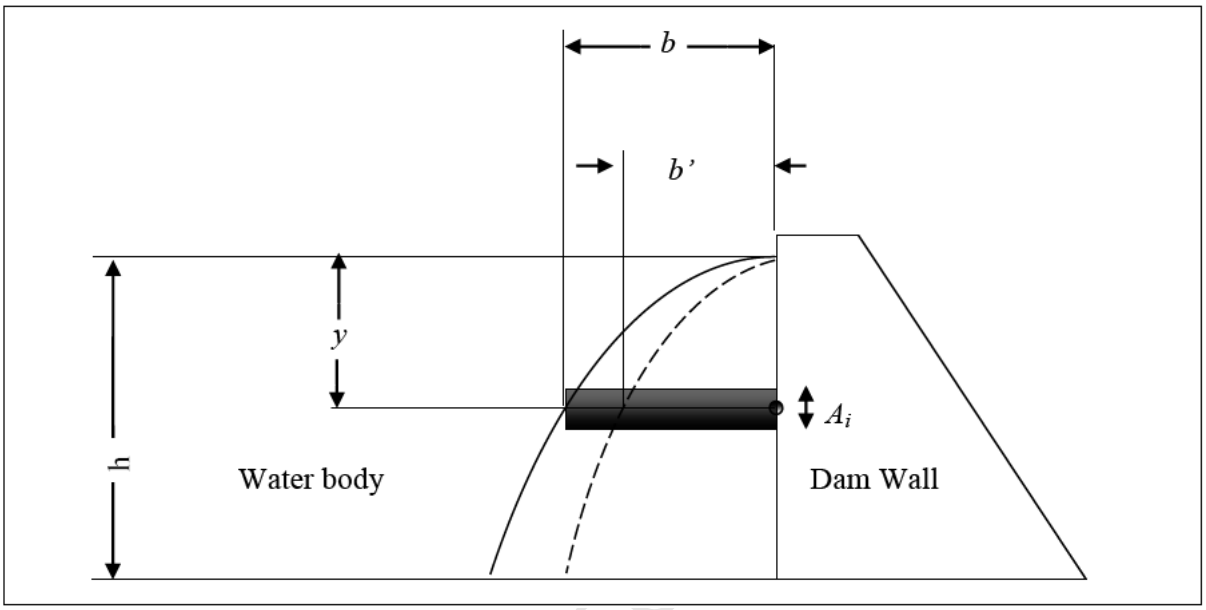

Figure 2.1: Body of water which may be considered to move with the dam wall shown by a bold curve. The dotted curve shows equivalent body of concrete.

The parameter *y* refers to the depth of the water from the water surface to the point of interest while the parameters *b* and *b'* are the depth dependent dimension which describe the respective parabolas for the masses of the water or equivalent concrete which move with the dam. The depth of the water in the reservoir is defined by the parameter *h*.

$$b' = 0.38 \times \sqrt{(h \times y)} \tag{2.6}$$

$$b = \frac{7}{8} \times \sqrt{(h \times y)} \tag{2.7}$$

The added mass of water m_{ai} at point i is obtained by multiplying the mass density of water ρ_w by the volume of water tributary to point i. This derivation was for a 2-dimensional case hence it can be assumed that dam section extends one unit into the page and A_i is the height of the small water volume which is tributary to point i.

$$m_{ai} = \frac{7}{8} \times \rho_w \times A_i \times \sqrt{(h \times y)} \quad (2.8)$$

The calculated added mass matrix for the wetted upstream points is then added to the mass matrix of the structure as mentioned in Equation 2.5. After this is done, the dynamic properties can then be extracted.

The United States Bureau of Reclamation (USBR) Manual (1977) extends the application of the Westergaard method to 3-dimensional cases. This was done in order to make possible the use of the Westergaard method for arch dams' dynamic analysis. It is not advisable for any analysis of arch dams to be executed in 2-dimensions only as their crown cantilever's behaviour is not always representative and critical; this is normally the case in gravity dams.

The USBR Manual (1977) notes that the amount of water that is assumed to move with the dam is actually different for the different modes of vibration of the dam. For example, in this approach the dimensions *b* and *b'* given in Equations 2.6 and 2.7 above respectively only apply for the dam's first mode of vibration. The dimension *b* for the mass of water that moves in the second mode of vibration for any point in contact with the water is given in Equation 2.9.

$$b = \frac{2X}{3L} \times \sqrt{(h \times y)} \quad (2.9)$$

The parameters *h* and *y* are as described as in Figure 2.1. *L* is the length of contact of the water with the face of the dam at the height of point of interest and *X* is the distance measured from the vertical axis of the dam horizontally to the point of interest. Figure 2.2 illustrates these parameters further.

The USBR Manual method modifies the original Westergaard method by considering the flexibility of the dam wall. Clearly, once the flexibility of the dam is considered, it would imply that the added mass function would then depend upon the shape of the vibration mode considered. So, no one function will be exactly valid for all vibration modes of the dam. However it has been shown that the formulations for a rigid dam can still be used to an acceptable degree of accuracy to account for the hydrodynamic effects for all modes of a flexible structures (Goyal and Chopra, 1989 cited by Davey et al. (2006)).

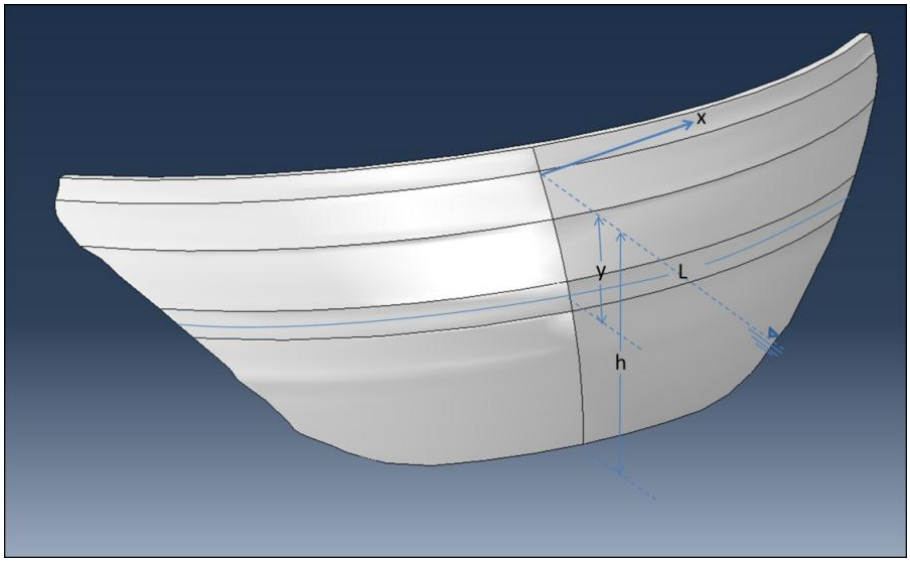

Figure 2.2: The parameters used to describe the added mass in the USBR Manual.

Kuo (1982) extended the original Westergaard method to allow the method to account for both flexibility and upstream dam face curvature and hence extend the application of the method to other dam types. A typical curved dam wall on which the extended Westergaard method is applicable to is shown in Figure 2.3. This formulation by Kuo is often referred to as the generalized Westergaard method.

The generalized Westergaard method recognises that the hydrodynamic pressure exerted on any point of the upstream face of the dam, due to the total acceleration normal to the dam face at that point, is equal to the inertia force produced by a prismatic body of water of unit cross section with length b, which is defined in Equation 2.7. This water body is assumed to be attached strongly normal to the dam face at that point and moving back and forth with the dam in the normal direction without friction (Kuo, 1982).

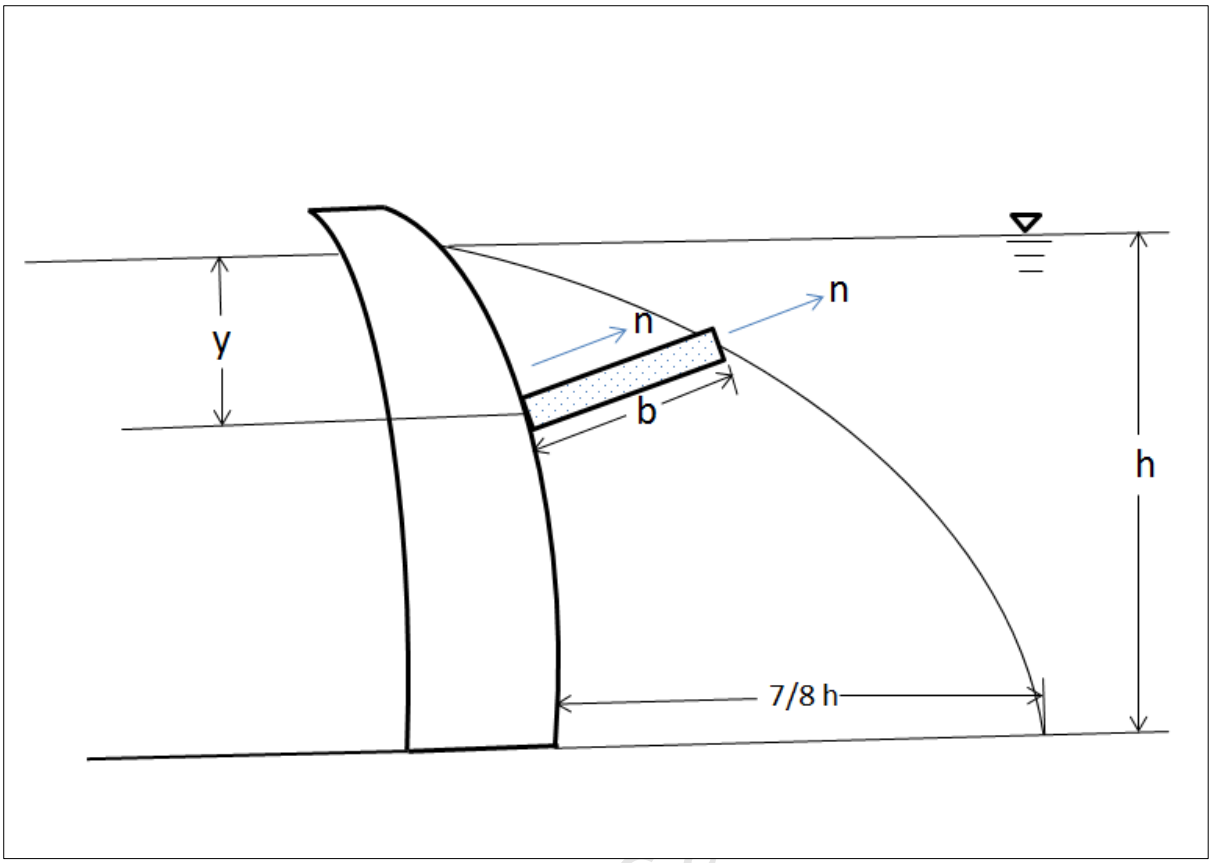

Figure 2.3: A curved upstream face for which the generalized Westergaard method is applicable.

The normal hydrodynamic pressure $\boldsymbol{P}_n$, at any wetted point on the upstream wall is proportional to the total normal acceleration $\ddot{\boldsymbol{u}}_{\boldsymbol{n}}$ at that point (Federal Energy Regulatory Committee, 1999),

In mathematical form:

$$\{\boldsymbol{P}_{\boldsymbol{ni}}\} = \alpha\{\ddot{\boldsymbol{u}}_{\boldsymbol{n}}\} \tag{2.10}$$

$$\alpha = \frac{7}{8}\rho_w\sqrt{(h \times y)} \tag{2.11}$$

The parameter α is known as the Westergaard pressure coefficient and it is the product of the length parameter *b*, which has already been described in Equation 2.7, and the density of water ρ_w.

$\ddot{\boldsymbol{u}}_{\boldsymbol{n}}$, the total normal acceleration at a node "*i*", is resolved into a sum of the ground acceleration $\ddot{\boldsymbol{u}}_{\boldsymbol{g}}$ and acceleration at node "*i*" relative to the base of the dam which is $\ddot{\boldsymbol{u}}$. A row vector of direction cosines of the normal vector λ_i at a point of interest "*i*" and a transformation matrix β_i are used to achieve this. β_i is a (3×3) displacement transformation

matrix of which the entry β_{jk} stands for the acceleration of node "*i*" in the j-direction due to a unit ground acceleration in k-direction while the dam is undergoing rigid body motion (Kuo, 1982).

$$\{\ddot{\boldsymbol{u}}_{\boldsymbol{n}}\} = \lambda_i(\{\ddot{\boldsymbol{u}}\} + [\beta_i]\{\ddot{\boldsymbol{u}}_{\boldsymbol{g}}\}) \tag{2.12}$$

Combining Equations 2.10 and 2.12 results in Equation 2.13 below and remembering that the normal force $\boldsymbol{F_{ni}}$ at a node *"i"* is a product of the normal pressure and the surface area A_i tributary to point *"i"* also gives the hydrodynamic force formulation in Equation 2.14.

$$\{\boldsymbol{P_{ni}}\} = \alpha\{\ddot{\boldsymbol{u}}_{\boldsymbol{n}}\} = \alpha\,\lambda_i(\{\ddot{\boldsymbol{u}}\} + [\beta_i]\{\ddot{\boldsymbol{u}}_{\boldsymbol{g}}\}) \tag{2.13}$$

$$\boldsymbol{F_{ni}} = -\boldsymbol{P_{ni}}A_i = \alpha\,\lambda_i(\{\ddot{\boldsymbol{u}}\} + [\beta_i]\{\ddot{\boldsymbol{u}}_{\boldsymbol{g}}\})A_i \tag{2.14}$$

The last step involves resolving the normal force $\boldsymbol{F}_{ni}$ into Cartesian components. This is done in Equation 2.15. The positive direction in this derivation is assumed to be outward and normal from the dam face.

$$F_i = \lambda_i^T \boldsymbol{F_{ni}} \tag{2.15}$$

Combining Equation 2.14 and 2.15 results in Equation 2.16 below;

$$F_i = -\alpha A_i \lambda_i^T \lambda_i(\{\ddot{\boldsymbol{u}}\} + [\boldsymbol{\beta_i}]\{\ddot{\boldsymbol{u}}_{\boldsymbol{g}}\}) \tag{2.16a}$$

$$= -[M_{ai}](\{\ddot{\boldsymbol{u}}\} + [\boldsymbol{\beta_i}]\{\ddot{\boldsymbol{u}}_{\boldsymbol{g}}\}) \tag{2.16b}$$

Where

$$[M_{ai}] = \alpha A_i \lambda_i^T \lambda_i \tag{2.17}$$

M_{ai} is a full (3×3) added mass matrix associated with a node *"i"* on the upstream face of the dam (Ghanaat, 1993). The difference between the original and generalized Westergaard methods is the presence of the symmetric matrix in the latter. This matrix will be referred to as a matrix *f* for the rest of this thesis.

The component of the normal acceleration which relates to the ground motions can be assumed to be almost zero for non-seismic excitations. This is because there are hardly any ground motions during normal operation of the dam other than the limited ones that may occur due to the water that might overspill when the dam is full.

In light of this information, for ambient vibrations Equation 2.16b can be approximated as follows:

$$F_i = -[M_{ai}]\ddot{\boldsymbol{u}} = -\alpha A_i \boldsymbol{\lambda}_i^T \boldsymbol{\lambda}_i \ddot{\boldsymbol{u}} \quad (2.18)$$

At this stage, it is important to highlight that all of the Westergaard method expressions were formulated on the basis of an earthquake induced movement which is very different from the ambient dynamic behavior of the dam. However, the method has been used for both earthquake and ambient behavior where it has been observed that it overestimated the added mass at times hence giving inaccurate results especially for seismic analysis (Lemos et al., 2008).

The magnitudes of the accelerations experienced by the dam during both earthquakes and ambient conditions are significantly different. Data of peak accelerations extracted from Mauvoisin dam shows that during an earthquake of magnitude 4.6 that occurred on 31st March 1996, peak accelerations that were observed at the dam crest had a magnitude of about 0.013g. On the other hand, typical time-history from a continuous automated ambient vibration monitoring of the same dam for an acceleration record close to the crest show a peak value of 11μg (Darbre and Proulx, 2002).

The significance of the different peak acceleration magnitudes is that higher magnitudes experienced during seismic activities result in great pressures on the water forcing it to vibrate immensely such that the compressibility of the water cannot be ignored anymore. It turns out that for such cases the dynamic pressures depend on magnitude and the nature of the exciting acceleration (Pani and Battacharyya, 2008). On the other hand, during ambient day to day operation of the dam, modest pressures are observed and these pressures do not depend on the magnitude of the exciting acceleration. In this case, the water can be assumed to be incompressible since the dynamic deformations are relatively small.

The Westergaard added mass assumes the water in the dam is incompressible. With this in mind, the author postulates that for the case of the ambient day-to-day dynamic behavior of an arch dam for which the dynamic pressures and deformation are relatively small, the method can still be used to give reasonable results. The Westergaard method has been used throughout the years as an easily applicable method and an alternative to a more cumbersome approach of using fluid finite elements. Improvements, criticisms and evaluations of the

method have been done over the years and this study also attempts to contribute positively to the use of the method.

2.3 Galerkin finite element added hydrodynamic mass model

Just like the Westergaard added mass method, this model attempts to estimate the hydrodynamic pressures generated from the incompressible fluid-structure interaction. Once they are found, the pressures are lumped into equivalent hydrodynamic nodal forces, from which the added mass coefficient matrix can be deduced (Kuo, 1982).

This method uses the pressure wave equation for incompressible and inviscid fluid mentioned in Equation 2.19 for the solution of the pressures. ∇^2 is the Laplace operator in three dimensions and $\boldsymbol{P}$ is the hydrodynamic pressure in excess of the static pressure in the fluid domain.

$$\nabla^2 \boldsymbol{P} = 0 \qquad (2.19)$$

The boundary condition assumptions made in the solution of this pressure wave equation are very important. Most reservoirs are generally irregular in geometry which makes it very difficult to find closed form solutions of Equation 2.19. Therefore, a numerical solution based on the finite element method is used. A finite element mesh of a fluid domain which extends a distance three times the height of the dam in the upstream is assumed to be good enough to be representative of the entire reservoir.

In general, when the Westergaard method is compared to the finite element based Galerkin method, the Westergaard method gives higher hydrodynamic pressures and hence higher added masses (Kuo, 1982). The effect of the diverging reservoir wall angles can be captured by the boundary conditions in the modelling when the Galerkin finite element method is used but when the Westergaard method is used the effect cannot be captured. This is one of the reasons these two methods can give different results. The overestimation of the added mass by the Westergaard method due to the diverging reservoir walls depends on the angle of divergence of the walls (Kuo, 1982).

2.4 Extraction of natural frequencies using decoupled modes

This analysis is based on the Eulerian approach of solving the structure-fluid interaction. In the Eulerian formulation normally the variables are displacements in the dam wall and pressures in the fluid (Bayraktar et al., 2011).

For the case of a flexible dam wall and compressible water in the reservoir, the fluid and structure interaction of the impounded water and the dam wall results in a coupled system. This coupled system can be described with the help of Equation 2.20 which has been written in the standard Galerkin variation formulation of pressures and displacements (Tiliouine and Seghir, 1998). This formulation can be used in finite elements.

$$\begin{bmatrix} \boldsymbol{M_s} & \boldsymbol{0} \\ \rho_w \boldsymbol{Q^T} & \boldsymbol{M_F} \end{bmatrix} \begin{Bmatrix} \ddot{\boldsymbol{u}} \\ \ddot{\boldsymbol{P}} \end{Bmatrix} + \begin{bmatrix} \boldsymbol{C_s} & \boldsymbol{0} \\ \boldsymbol{0} & \boldsymbol{C_F} \end{bmatrix} \begin{Bmatrix} \dot{\boldsymbol{u}} \\ \dot{\boldsymbol{P}} \end{Bmatrix} + \begin{bmatrix} \boldsymbol{K_S} & -\boldsymbol{Q} \\ \boldsymbol{0} & \boldsymbol{K_F} \end{bmatrix} \begin{Bmatrix} \boldsymbol{u} \\ \boldsymbol{P} \end{Bmatrix} = \begin{Bmatrix} \boldsymbol{F_g} \\ \boldsymbol{0} \end{Bmatrix} \tag{2.20}$$

Equation 2.20 is not really made out of 2×2 matrices but it is represented so as to show the distinction between terms associated with the displacement, $\boldsymbol{u}$ and terms associated with the pressure, $\boldsymbol{P}$. The entries $\mathbf{M_s}$, $\mathbf{C_s}$ and $\mathbf{K_s}$ are as described in section 2.1 while ρ_w is the water density. The terms with the subscript *s* refer to the dam wall while those with the subscript *F* refer to the impounded water body. $\mathbf{F_g}$ refers to the driving force and **Q** is the transformation matrix which converts nodal pressures into hydrodynamic forces (Tiliouine and Seghir, 1998).

This Eulerian based equation is specially difficult since the matrices are not symmetric. Even though there are unsymmetrical eigen-solvers available, they are very time-consuming from the execution point of view and also complicated from programming aspects. Furthermore, even though symmetrization of the matrices is possible, it requires introduction of additional variables which creates complications in computer programming (Tiliouine and Seghir, 1998).

Sani and Lotfi (2010) solve the dynamic problem of the arch dam-reservoir system by introducing fictitious decoupled systems whose mode shapes are found and then used to compute the actual mode shapes. The fictitious mode shapes are known as ideal coupled modes as they represent mode shapes of ideal systems. The two ideal systems are the incompressible fluid system and the massless dam wall system. The analysis of the incompressible fluid system generates mode shapes of the dam with the reservoir water assumed to be incompressible while the massless dam wall system analysis will generate

mode shapes of the reservoir with rigid walls everywhere except at the free surface (Sani and Lofti, 2007).

In this ideal-coupled modal approach, the dam is discretized by solid finite elements, while, the reservoir is divided into parts, a near-field region in the vicinity of the dam and a far field part assumed as a prismatic channel, which extends to infinity. The former region is discretized by fluid finite elements,while the three-dimensional fluid hyper-elements are utilized to model the reservoir far-field region. This is illustrated in Figure 2.4.

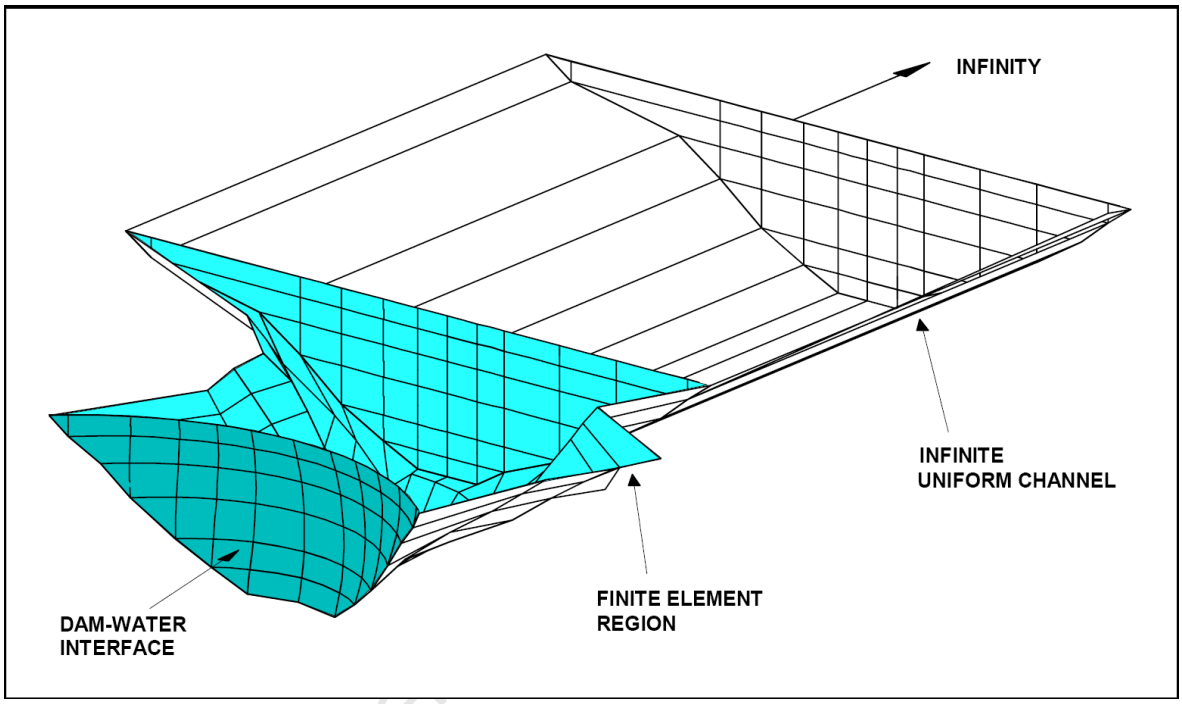

Figure 2.4: Shows typical fluid element region and a far field infinite region which can be modelled by hype-elements Courtesy of United States Army Corps of Engineers (USACE) (2007).

The procedure for the ideal-coupled modal approach is outlined below for a dam with a finite reservoir system.

Equation 2.20 is rewritten below for easy reference.

$$\begin{bmatrix} \boldsymbol{M_s} & \mathbf{0} \\ \rho_w \boldsymbol{Q^T} & \boldsymbol{M_F} \end{bmatrix} \begin{Bmatrix} \ddot{\boldsymbol{u}} \\ \ddot{\boldsymbol{P}} \end{Bmatrix} + \begin{bmatrix} \boldsymbol{C_s} & \mathbf{0} \\ \mathbf{0} & \boldsymbol{C_F} \end{bmatrix} \begin{Bmatrix} \dot{\boldsymbol{u}} \\ \dot{\boldsymbol{P}} \end{Bmatrix} + \begin{bmatrix} \boldsymbol{K_S} & -\boldsymbol{Q} \\ \mathbf{0} & \boldsymbol{K_F} \end{bmatrix} \begin{Bmatrix} \boldsymbol{u} \\ \boldsymbol{P} \end{Bmatrix} = \begin{Bmatrix} \boldsymbol{F_g} \\ \mathbf{0} \end{Bmatrix} \tag{2.20a}$$

The free vibration form of Equation 2.20a without the damping is given in Equation 2.21 below. It can also be assumed that the dam's response in the form of displacements and pressures will be harmonic (Sani and Lotfi, 2010);

$$\begin{bmatrix} -\omega^2 \mathbf{M_S} + \mathbf{K_S} & -\mathbf{Q} \\ -\boldsymbol{\omega^2} \rho_w \mathbf{Q^T} & -\omega^2 \mathbf{M_F} + \mathbf{K_F} \end{bmatrix} \begin{Bmatrix} \boldsymbol{u} \\ \boldsymbol{P} \end{Bmatrix} = \begin{Bmatrix} \mathbf{0} \\ \mathbf{0} \end{Bmatrix} \tag{2.21}$$

Considering only the lower partition of Equation 2.21 and letting $\mathbf{M_F}$ equals zero for the assumed incompressibity of water, one would have:

$$-\omega^2\rho\mathbf{Q^T}\boldsymbol{u} + \mathbf{K_F}\boldsymbol{P} = \mathbf{0} \tag{2.22}$$

Solving Equation 2.21 for the pressure in terms of the displacement field yields the following:

$$\boldsymbol{P} = \omega^2\rho_w\, \boldsymbol{K_F^{-1}}\, \mathbf{Q^T}\, \boldsymbol{u} \tag{2.23}$$

Subtituting this relation in the upper partition equation of Equation 2.21 results in the following simplified form of the first ideal eigenproblem:

$$(-\omega^2(\mathbf{M_s} + \mathbf{M_a}) + \mathbf{K_S})\boldsymbol{u} = \mathbf{0} \tag{2.24}$$

With the following matrix definition being used:

$$\boldsymbol{M_a} = \rho_w \boldsymbol{Q}\ \boldsymbol{K_F^{-1}}\, \mathbf{Q^T} \tag{2.25}$$

Matrix $\boldsymbol{M_a}$ is referred to as added mass matrix that is usually obtained for the fluid-structure interaction problems in the case of incompressible fluid assumption (Sani and Lotfi, 2010). This is an equivalence to the added mass matrix discussed earlier in the Westeergaard method. However, in this case, the mass is added through the use of fluid finite elements in an Eulerian approach.

The second stage of this ideal eigen-problem which involves using the assumption of the massless dam wall, i.e. the corresponding mode shapes are entirely due to the water body restrained from all sides. This corresponds to omitting the matrix $\mathbf{M_S}$ in Equation 2.21. Having omitted $\mathbf{M_S}$, the task is then to use the upper partition of Equation 2.21 to solve for the displacements $\boldsymbol{u}$ in terms of the pressures $\boldsymbol{P}$. This leads to:

$$\boldsymbol{u} = \boldsymbol{K_S^{-1}Q}\, \boldsymbol{P} \tag{2.26}$$

Thereafter, substitute this relation in the lower partition equation of Equation 2.21 to obtain the simplified form of the second ideal eigen-problem:

$$(-\omega^2(\mathbf{M_F} + \mathbf{G_a}) + \mathbf{K_F})\mathbf{P} = \mathbf{0} \tag{2.27}$$

Where $\mathbf{G_a}$is defined as:

$$\boldsymbol{G_a} = \boldsymbol{\rho}\, \mathbf{Q^T}\, \boldsymbol{K_s^{-1}}\, \mathbf{Q} \tag{2.28}$$

Sani and Lotfi (2010) suggest that the two ideal eigen-problems represented by both Equations 2.24 and 2.27 may be combined in one relation to yield the following:

$$\begin{bmatrix} (-\omega^2(\mathbf{M_s} + \mathbf{M_a}) + \mathbf{K_S}) & 0 \\ 0 & -\omega^2(\mathbf{M_F} + \mathbf{G_a}) + \mathbf{K_F} \end{bmatrix} \begin{Bmatrix} \boldsymbol{u} \\ \boldsymbol{P} \end{Bmatrix} = \begin{Bmatrix} \mathbf{0} \\ \mathbf{0} \end{Bmatrix} \quad (2.29)$$

Due to the symmetry of the matrix in Equation 2.29, the solution to the above combined eigen-value can be easily found by standard multiple degree of freedom dynamic system solving techniques provided that the matrices are computed correctly. The effects of the reservoir far-field region are then added to the near field region which has just been discussed (Sani and Lotfi, 2010).

However, in this work, the effects of the far field region are not discussed as it is mainly concerned with the treating of the radiation condition. In this case, the radiation condition refers to the propagation of energy waves away from the dam wall to infinity (Sani and Lotfi, 2010). This is a important scenario in seismic analysis where the effects of these waves can be significant. However, for a normal day-to-day operation of the dam in ambient conditions the propagation of waves to infinity can be assumed to have insignificant effects on the dynamic behaviour of the dam since the magnitude of the waves is likely to be very small.

Hence, of much interest to this project, is the near field system which is made out of an incompressible fluid which uses normal finite elements.

The ideal-coupled modal approach was discussed to illustrate that for the case of an ideal system of an incompressible fluid, the ideal-coupled modal approach show some similarities to the added mass methods discussed in section 2.1. This is through the use of the near-field part of the reservoir in the ideal modal coupled approach. Sani and Lotfi (2010) used the ideal-coupled method on Morrow Point dam to extract the natural frequencies of the model of the full dam. It does not appear that there was any comparison on the study on how the results of the ideal-coupled analysis compare to field results. The comparison is made in Table 2.1 with field results captured on the same dam by Duron (1987) and some other contemporary analytical results.

Table 2-1: Comparison between measured and computed resonant frequencies for a full Morrow Point dam.

	Natural frequencies			
Mode Number	Experimental Duron (1987)	Sani and Lotfi (2010) (Incompressible fluid assumption)	Westergaard added mass (Noble, 2002)	Tan and Chopra (1996)
1	2.95	2.57	2.62	2.82
2	3.30	2.82	2.76	*
3	3.95	4.15	4.34	*
4	5.40	4.80	5.30	*
5	6.21	5.95	5.90	*

*This natural frequencies were not identified in the study.

Table 2.1 shows that the results from the analysis carried out using the Westergaard added mass formulations to represent the arch dam interaction with the water body are comparable to those achieved through the use of the ideal-coupled mode approach where the incompressible fluid assumption is made. The latter approach is clearly more demanding than the added mass approach in terms of the computational cost. This is because the ideal-coupled approach requires one to model the water body using finite elements.

Furthermore, the aim of this work is to develop and calibrate a model which can be used to assess the day to day behavior of the dam. The water level changes overtime in the dam hence this would have to be captured in the model as well by changing the level of the elements. It is speculated that this would prove to be very cumbersome. The same can be said about the substructure method which was used in Tan and Chopra (1996) as it also utilizes fluid finite elements

On the other hand, Ghanaat (1993) suggested that the use of the Westergaard method should only be limited to the feasibility or preliminary studies. This is due to that it only provides a rough estimate of the hydrodynamic forces acting on the face of an arch dam as it ignores the compressibility of water, which for most arch dams, one cannot simply ignore. This comment was however relevant to seismic analysis of dams. It is postulated that as long as the inaccuracies of the added mass method can be established and quantified for different dam and reservoir geometries, the method can prove to be a strong tool that can be used in the years to come for dam assessment and monitoring purposes. The normally observed tendency of the Westergaard added mass approach to overestimate the added mass is observable in Table 2.1 through the generally higher frequencies when compared to field. This can be

concluded only provided it is assumed the dam behavior has not changed over time since the field data is very old.

2.5 Effect of the opening and closing of contraction joints in arch dams

Nonlinear behaviour can be expected in the dam walls of arch dams. There are two main sources of nonlinear behaviour dam walls namely; concrete cracking and the closing and opening of the contraction joints. Many arch dams have contraction joints and one reason for this is to control tensile forces that can be caused by concrete shrinkage and temperature variations. The opening of a joint relieves tensile stresses across the joint (USACE, 2007).

Furthermore the need for contraction joints facilitates easy arch dam construction as they can be built as cantilever monoliths separated by the vertical contraction joints (USACE, 2003). Nonlinearities associated with high compressive stresses are hardly ever experienced in the dam walls of concrete arch dams under normal ambient conditions.

The contraction joints are usually grouted at the completion of the dam construction or in stages and may also include shear keys for additional resistance. However, contraction joints have limited tensile resistance and can open and close any time when the dam wall is excited (USACE, 2007). This kind of behaviour can be expected to be very crucial for cases in which the source of excitation is a strong one, for example, an earthquake.

One other important aspect which affects the closure and opening of contraction joints is the level of the water in the reservoir. This phenomenon was observed by Darbre et al. (2000) and Proulx et al. (2001) in the studies carried out in Mauvoisin dam and Emosson dam respectively, in which, particular attention was paid to the variation of the resonance frequencies with changes in the water level. It was observed that the resonance frequencies initially increase with rising water level and then decrease with a further rise. The proposed explanation for this observation was that at lower water levels the effect of the dam becoming stiffer due to the closing of the vertical construction joints under increasing hydrostatic pressure prevails over the effect that is brought about by the augmentation of the mass of the entrained water. The latter effect however prevails at higher water levels (Darbre et al., 2000).

Two approaches which are normally used in the finite element modelling of cracks and joints were identified in literature namely the smeared crack approach and the use of joint elements.

In the smeared crack method approach, nonlinearities associated with cracks and joints are included in the finite element modelling by allowing modifications of properties at the integration points of the regular finite elements (Hall, 1996). According to Hall (1996), the smeared crack method is computationally more efficient and exhibits better convergence while still showing useful results when compared to inter-element nonlinear springs which are sometimes also used to model joints and cracks.

Inter-element nonlinear springs are just one of the many other types of joint elements in finite element modelling. These kinds of springs are normally assigned to have an infinite strength in compression and to have a given strength in tension. They are inter-element springs; which means that they span the joint connecting the nodes of the finite elements on opposite sides. Representation of the gradual opening and closing of contraction joints with the use of joint springs in arch dams requires a multiple finite element discretization in the thickness direction because if the dam is modelled using a single layer of elements along its thickness in conjunction with joint springs, the solution is likely to be very inaccurate (Dowling, 1987).

On the other hand, using several elements in the thickness direction connected by contact springs at a joint or crack would be more accurate but it said to be more computationally expensive. It is hence advisable that if an arch dam is a thick one which needs not be modelled using several elements in its thickness direction, alternatives such as the smeared cracking method are used for the joints or cracks nonlinear behaviour representation (Hall, 1996).

2.6 Chapter summary

This chapter specifically focused on the techniques used to model the dynamic interaction of the water body and the dam wall in arch dams.

Similarities were identified between two methods used to represent the dynamic interaction of the arch dam and the water body, namely the added mass approach and part of the ideal-coupled mode approach. The relevant part of the ideal-coupled method is where the mode shapes are found using the assumption of incompressible water body in the dam. Both methods give rise to the added mass concept, where any other properties of the water besides its mass are considered irrelevant in the analysis.

Despite this similarity, the ideal coupled method models the water using finite elements which makes it relatively complicated. On the other hand, despite its ease of application, the Westergaard method generally overestimates the added mass of water that is assumed to move with the dam during a dynamic action. It is however postulated that the Westergaard added mass technique can be improved through studies where the results that it produces can be compared to experimental field results. It is through such studies that the inaccuracies of the method can be quantified for different dam reservoir shapes and dam wall geometries. This study will adopt such an approach to assess the viability of use of the Westergaard added mass formulations to represent the interaction of the water body and a dam wall during an ambient dynamic action

CHAPTER 3

ARCH DAM FOUNDATION MODELS

3.1 Introduction

This section will describe models used to represent the foundation behaviour under a dynamic loading. The problems normally encountered in the modelling of foundation-dam wall dynamic behaviour will also be discussed together with respective solution.

3.2 Massless foundation approach

Much of the work that has been done on the dynamic interactions between the dam and the foundation is biased towards safety of dams under seismic loads. Earthquake effects are transferred from the source in the form of underground waves. The dam then experiences the effect of the earthquake as a result of the movement of the foundation. In order to accurately assess the safety of dams in the event of earthquakes, the magnitude of the critical acceleration that can be experienced by a dam needs to be known to a reasonable degree of accuracy. The magnitude of these accelerations on an already existing dam can be measured by the help of seismometers which are normally located at the interface of the dam wall with the foundation.

It is clear that in order to correctly formulate the dynamic response analysis for a dam, it is necessary to include a significant amount of the foundation material in the dam model. Having included the foundation in the modelling, the major challenge that follows is ensuring that the seismic input to the foundation is specified as accurately as possible. It also needs to be ensured that the propagation of the seismic input waves inside the foundation model is as close to the actual field scenario as possible.

Generally, either of two different approaches is used to specify the seismic input to models: 1) it may be defined as motions applied at the boundaries of the foundation; 2) or it may be prescribed as ‘free-field’ motions of the interface between dam and foundation. These ‘free-field’ motions are the ones that would have occurred at the nodes of the foundation block in contact with the dam if the dam were not present (Zienkiewicz et al., 1984).

The massless foundation model assumes the mass of the foundation block is zero. The foundation block in this case functions simply as a spring system in the interaction mechanism; without mass the rock does not develop vibration waves to modify the properties of the waves as they propagate through the foundation (Zienkiewicz et al., 1984).

Normally, in this method ground level accelerations measured from previous earthquakes which are also known as free-field accelerations time history are applied uniformly at the truncated foundation base. Since the wave propagation velocity in the assumed massless rock approaches infinity, the input motions are transmitted instantaneously through the foundation rock to the dam-foundation interface, and the motion at the interface would be the same as the input one. This makes the method highly favourable in that aspect as it allows for the use of the actually measured earthquake motions at the free field surface as the boundary input (Chuhan et al., 2009).

Hence, the massless foundation model avoids one of the major difficulties inherent in the boundary input approach and has been used extensively for that reason. However, Chuhan et al. (2009) mention that this massless foundation approach only considers the foundation flexibility and ignores the dam-foundation inertial interaction. One other disadvantage with this method as indicated by Chuhan et al. (2009), is that it overestimates the response of the dam both in the linear and the non-linear analyses.

Literature indicates that the EACD-3D and the Smeared Crack Arch Dam Analysis programs which were developed by Fok et al. (1986) and Hall (1996) respectively use this assumption of a massless foundation. In a study done by Proulx et al. (2004) on Mouvoisin dam is Switzerland, in which numerical analyses of earthquake responses of three dams was done and compared with results from in-situ measurements, it was found that damping ratios as high as 8-15% (while the normal range of damping ratio of dams is about 5% in design practice) were needed for approximately matching the field response records of the dams which further highlights the inaccuracy of the massless foundation assumption.

Furthermore, on a study carried out in Murrow Point dam, it was discovered that the use of the massless foundation on the model of the dam predicted the behaviour which did not match the measured response. For example, the predicted stresses were at times 2-3 times more than the actual stresses. This can lead to erroneous conclusion that the dam needs remediation (Chopra, 2010).

3.3 Foundation with mass approach

There are generally two earthquakes data input methods available for use with the foundation with mass approach, namely the deconvolution and the free-field input methods.

1) Deconvolution Input Method

As mentioned earlier, the free field surface motions are significantly different from the motions at depth. The former are considerably amplified by reflections as compared to the latter. Seismometers located at the surface of the ground measure the free field surface motions.

If the mass of the foundation is to be considered in the analysis then it is highly advisable that the earthquake motions at depth are known so that they can be introduced accordingly at the truncated foundation base. The difficulty normally encountered is how to determine these at depth motions given the free field ones. The procedure of determining this is known as the deconvolution analysis.

In the deconvolution analysis, first the foundation block alone is analysed alone to determine the motion at depth that would have produced the measured free field surface motions. The result of this preliminary analysis which is performed in the frequency domain is then used as the input to the boundary of the foundation block supporting the dam (Zienkiewicz et al, 1984).

2) Free-Field Input Method

In this method, the equations of motion are formulated directly in terms of the free-field input. Earthquake excitations are therefore imposed as the free-field motions at the dam-foundation interface directly. Both the latter two methods, namely the deconvolution input and the free-field input models are equivalent if the radiation damping and input mechanisms are considered appropriately (Chuhan et al., 2009).

3.4 Foundation size models

The preceding sub-topic has outlined how important it is to include the foundation in the dynamic analysis of arch dams. When this is done, at some depth at which the boundary of this hypothesized portion of the foundation rock lies, the conditions are usually assumed to be

rigid. This is one of the limitations associated with this approach in that in concrete dam sites where rocks usually extend to large depths, there is no obvious rigid boundary.

However, studies have been done which show that depending on the ratio of foundation deformation modulus to the dam elastic modulus the extent of the representative foundation model can be estimated. Whether a foundation model is representative or not is decided upon on the basis of whether the increase of dimensions affects any of the deflections, stresses or natural frequencies in the dam. For example, for a ratio of the foundation's deformation modulus to the dam's elastic modulus of about 1, the minimum radius of the semi-circular foundation can be chosen to be equivalent to the dam wall height (U.S. Army Corps of Engineers, 1994).

In seismic analysis, the artificial boundary conditions have an effect of reflecting radiation waves from the dam model, which is not what exactly happens on site. In order to solve this problem, several techniques are employed including absorbing elements, radiating boundaries and infinite elements (Aznarez et al., 2006). These techniques are applicable to the seismic analysis of arch dams where the excitation motion is significant and hence the secondary effects of radiation waves are important. For the case of ambient conditions of the dam, the secondary effects are likely to be insignificant as the excitation forces are normally of smaller magnitudes.

However for earthquake induced radiation waves, in order to avoid their reflections in models, truncated foundation with non-reflecting boundaries needs to be introduced such that the radiated waves can propagate through towards infinity. The viscous spring boundary input model is one such input method which ensures that waves can propagate through towards infinity.

3.5 Viscous-spring boundary input model

Chuhan et al. (2009) use the viscous-spring input model to study the arch dam-foundation interaction.They argue that this method is very efficient and convenient to incorporate in the finite element code and has sufficient accuracy without much increase in computational efforts. In this method, pairs of dashpots and springs are installed in all nodes of artificial boundaries. Each node on the artificial boundary contains three pairs of dashpots and springs, i.e. one in the normal direction of the boundary plane and the other two in the tangential directions.The dashpoints and the spring are both assigned values of viscous damping and

stiffness respectively in all three directions. Chuhan et al. (2009) indicates that the acceleration time histories which normally act as an input parameter are, in this method, replaced by equivalent force input on the artificial boundaries.

3.6 Nonlinear behavior in the foundation

In the foundation, nonlinearities can be expected due to the presence of joints, faults etc. It can be assumed that nonlinear behaviour associated with these joints is in some way analogous to the one associated to cracks in concrete as both of cracks and joints are simply discontinuities in concrete and foundation rock respectively. The interface between the dam wall and the foundation also can at times need to be modelled by nonlinear methods.

Rock masses often exist as blocks which are separated from each by zones of small thickness which corresponds to modifications or degradations of the mechanical properties of the rock matrix. These zones are known as joints and they normally represent areas of weakness along which failure can occur. The overall behaviour of rock media is strongly affected by the mechanical properties of the joints (Maghous et al., 2008).

Hence, in the finite element models of the dam foundation, a deformation modulus is used instead of the normal elastic modulus to define the stiffness properties of the foundation. According to the Arch Dam Design Manual (1994), the deformation modulus is defined as the ratio of applied stress to elastic plus inelastic strains and thus includes the effects of joints, shears and faults. Deformation modulus is obtained by in situ jacking tests or it can be estimated from elastic modulus of the rock using a reduction vector. Estimation of the deformation modulus using the rock mass rating system is common in literature.

Just like in the superstructure, the use of joint elements is normally employed in finite element analysis to model the discontinuities. Modelling these nonlinear effects requires calculating the behaviour of the dam progressively with time (time domain analysis). On the other hand, according to Darbre (2000), when considerations of the infinite domains are made in the dynamic analysis of arch dams, a use of a solution algorithm working in the frequency domain is required. Infinite domains include the foundation and the hydrodynamic mass of the reservoir. This has been a major problem in the field of dynamic behaviours of arch dams as it means that there cannot be any program which can be built which can accordingly account for the nonlinearities and simultaneously include the infinite domains.

It is also agreed that the finite element does not handle infinite domains very well, hence, the need for use of truncation boundaries in the modelling of infinite domains using finite elements (Seghir et al., 2009). Elimination of any or both of the infinite domains without loss of accuracy of the results can help solve this problem. The use of the added mass formulation eliminates one infinite domain namely, the reservoir water domain.

3.7 Chapter summary

This chapter covered the approaches used in literature to model the rock medium on which arch dams are founded. Many of these representations attempt to model some field behaviour which is normally observed during a seismic occurrence. The zero foundation rock mass approach is the one approach that has been mostly used in literature as it is able to model with great accuracy the passage of waves inside the foundation. The passage of waves is a phenomenon which is more relevant to the seismic safety of dams than it is for ambient dynamic dams' behaviour. Despite its proven ability in that aspect, it is highly inaccurate when it comes to representing the dam wall-foundation rock interaction (Chopra, 2010).

It was decided that the foundation with mass approach would be used in this study given that foundation size calibration was still to be done. This is a scenario where the foundation size is increased until any further increase does not affect the natural frequencies and mode shapes significantly anymore. If the massless foundation approach were used, it is speculated that the increase would have no effect on the natural frequencies. This behaviour would not represent field behaviour as in reality the foundation size does affect the dynamic behaviour of the dam wall.

CHAPTER 4

DEVELOPMENT OF THE FINITE ELEMENT MODEL OF ROODE ELSBERG DAM

4.1 Introduction

Roode Elsberg is a double-curvature concrete arch dam with a nearly centrally situated uncontrolled spillway as shown in Figure 4.1. It is located in Worcester, in the Western Cape in South Africa. Its full capacity is about 8.2 million m^3 of water and this water is used for irrigation purposes of the nearby wine plantations. The dam crest is about 72m above the point of lowest foundation. The crest length from one abutment to the other is about 274m.

Figure 4.1: Roode Elsberg Dam.

4.2 Dam geometry

4.2.1. The superstructure

All the necessary information regarding the geometry of the Roode Elsberg dam's superstructure was extracted from the design drawings 43036 and 43938 (DWA, 1971). This information was then input into a finite element program, ABAQUS Professional 6.10.

Roode Elsberg dam is a one-centred arch dam which means that all the lines of centres of the arches lie on the same reference plane. The local zero level was set at a reduced level of 515.1m which is about 3m below the river bed level. All the arch units from the crest down to the local level of 27.4m are of uniform thickness. This is reflected in that for all levels above 27.4m, the loci for the line of centres of both the extrados and the intrados coincide. The two loci differ for all arch units lower than this level which translates to varying thickness for these arch units. This information is depicted in Figure 4.2. The extent of the arch units on both sides of the reference plane is defined by the subtended angles between the reference plane of the dam and the cushion line at various levels. The subtended angles are measured at different levels along the line of centres of the arch units' meridians.

The pictorial representation of the model that was constructed using this information is shown in Figure 4.3.

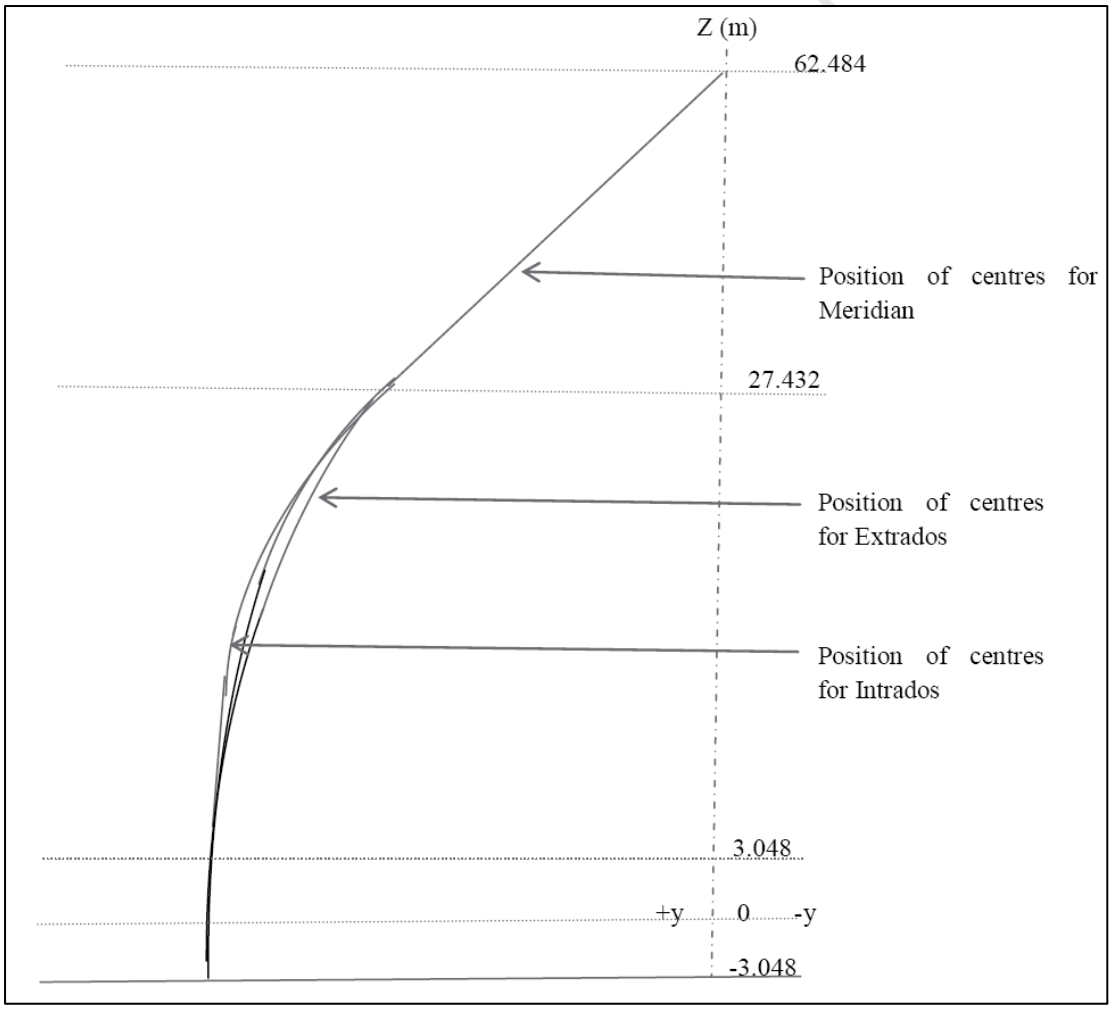

Figure 4.2: The profile of the position of centres of the meridian, intrados and extrados.

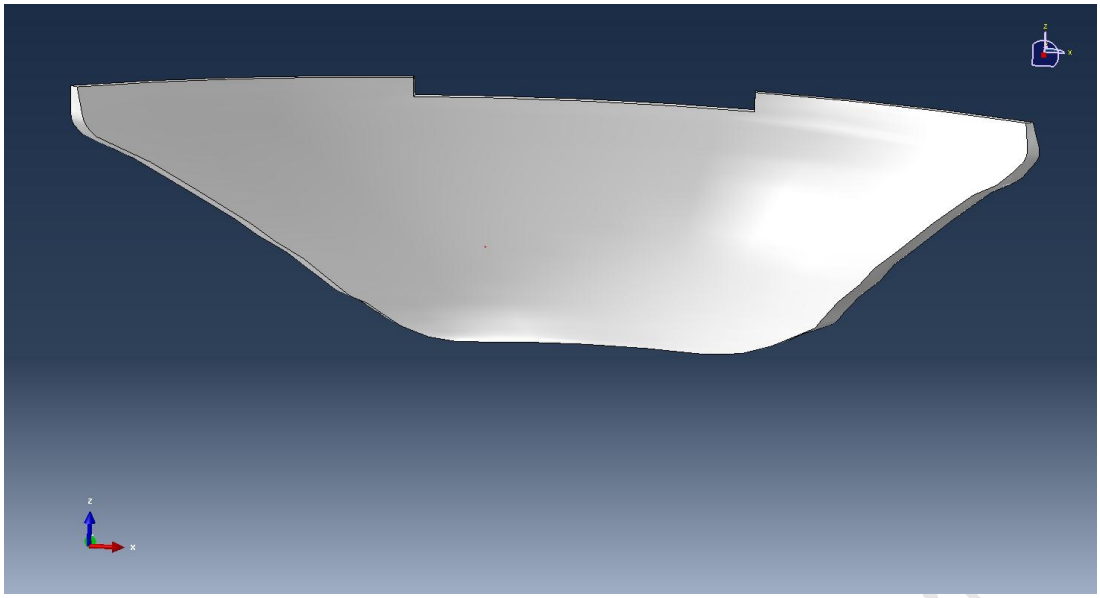

Figure 4.3: The dam arch drawn according to the design drawings, downstream view.

The canyon on which Roode Elsberg dam is built must have not allowed for a construction of a symmetric dam hence the inclusion of the cushion in the dam design and structure. The cushion is also often known as the pulvino in dam engineering. The construction instructions given in the design drawing 43936 were used as guidelines in defining the geometry of the cushion. It was mentioned that from the reduced level of 515.1m to the crest of the dam, the cushion line was to be carried horizontally with the same projection of 3.05m until meeting the solid rock line. This information was input into Abaqus Professional 6.10 to create a pulvino part shown in Figure 4.4.

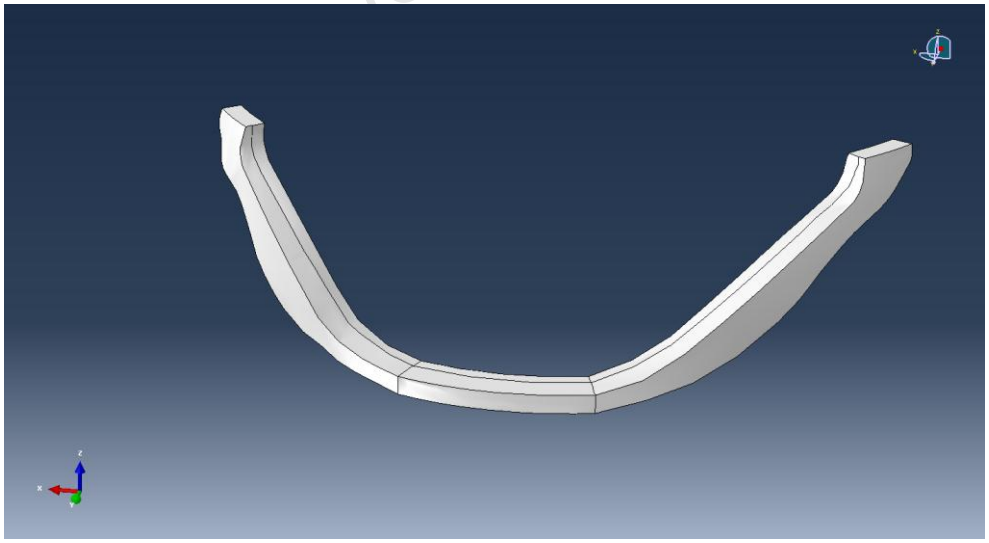

Figure 4.4: The pulvino, upstream view.

4.2.2. The foundation

The geometry of the foundation was based on the guidelines provided by the Arch Dam Design Manual (1994) which mentions for a ratio of the foundation's deformation modulus to the dam's elastic modulus of about 1, the minimum radius of the semi-circular foundation can be chosen to be equivalent to the dam wall height as a starting point to a parametric study in which the foundation size is increased until the increase of which has no effect on the static stresses, natural frequencies and mode shapes of the system. The rectangular foundation of depth equal to the dam height, as shown in Figure 4.5, was chosen as the starting point in the validation of the Roode Elsberg arch dam model.

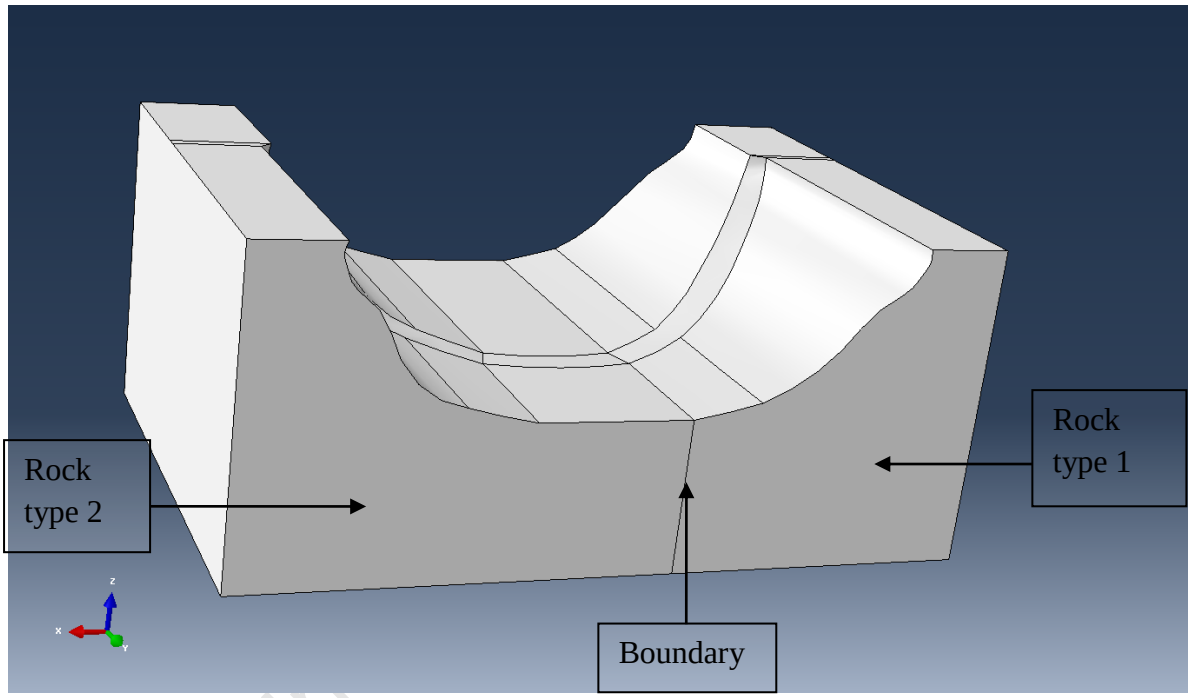

Figure 4.5: The initial foundation model of the Roode Elsberg dam, upstream view. The different rock types foundations as proposed by O'Connor (1985) are also shown.

4.3 The material properties

4.3.1. The dam wall concrete

For the initial stages of the analysis, linear behaviour, isotropy and homogeneity were assumed for the dam wall concrete. With these material behaviours having been assumed, only a few material properties for the dam concrete had to be estimated. These are the sustained dynamic modulus of elasticity, the dynamic Poisson's ratio and the unit weight of the concrete. In order to estimate the current dynamic modulus of the dam concrete, first the 28 day static elastic modulus had to be estimated.

The static elastic modulus of concrete was determined from the correlation between concrete's 28 day mean strength and the static elastic modulus mentioned in Fulton's concrete technology book (2009). The kind of aggregate in the concrete was used as the variable which determines the concrete elastic modulus in the correlation graphs. It was therefore essential that a good assumption is made on what aggregate was used in the Roode Elsberg dam concrete. It was hence deduced that the local Table mountain quartzite could have been used as it was readily available on the dam site. The working drawings indicated that the desired 28 day strength of dam wall concrete was 29MPa, with which the correlation was done in the correlation graphs to give a 28 day static elastic modulus of 31GPa. An extract, from working drawings, of the design data for the Roode Elsberg, is shown in Table 4.1.

There is however a difference between a 28 day static elastic modulus and a long term sustained static elastic modulus. The latter includes the effects of creep. According to the effective modulus creep theory; the sustained static elastic modulus is lower than the 28 days static elastic modulus. Fulton (2009) was still referred to in this case for the guidelines on how to convert the 28 day static elastic modulus to the sustained static elastic modulus and then to the dynamic modulus. The relevant Equations used to account for creep and dynamic behaviour are mentioned as Equation 4.1 and Equation 4.2 respectively where E_c is the 28 day static elastic modulus, E'_c is the sustained static elastic modulus, E_d is the dynamic modulus and φ is the creep factor. A creep factor of 0.35 was chosen as advised in the Engineering guidelines for the evaluation of hydropower projects (1999). After all these calculations, it was decided that a dynamic modulus of 40GPa was to be used.

$$E'_C = \frac{E_C}{1+\varphi} \tag{4.1}$$

$$E'_C = 1.25E_d - 19 \tag{4.2}$$

The choice of the first trial of the Poisson's ratio for the concrete to be used in the analysis was based on the guidelines provided in the Arch Dam Design Manual (1994), which states that for dynamic analysis of arch dams a Poisson's ratio of 0.22 can be assumed. The density of 2400kg/m^3 for the dam wall was used in this study as it was previously assumed in the design of the dam. That is according to the extract from the design drawings in Table 4.1.

Table 4-1: Extract from the design drawings of Roode Elsberg Dam.

	Design Data	
	Property	Metric System
1	Concrete Specifications	
	2.5% min. strength[1]	20.7MPa
	Allowable standard deviation	4 .1MPa
	Mean strength	29.0MPa
2	Design Stresses	
	Concrete	
	a) Tensile	1.7MPa
	b) Compressive	6.9MPa
	Steel	
	a) Tensile	8.3MPa
	b) Compressive	12.4MPa
3	Foundation type	
	Table mountain quartzite sandstone	
4	Coefficient of expansion of concrete	5.5×10^{-6} /°F
5	Concrete density assumed	2400kg/m^3

4.3.2. The foundation material

The foundation rock material was assumed to obey linear behaviour as the deformations in the rock can be expected to be small. From the design data in Table 4.1, it can be observed that the foundation rock is of Table Mountain quartzite sandstone type. According to Alexander and Mindess (2005) , samples of this type of sandstone can have a modulus of elasticity that varies for a wide range of values with a mean of about 60GPa. On being reduced to the afore-mentioned deformation modulus, in order to account for the faults and

[1] Only 2.5% of the tested concrete specimens were allowed to have strength of less than 20.7MPa.

joints in the massive foundation rock, this value can be expected to be much lower than 60GPa.

According to the tests done on the foundation rock (O'Connor, 1985), the foundation rock on the left abutment clearly has very different elastic deformation properties from the right abutment. It is however not very clear of where exactly does the boundary that separates the softer rock from the harder rock lies. O'Connor decided on the boundary as shown in Figure 4.5. Rock 1 had a deformation modulus of 29.5GPa in the two perpendicular horizontal directions and 6.9GPa in the vertical direction while Rock 2 had a deformation modulus of 23GPa in the perpendicular horizontal directions and 3.1GPa in the vertical direction.

O'Connor's values are definitely old but they give an idea of the current field properties. Unlike O'Connor (1985), the foundation rock was assumed to be orthotropic with Rock1 and Rock 2 having a dynamic deformation modulus of 25GPa and 20GPa respectively. A basis for this choice was the test results of the Rock Mass Rating (RMR) system (Bieniawski, 1989). Using this system, RMR values of 54 and 41 were determined for the right and left abutments respectively. These values are input into Equation 4.3 (Serafim and Pereira, 1983). The deformation moduli, *E* values obtained from Equation 4.3 were then converted into dynamic values. A material density of 2500 kg/m^3 and the Poisson's ratio of 0.25 for the foundation rock were also assumed.

$$E = 10^{(RMR-10/40)} \quad (4.3)$$

Evidence of the differential properties between the two abutments is evident in the design drawings as well. The drawings reveal that the right flank (Rock 2) was particularly troublesome as boreholes indicated that the rock was highly weathered down to the design excavations depth requiring that the actual excavations depths went somewhat deeper. Hence the excavation drawings for the right flank had to be specially revised.

4.4 Model assembly and definition of boudary conditions

4.4.1. Defining the assembly and the interaction between parts

The created Roode Elsberg dam model consisted of the three distinct parts, namely the dam arch, the pulvino and the foundation. The three parts were each created on the coordinate space that corresponds to the space that it occupies on site. Therefore, there was no need to

employ any position constraints when the instances were assembled together. The assembled parts are as shown in Figure 4.6.

Interactions however needed to be defined between the instances. It was decided that the constraint that does not allow any slipping between the surfaces between which it is applied were to be employed to describe both the contacts between the dam wall arch and the pulvino and also between the pulvino and the foundation. In case of rotations, the constraint was that the nodes which are in contact on the two surfaces be allowed to move by the same displacements.

4.4.2. Model boundary conditions

It is only in the foundation part where the boundary conditions were imposed. All the outside surfaces were assumed to be fixed.

4.5 The meshing process

Meshing refers to the process whereby the part geometry is discretized into smaller assemblage of finite elements. This is one of the most important steps in any finite element modelling procedure as the basis of any finite element solution procedure is that there should be small elements for which matrices of the variables are calculated which can then be used to derive the global matrices of the variables.

4.5.1. Mesh size refinement and optimization

It is normal in the use of finite elements to refine and optimise the mesh size. This is done by decreasing the mesh size, up to the point where the increase in mesh density does not affect the final solution significantly. This is an optimization problem because a finer mesh means a longer time is needed for the computer to solve the problem, so there is a trade-off between mesh density and computational time. This was carried out in this study as well to determine the optimum mesh size, the mesh size as shown in Figure 4.6 was determined to be of the optimum size.

Further information on the number of elements used, the kind of elements and the form of integration is used on the elements on the model is presented in Appendix 1.

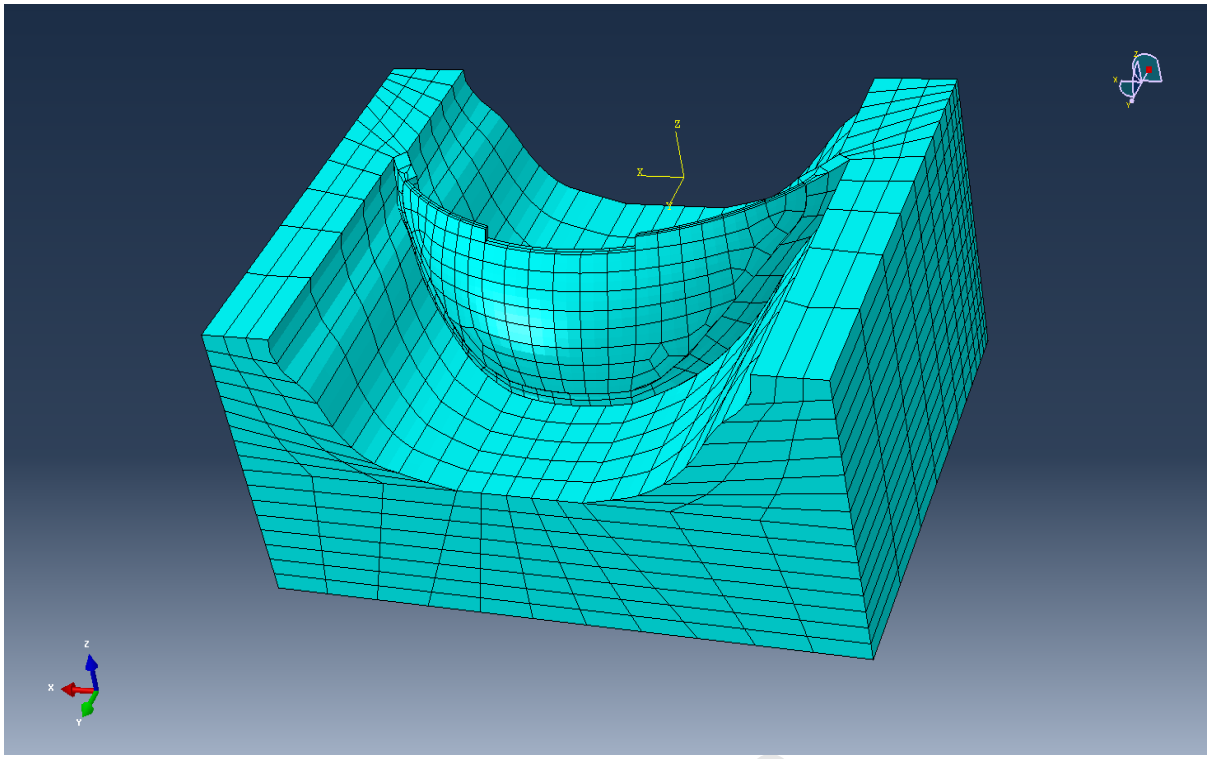

Figure 4.6: The assembled parts and their respective meshes in the mesh module.

4.5.2. Mesh verification

The developed mesh as shown in Figure 4.7 was then checked for any errors. The foundation mesh was the only one which was found to be slightly problematic as there were several elements of the mesh that had unacceptable aspect ratio, minimum angles and maximum angles. Table 4.2 summarizes the results of the mesh verification process.

Table 4-2: Summary of the detected faults in the foundation mesh.

Detected fault	Number of faulty elements	Percentage of total elements
Unacceptable aspect ratio ≥ 8	41	2.4
Minimum angle ≤10°	14	0.8
Maximum angle ≥160°	56	3.4

Due to these identified faults it was decided that a better foundation model would be developed.

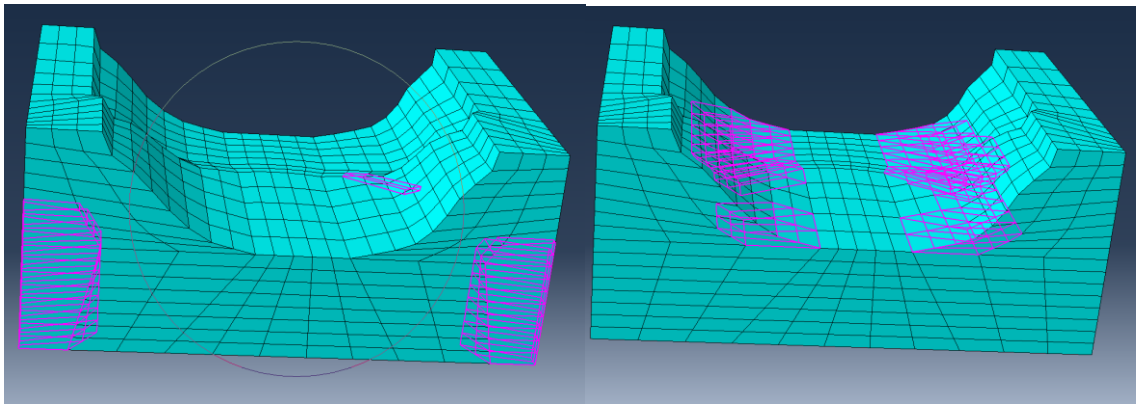

Figure 4.7: The highlighted elements on the left picture show elements of unacceptable aspect ratio while on the right the highlighted elements have at least one face angle of more than 160°.

4.6 The new foundation part

The proposed foundation model is shown in Figure 4.8. Even though it showed less of the afore-mentioned faults in its mesh, it however depicted another problem which was that there were some mesh gaps detected. This problem was due to the fact that the mesh was created using a bottom-down swept technique but given that the source side did not consist of simply connected surfaces which have small angle variations among them, it was not easy to create a good mesh.

Figure 4.9 shows that the pulvino is slightly embedded in the foundation rock. The foundation model in Figure 4.8 tried to capture this embedment of the pulvino in the foundation but this came with a cost of a faulty foundation as mentioned above. This embedment was then removed to produce a better and almost faultless foundation model shown in Figure 4.10.

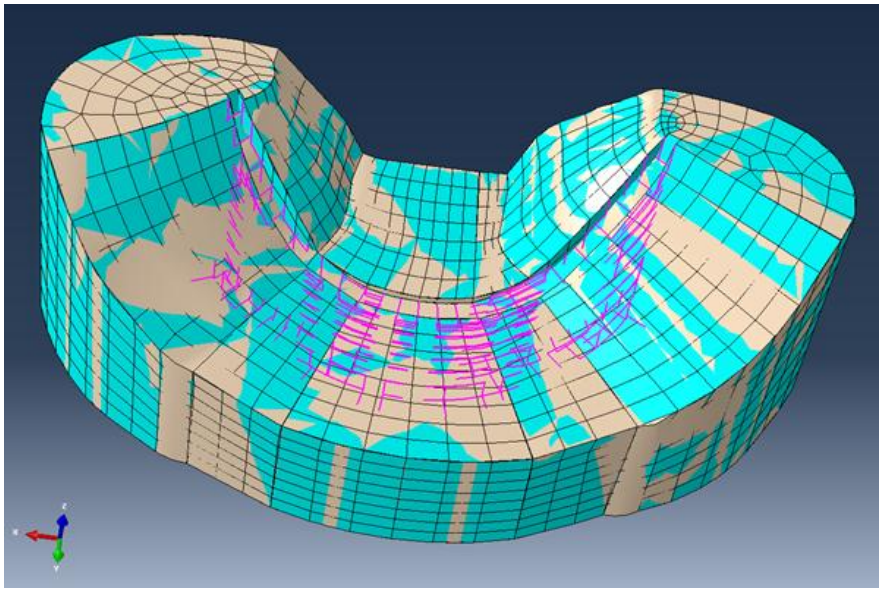

Figure 4.8: The faulty mesh of the dam foundation showing the mesh gaps.

Figure 4.9: Shows how the pulvino is embedded in the rock foundation on site.

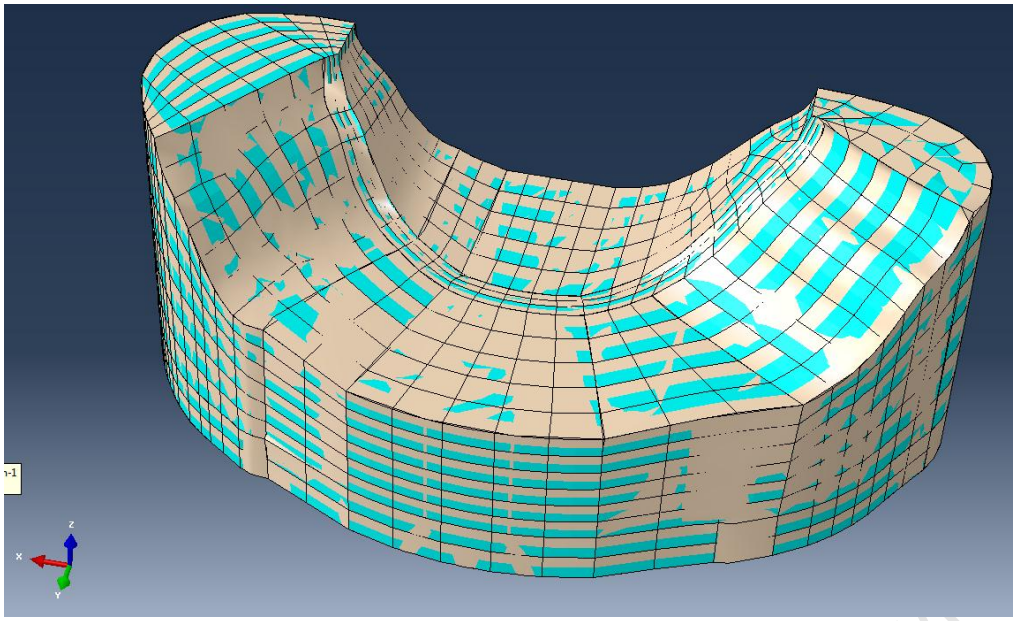

Figure 4.10: The final dam foundation model.

4.7 Dam wall partitions and the application of the Westergaard method

At first, it was decided that the added mass was to be added on the wetted upstream nodes of the orphan meshes as nodal point mass.

If only the original Westergaard method is applied and not the extended method, the magnitude of each nodal point mass depends on the water depth; height of the node above the base and the tributary area assigned to that particular node .The full calculation of the added masses for the different nodes for the full dam is attached in Appendix 2.

The application of the original Westergaard method using the point mass approach in Abaqus Professional 6.10 is normally executed through the use of the orphan mesh. However, the use of an orphan mesh would in future make the combined analysis of both thermal and ambient dynamic behaviour very difficult. This is partly because partitioning, which is an indispensable tool for such an analysis, is limited in orphan meshes.

It was hence decided that an application which introduces the added mass as a change in density of the structure will instead be applied. Over the area on which the added mass will be applied, there is likely to be a change of the parameter that is used to calculate the added mass e.g. the height. This calls for the use of the integration mathematical technique or a use of a parameter that can be considered representative for the whole area, e.g. the average height instead of integrating from one height to the other.

If however integration is used, it is advisable that the dam wall is partitioned. Once partitions are made then each added mass can be added on its respective partition. It has to be ensured that in each partition any of the parameters that is used to calculate the added mass does not vary much otherwise complicated integration might need to be done. The dam wall was hence partitioned as shown in Figure 4.11. Note that all the cell partitions have at least one horizontal partition to facilitate easy application of the added mass which varies with height.

The conversion of nodal masses into masses that are applied on the surface was carried out by first summing up all the nodal masses which lie entirely on any given surface. Then for the masses on the corners of the surface; their nodal masses were divided by either four or two depending on the position of a node.

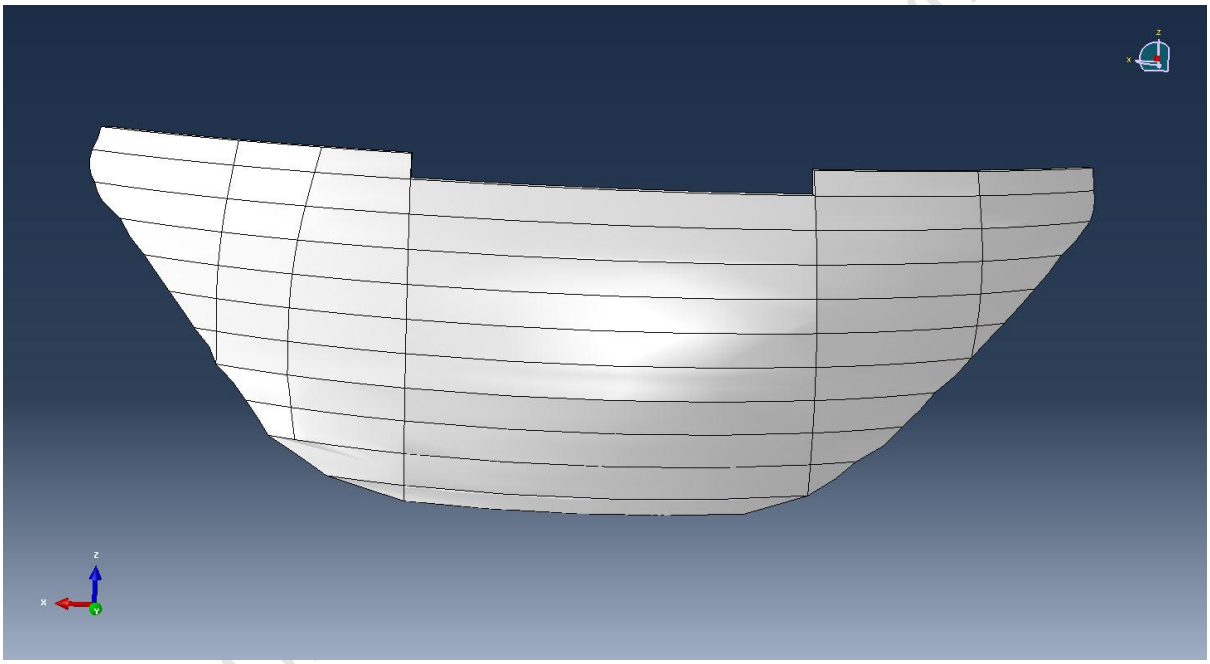

Figure 4.11: The dam wall part with all its cell partitions.

4.8 Natural frequencies extraction methods

Dynamic response of a structure to a given excitation force can either be carried out in the frequency domain or in the time domain. For linear systems which are solved in the frequency domain, the excitation force is assumed to be a superposition of a large number of harmonic excitations of different frequencies. The behaviour of the structure is then determined for each frequency of excitation and then the individual results are combined to obtain total dam response. In time domain, the response of a structure is obtained by following the action of the excitation force step by step (Darbre, 2000).

This section describes the natural frequencies extraction methods used in Abaqus Professional 6.10.

4.8.1. Subspace iteration method

A small set of base vectors is created, thus defining a subspace. This subspace is then transformed, by iteration and Ritz analysis, into the space containing the lowest few eigenvectors of the overall system. This is a basis of one advantage of the subspace method which is that the extraction of the eigenvalues is in a reduced space, which will cause a rapid convergence to the eigenvectors in full space (Dassault Systems Simulia Corp., 2010).

However, the choice of starting vectors is also important because if these are chosen such that they span the space of the eigenvectors as completely as possible rapid convergence can be achieved. The number of base vectors carried in the iterations is also of importance as if more vectors are used, the number of required iterations is reduced, but each iteration takes longer. The default value used in Abaqus has been found to be effective and optimum (Bathe, 1996).

4.8.2. Lanczos iteration method

Theoretically, the basic steps of the Lanczos method transform the generalized eigenproblem in Equation 4.4 into a standard form with a tri-diagonal coefficient matrix. The applied transformation for every Lanczos run is stated in Equation 4.4.

$$[\boldsymbol{K}]\{\boldsymbol{\Phi}\} = \omega^2[\boldsymbol{M}^*]\{\boldsymbol{\Phi}\} \tag{4.4}$$

$$[\boldsymbol{M}^*]([\boldsymbol{K}] - \sigma[\boldsymbol{M}^*])^{-1}[\boldsymbol{M}^*]\{\boldsymbol{\Phi}\} = \theta[\boldsymbol{M}^*]\{\boldsymbol{\Phi}\} \tag{4.5}$$

$\boldsymbol{M}^*$and $\boldsymbol{K}$ are the structure's mass and stiffness matrices respectively. If, however the fluid-structure interaction is considered using the added mass concept, then $\boldsymbol{M}^*$ represents both the mass of the structure and the added water mass. ω is the undamped natural frequency of the

structure and $\boldsymbol{\Phi}$ is the corresponding mode shape. σ is the shift, θ is the eigenvalue of the transformed Equation and these two variables are related to ω by Equation 4.6. This transformation allows rapid convergence to the desired eigenvalues. The same eigenvectors apply to Equation 4.4 as in the transformed problem in Equation 4.5.

$$\omega^2 = \frac{1}{\theta} + \sigma \tag{4.6}$$

The Lanczos method is generally faster when a large number of eigenmodes is required for a system with many degrees of freedom (Dassault Systems Simulia Corp., 2010). Hence it was chosen for the analysis.

4.9 Finite element model calibration methods

It was indicated in the introduction chapter that it is normal for an analytical model to be inaccurate especially in the case of complex structures. The inaccuracies of the model can be due to difficulties in the modelling of joints, materials behaviour, boundary conditions and damping. Assuming that the experimental measurements are taken without error, the lack of correlation between model predictions and observations is resolved by calibrating the model (Mottershead and Friswell, 1993). There are several methods adopted in literature on how to effectively calibrate models and this section discusses some of these methods.

According to Modak et al. (2002), model updating methods can be broadly classified into non-iterative methods, also known as direct methods and iterative methods. The former assume that one of the following three quantities, namely the measured modal data, the analytical mass matrix or the analytical stiffness matrix is taken as reference and the remaining quantities are updated. A specific example of this would be to assume that the mass matrix is correct and hence taken as reference, while the measured eigenvectors are updated by minimizing the weighted Euclidean norm of the difference between the measured and the analytical eigenvectors subjected to the orthogonality constraints. The updated eigenvectors are then used to update the stiffness matrix (Modak et al., 2002).

It is however argued that event though these the standard direct methods yield updated matrices that reproduce measured modal data exactly, their drawback is that real structural connectivity is generally not maintained and the suggested corrections are not physically meaningful (Modak et al., 2002).

On the other hand, in iterative model updating techniques result in physically realizable models. These techniques rely on minimizing an objective function that is generally a non-linear function of selected updating parameters. However, the computational time required by the minimization procedure makes these techniques infeasible for use in a real-time fashion to correct the model parameters as the system changes (Atalla, 1996).

It is important to highlight that the above mentioned techniques are normally used to match both the mode shapes and natural frequencies of the analytical analysis to the experimental results. In case only the mode shapes need to be matched, techniques such as Modal Assurance Criterion (MAC) are normally used. Often in dam engineering, provided the physical behaviour is well captured on the model with sufficient number of degrees of freedom, the mode shapes do generally match between the analytical results and the experimental results. In that case, it is normal to just identify where the deficiencies in the model are then correct them. In most cases, these deficiencies are a result of using wrong material properties in the model. Once the deficiencies are identified, modifications are made as necessary to match the results. This approach was adopted by Sevim et al. (2009) in the calibration of the finite element model of Berke arch dam.

4.10 Chapter summary

This chapter described the process of developing the finite element model of Roode Elsberg dam in Abaqus Professional 6.10. It was desirable that a model which could be used in the future related studies on the dam is created. An example of this is a coupled displacements and temperature study where the thermal effects on the dynamic behaviour are investigated. While creating a multipurpose model might not be easy given that every analysis is highly specialised and different, an attempt was made for this to be achieved. For example, the application of the added mass using nodal masses was discarded for a more versatile approach of using non-structural masses.

The geometry was input in the program with the help of the design drawings of the dam. One major challenge that was encountered at this stage was the choice of material properties to be used in the analysis. This was because there was not enough field material testing which was carried out prior to the development of model. However, guidelines were resorted to wherever decision had to be made in the absence of data.

Familiarity with the program Abaqus was of great importance in the development of the model. This is because even though there are specific modules on which one works on in Abaqus 6. 10, these modules are actually related as normally what one does in one module affects what happens in other modules. Some key aspects of the modelling and some insight into Abaqus Professional 6.10 operations are included in Appendix 1.

CHAPTER 5

RESULTS AND DISCUSSION

5.1 Introduction

This chapter presents and discusses the results gathered from the operational modal analysis and the analytical modal analysis of Roode Elsberg dam. It is anticipated that there will be some differences between these two sets of results due to uncertainties in the material properties and boundary conditions used in the analytical model to represent real conditions. Hence, an attempt to calibrate the finite element model to produce similar results to the operational modal analysis results will also be presented in this chapter.

The calibration of a model of a structure which consists of as many components as an arch dam is likely to be in stages. Each of these stages deals with one component of the model, usually starting from a component which is assumed to be least complicated and ending with a more complex one.

Since the main focus of this work is to look at the representation of the dam wall- water interaction using the Westergaard method, it was decided that the foundation size calibration would be the first step of the whole model calibration process. The application of the Westergaard method would then follow after the foundation size calibration.

5.2 Operation modal analysis (OMA)

5.2.1. Data collection

Ambient vibration measurements on Roode Elsberg Dam were carried out in irregular intervals from December 2008 to June 2011. Response measurements were done in three dimensions. The galleries in Roode Elsberg Dam are both near foundation level and hence the dam's response was best captured at the crest at locations 2-9 in Figure 5.1. The rest of the shown locations were inaccessible. Each position represents the centre of a block (Moyo and Oosthuizen, 2011).

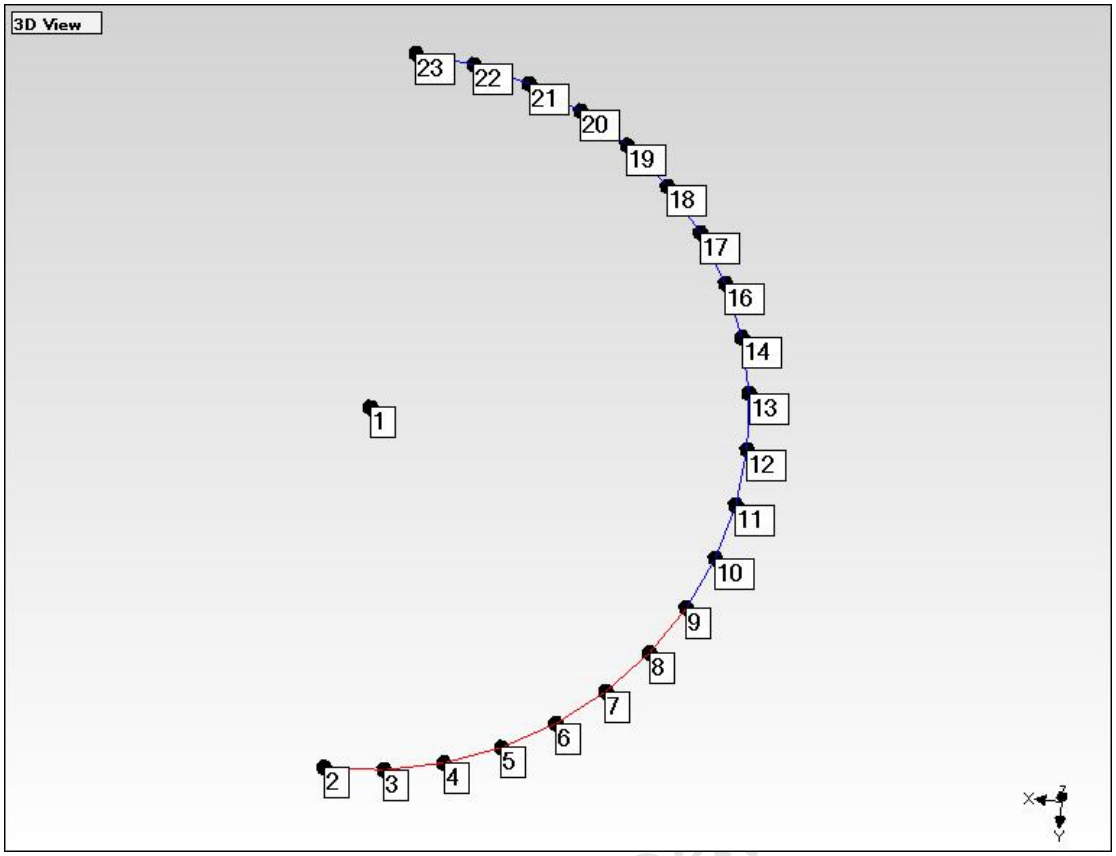

Figure 5.1: Measurement locations: Roode Elseberg dam crest.

Roving force balance accelerometers with a resolution down to 1µg and intrinsic noise of 7 µg (0-10Hz) and 70 µg (10-500Hz) and a set of three seismic piezoelectric accelerometers were used as reference. The force balance accelerometers have a nominal sensitivity of 6V/g while the piezoelectric accelerometers have a nominal sensitivity of 1V/g. Data acquisition was via the National Instruments 8 channel dynamic signal analyser (NI PCI 4472B). All 8 inputs are simultaneously sampled with a 24bit resolution at 1000Hz. Power supply was provided by means of a portable generator (Moyo and Oosthuizen, 2010).

5.2.2. Experimental natural frequencies

The dam's response that was captured by the testing includes the natural frequencies and mode shapes. The time variance of the natural frequencies for the mentioned time interval of December 2008 to June 2011 is presented in Figure 5.2.

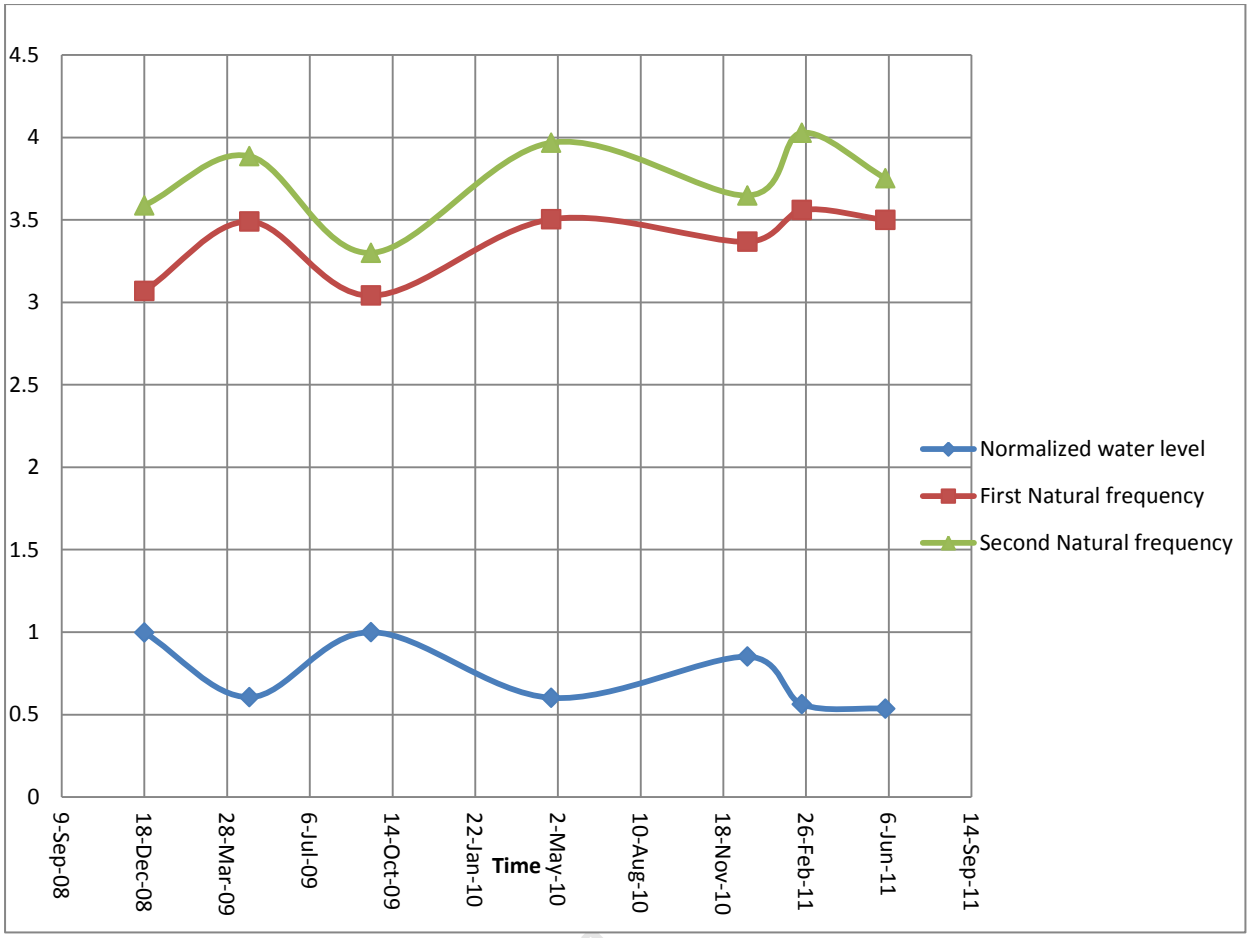

Figure 5.2: Variation of the first two natural frequencies with time.

The change of the natural frequencies with time shown in Figure 5.2 suggests that generally in late summer and autumn in the Southern hemisphere, the water level in the dam is at its lowest. It is hence during that time when the natural frequencies are expected to be the highest since the mass has an inverse proportionality with the frequencies. Figure 5.2 confirms this behaviour.

The variation of the natural frequencies with water level was very difficult to capture in the dam since the dam water level has never been very low for the period in which the tests were being done. Hence, there is insufficient data for lower water levels. Also it might also be very difficult to analyse and make conclusive remarks out of the collected data since the temperature was not constant in the water levels and natural frequencies data collected.

Despite the mentioned setbacks, there was some data captured for the variation of the natural frequencies with water level and it is presented in Figure 5.3

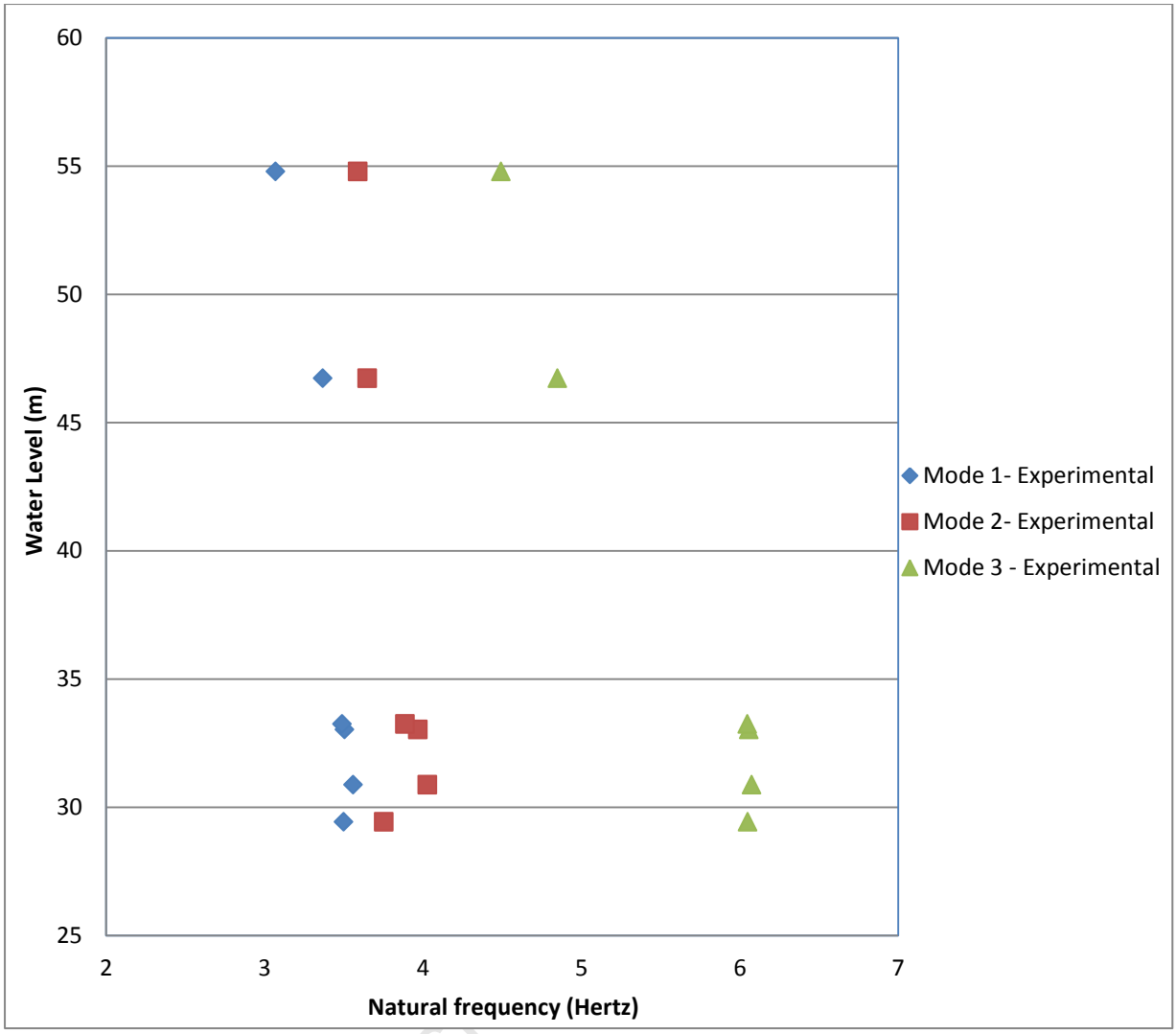

Figure 5.3: Some experimental results which were extracted from Roode Elsberg Dam.

The expected behaviour of the natural frequencies which increase with decreasing water level up to a certain water level is observable. The natural frequencies should then slightly decrease as described in section 2.5 of chapter 2 of the literature review. A very slight decrease can be expected though for Roode Elsberg dam as described in the next paragraphs.

The fact that Roode Elsberg dam experiences lower water levels in late summer when the temperatures are high, might have crucial implications to the contraction joint behaviour and hence natural frequencies of the dam when these are monitored for increasing water levels in the dam. The contraction joint behaviour described in section 2.5 mentions that for increasing water levels but at lower water levels in the dam the effect of the dam becoming stiffer due to the closing of the vertical construction joints under increasing hydrostatic pressure prevails over the effect that is brought about by the augmentation of the mass of the entrained water.

In addition to this, during times of lower water levels in the reservoir, it is normal for arch dams to experience zones of horizontal tensile stresses on the downstream or upstream dam faces near the base (U. S. Corps of Engineers, 1994). Evidence of this in Roode Elsberg dam is a crack in the upstream face of the dam which has been detected by the deformations monitoring system installed on the dam (O'Connor, 1985).

In response to these stresses, the contraction joints relieve the tensile stresses by opening up. This has the effect of reducing the overall stiffness of the dam wall. In Roode Elsberg dam, the temperatures are normally high when this happens as described. If the concrete temperature happens to be higher than the closure (grouting) temperature of the dam, then compressive stresses will develop in the arches, a phenomenon which counteracts the opening of the contraction joints (U. S. Corps of Engineers, 1994).

Hence, there are two phenomena whose effects counteract each other namely, the positive pressures which induce compressive stresses and the lowering of the water level which can bring about tensile stresses around the base of the dam. This means that in Roode Elsberg dam natural frequencies are likely not to decrease considerably at lower water levels when the frequencies are monitored with varying water levels.

5.3 Comparison of OMA results and the analytical modal analysis results

Firstly, it was discovered that the OMA mode shapes of Roode Elsberg did not change with water level in the dam. For the comparisons of the mode shapes of the analytical model with the experimental results, the mode shapes of a similar dam to Roode Elsberg namely Kouga dam were used. The experimental mode shapes of Kouga Dam were used for comparisons instead of the Roode Elsberg ones because the mode shapes of the latter could not be fully extracted due to inaccessibility of the spillway portion of the dam. Both dams were designed and built around the same time in the 1960s (Moyo and Oosthuizen, 2010). The comparison between the first three analytical mode shapes and the corresponding experimental ones is shown in Figures 5.4 to 5.6.

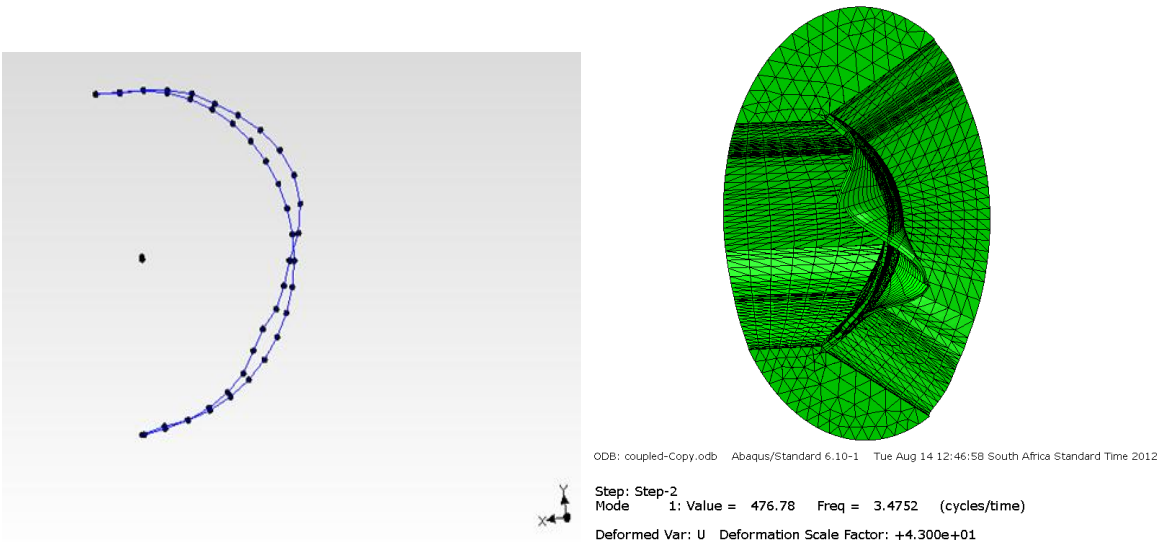

Figure 5.4: The comparison of the first mode of Kouga dam (Left) with the first one of the analytical model of Roode Elsberg dam (Right).

Figure 5.4 shows that the first mode shape or Kouga dam is an anti-symmetric mode which compares very well with the first mode of the analytical model of Roode Elsberg dam. The latter is also an anti-symmetric mode.

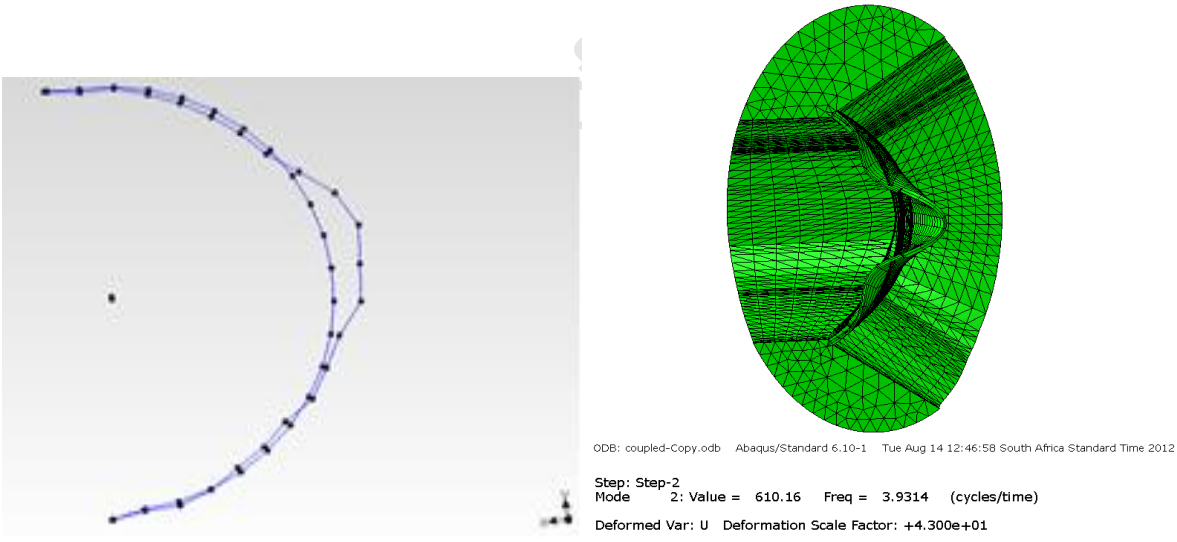

Figure 5.5: The comparison of the second mode of Kouga dam (Left) with the second one of the analytical model of Roode Elsberg dam (Right).

Figure 5.5 shows that the second mode shape or Kouga dam is a symmetric mode which compares very well with the second mode of the analytical model of Roode Elsberg dam. The latter is also a symmetric mode.

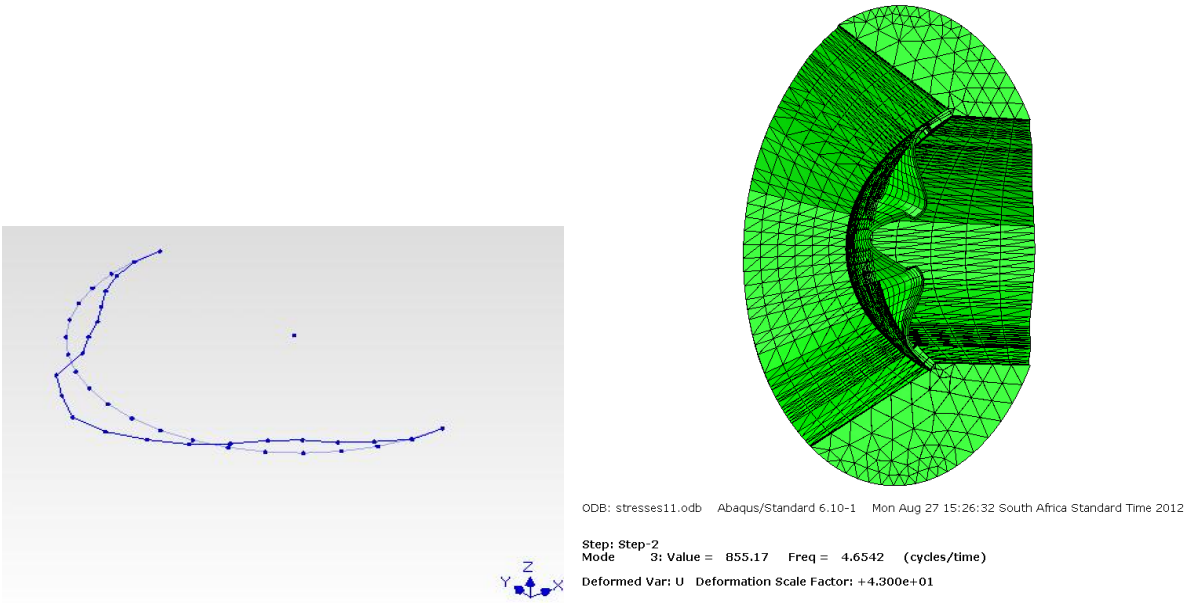

Figure 5.6: The comparison of the third mode of Kouga dam (Left) with the third one of the analytical model of Roode Elsberg dam (Right).

Figure 5.6 shows that the third mode of the analytical model of Roode Elsberg dam is a symmetric mode. The experimental third mode of Kouga dam is also shown on the left and the two do look similar. The slight difference between the two modes might be due to that Kouga has a slightly longer arch profile than Roode Elsberg. The rest of the mode shapes comparison is carried out in the Appendix.

Through the comparison carried out in Figures 5.4 to 5.6 and in the Appendix, it was concluded that the observed analytical mode shapes matched fairly well with those observed in Kouga Dam. Hence, there was no need to calibrate the model in that respect but rather calibrate with respect to natural frequencies which at this stage were still not matching with the experimental results. This then called to for the use of the Westergaard method to account for the dam-water interaction in the dam.

Prior to that, it had to be ensured that the uncertainty concerning the size of a representative foundation size is solved. This was done by increasing the foundation size until any further increase has no effect on the calculated natural frequencies. The results of this calibration of the foundation size are presented in the next section.

5.4 Foundation size calibration

An empty dam model was chosen for this calibration in order to minimize the number of uncertain parameters in the model to be calibrated for foundation size. If the full capacity dam model was to be used for the foundation calibration model, another unknown would have been introduced and it would have been difficult to track down how a parameter of interest, which in this case is the foundation size, influences the natural frequencies. An example of an increased foundation is shown on the right in Figure 5.7.

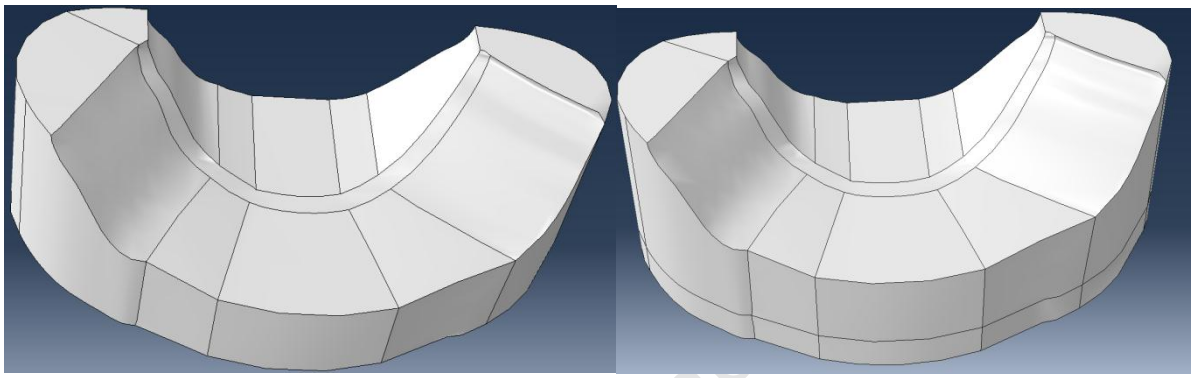

Figure 5.7: An increased standard foundation model shown on the right. On the left, a standard foundation model is shown.

The foundation size was increased by offsetting and extending all the boundary surfaces of the standard foundation size outwards. For a ratio of dam elastic modulus to foundation rock deformation modulus of close to one, the standard foundation is the one that extends a distance that is equal to the dam height in all direction. The results of the foundation size effect study are presented in Figures 5.8 and 5.9 for lower and higher modes respectively.

The results in Figures 5.8 show that for lower modes the foundation size increase has a very small effect on the natural frequencies. However for the higher modes, an increase in foundation size appears to have a considerable effect on the natural frequencies. For example, for the fourth natural frequency, an percentage increase of 35% in the foundation size results in a 0.2% decrease in the natural frequency while for the thirteenth mode the same percentage increase of 35% in the foundation size results in a 10% decrease in the natural frequency. Nonetheless, there is an observed convergence of the results in both higher and lower modes since for every subsequent increase in foundation size; the effect on the natural frequency keeps diminishing.

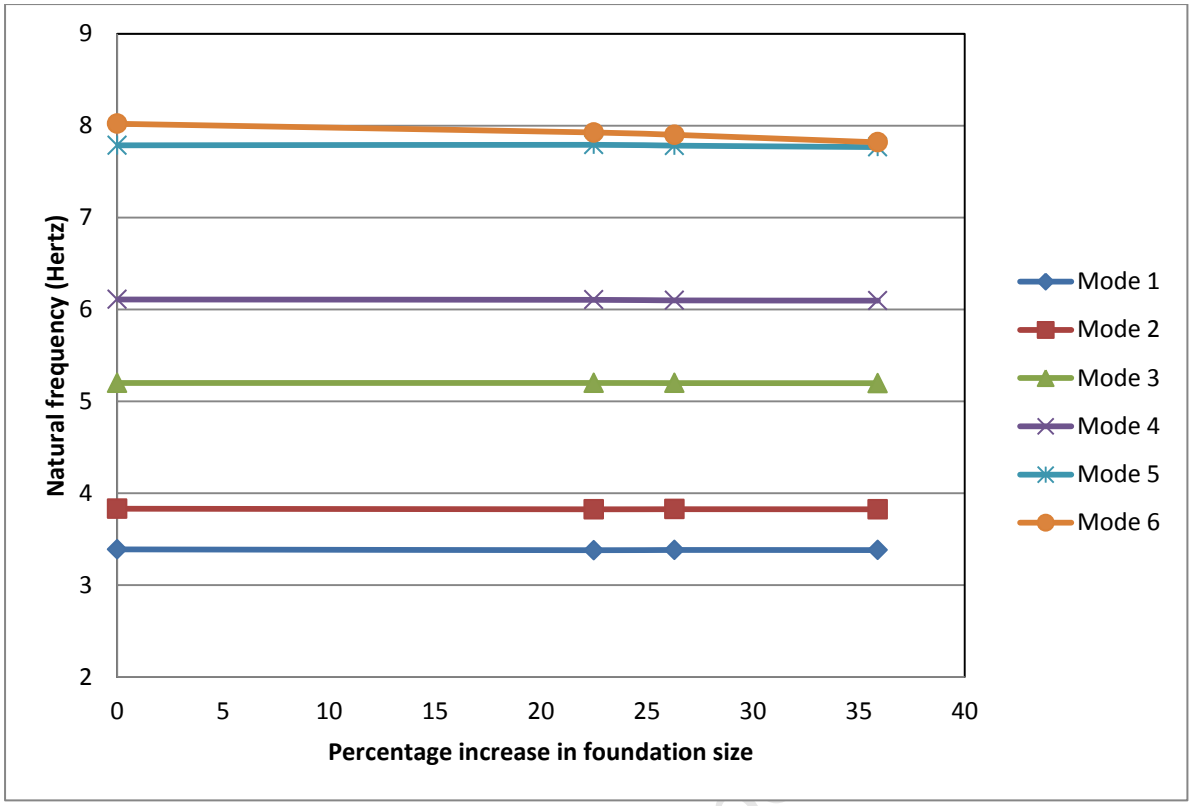

Figure 5.8: Natural frequencies for various foundation sizes for lower modes.

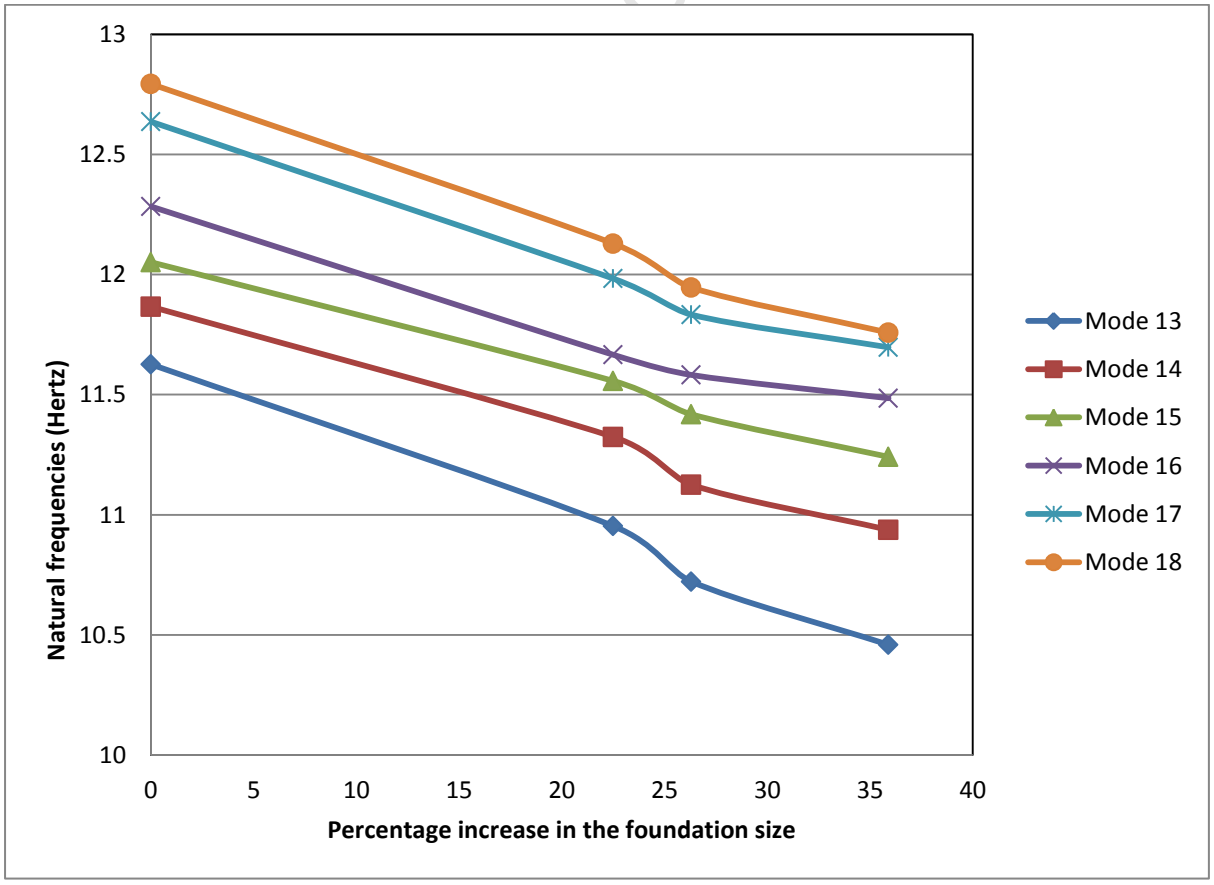

Figure 5.9: Natural frequencies for various foundation sizes for higher modes.

In linear dynamic behaviour analysis of structures using the mode superposition technique, it is normally assumed that the behaviour of a structure is governed by only a few of the lower modes. This means that the lower modes are of more importance than the higher ones. Hence, since the lower natural frequencies were relatively stable for a further increase in the foundation, it was decided that no further increase (beyond 35%) were to be done on the foundation size despite the behaviour of the higher natural frequencies.

Figure 5.10 justifies this decision clearly as even for higher natural frequencies the graphs generally get closer to each other for every increase in the foundation size. This implies convergence of the results.

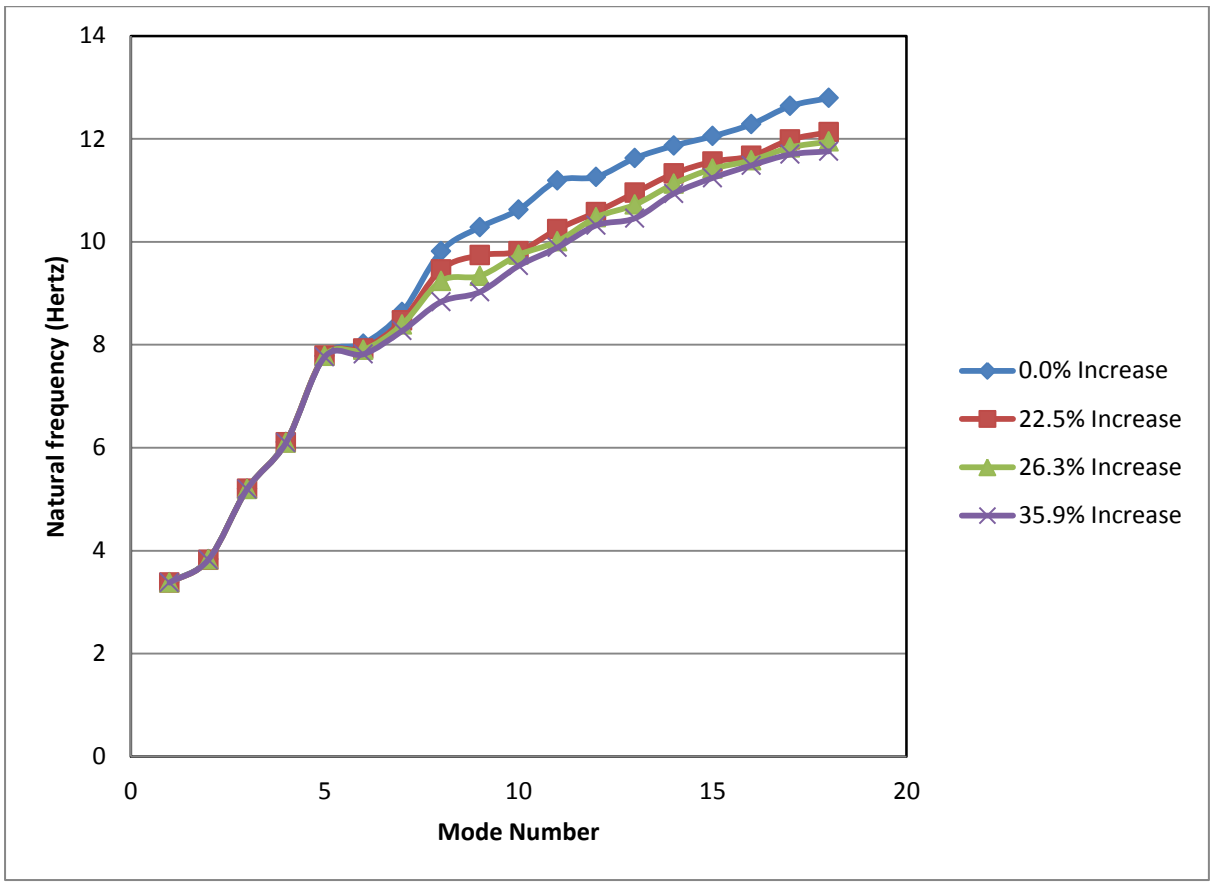

Figure 5.10: Variation of natural frequencies with foundation size for all the calculated natural frequencies.

5.5 The Westergaard method results

At first the added masses were calculated using the original Westergaard method and this would later be changed to the generalized Westergaard method which is applicable to the upstream curved Roode Elsberg dam.

The observed analytical natural frequencies proved to be too low as compared to the experimental ones. This is reflected in Tables 5.1 and 5.2 which summarize the comparison of the field results with the analytical ones where the original Westergaard method was used for a full dam and a half full dam respectively. The data for the full dam in Table 5.1 clearly shows higher percentage errors in the results than the Table 5.2 with data for a half full dam.

Table 5-1: Comparisons between the analytical frequencies found using the original Westergaard method with OMA results for a full dam.

Mode Number	**FEM with Original Westergaard Masses Results**	**Ambient Vibration Testing Results** (14^{th} December, 2008)	**Percentage Error (%)**
Mode 1	2.32	3.07	24
Mode 2	2.59	3.59	28
Mode 3	3.71	4.11	10
Mode 4	4.37	4.49	3
Mode 5	5.39	5.64	4
Mode 6	5.70	6.41	11

Table 5-2: Comparisons between the analytical frequencies found using the original Westergaard method with OMA results for a dam half empty

Mode Number	**FEM with Original Westergaard Masses Results**	**Ambient Vibration Testing Results**(21^{st} February, 2011)	**Percentage Error (%)**
Mode 1	3.24	3.56	9
Mode 2	3.63	4.03	10
Mode 3	5.07	4.91	-3
Mode 4	5.99	6.08	1
Mode 5	6.92	6.38	-8
Mode 6	7.63	7.19	-6

The mismatch of the results presented in Tables 5.1 and 5.2 suggested that the original Westergaard method was not applicable in this case as was previously hypothesized. The

mismatch was higher for a full dam data than for a half full one, which confirmed that the added water mass was the problem. Hence it was decided that the generalized Westergaard added mass method will then be used.

However, before the shift could turn completely from the original Westergaard method to the generalized one, several aspects had to be discussed first which are common to both methods. These include the effects of both the diverging reservoir walls and the non-symmetrical distribution of the water across the dam wall.

5.5.1. Effect of the orientation of the water body

The water body in Roode Elsberg dam is not symmetrical as the picture in Figure 5.11 suggests. However in the use of either the original or the generalized Westergaard method it is always assumed that the water body is symmetrically distributed across the dam wall. It is not only symmetry which is important in this case but also the average angle between the water body and the dam wall. Most dams have diverging reservoir walls while Westergaard assumed a prismatic reservoir.

Figure 5.11: An aerial photograph of Roode Elsberg Dam (Courtesy of Google maps, 2005).

Dams of diverging reservoir walls experience less dynamic pressures in the crown cantilever than the same sized prismatic dams under same ambient conditions (Kuo, 1982). Roode Elsberg dam, as shown in Figure 5.11, has an unsymmetrical distribution of the impounded water, with most of the water concentrated towards the Westward part of the skew reservoir. A considerable percentage of the water body is hence at an angle to the dam wall. The effects of asymmetric and diverging reservoir are likely to be even more significant for Roode Elsberg dam due to a presence of a kink just upstream of the dam wall which noticeably divides the water body into two parts.

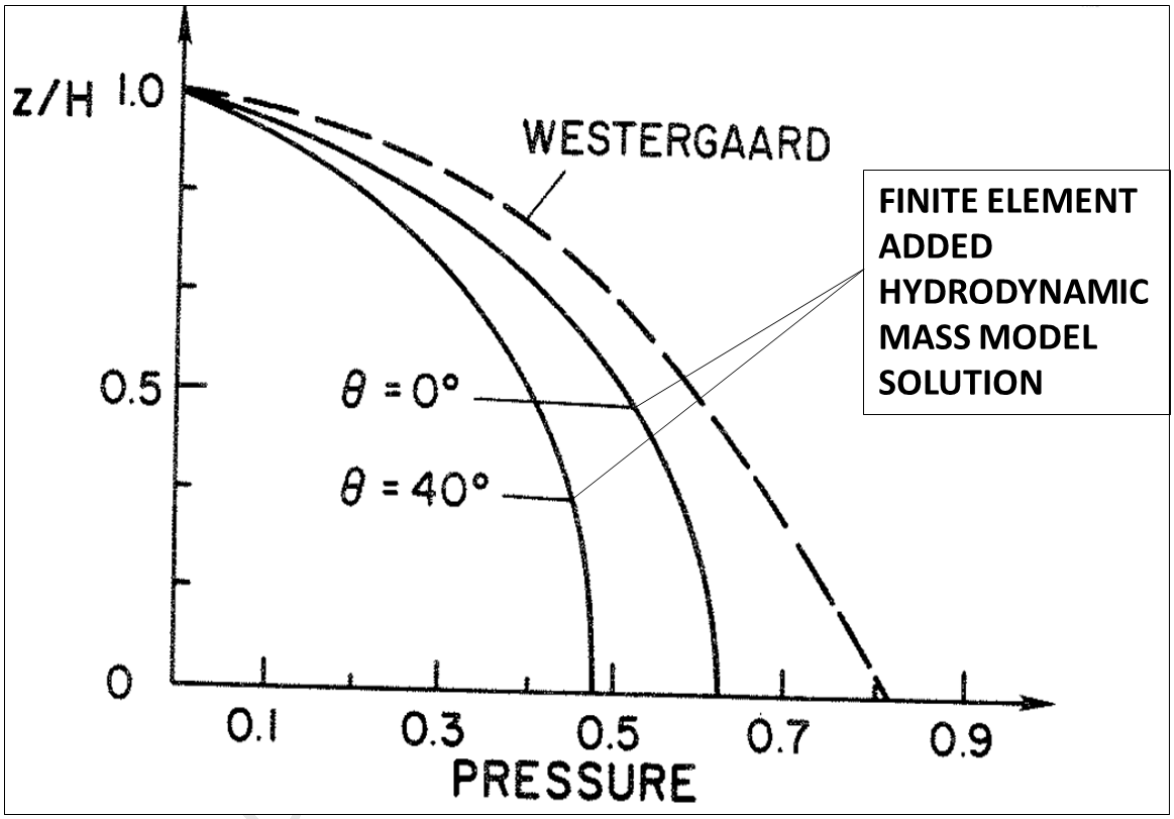

Figure 5.12: Pressure distributions at crown section of a cylindrical dam, showing the finite element fluid results compared to the Westergaard added mass ones. The reservoir wall diverging angle was varied from 0° to 40° for fluid finite elements (Kuo, 1982)

The angle between the West part of the water body and North is about 25°. It can be assumed that a component of this body in the North direction is the one that influences the dynamic behaviour of the dam. In that case, the added mass would have to be multiplied by a factor of cosine 25° ≈ 0.9. If Figure 5.12 is used and the position of the θ=25° graph is estimated using linear interpolation of the areas enclosed by the other graphs with the axes, it is found that a graph of θ=25° would enclose about 0.7 of the area enclosed by the Westergaard pressures graph. An average of 0.7 and 0.9 which is 0.8 is taken as the final factor that will be applied to the calculated generalized Westergaard added mass.

The eastwards lying water body is also at an angle to the North. This body of water however is very small compared to the westward lying water. In order to be on the conservative side, it was decided than no factor will be applied on this body of water.

Even with these reductions in the added mass, it was found that the added mass is still overestimated as the analytical frequencies were still lower when compared to the experimental results. The effect of the dam flexibility and curvature of the upstream dam wall which were also ignored in the derivation of the original Westergaard method were then looked at.

5.5.2. Effect of the dam flexibility and curvature of the upstream dam wall

The inaccuracy of the results from the analysis in which the added masses were calculated using the original Westergaard method called for the use of the generalized Westergaard method. As discussed in the literature review, in section 2.2, the difference between the two methods is the presence of a matrix which accounts for both flexibility and curvature in the generalized method. This matrix *f* is a dyadic product of a unit normal vector at a point with itself, as follows:

$$f = \lambda_i^T \lambda_i = \begin{pmatrix} \lambda_1 \\ \lambda_2 \\ \lambda_3 \end{pmatrix} (\lambda_1 \quad \lambda_2 \quad \lambda_3) \tag{5.1}$$

Where

$\lambda_i = (\lambda_1 \quad \lambda_2 \quad \lambda_3)$ is a row vector of direction cosines of the unit normal vector at a point of interest.

The matrix *f* is hence a symmetric (3×3) matrix.

All the intrados and extrados centres of the arches of Roode Elsberg dam lie along one reference plane. This means that at any height of the dam an arch of a circle is enough to describe a locus of points (at that height) on the upstream face. This helps as a parametric equation can be formulated which describes a locus of points at a certain height on the upstream face of the dam.

Suppose that, the centre of such a circle lies in the y-z plane, is at a height *h* and its y-coordinate is equal to *b*. The radius of the circle is assumed to be *r*. It is important to mention

that the circle has to completely lie in a horizontal plane of Equation z = *h*. Then its parametric Equation will be given as follows;

$$\boldsymbol{p}(\theta) = r\cos\theta\,\mathbf{i} + (b + r\sin\theta)\mathbf{j} + h\,\mathbf{k} \tag{5.2}$$

A unit normal vector to such a circle is given by:

$$\lambda_i = (-\cos\theta\,, -\sin\theta,\ 0) \tag{5.3}$$

From this a matrix *f* can be found as formulated in Equation 5.1.

$$f = \lambda_i^T\lambda_i = \begin{pmatrix} -\cos\theta \\ -\sin\theta \\ 0 \end{pmatrix}(-\cos\theta\,, -\sin\theta,\ 0) = \begin{pmatrix} (\cos\theta)^2 & \cos\theta\sin\theta & 0 \\ \cos\theta\sin\theta & (\sin\theta)^2 & 0 \\ 0 & 0 & 0 \end{pmatrix} \tag{5.4}$$

Equation 2.18 is re-written below for easy reference. The component of the normal acceleration which relates to the ground motions can be assumed to be almost zero for ambient conditions.

$$F_i = -[M_{ai}]\ddot{\boldsymbol{u}} = -\alpha A_i \boldsymbol{\lambda_i^T}\boldsymbol{\lambda_i}\ddot{\boldsymbol{u}} \tag{5.5}$$

Equation 5.5 can be written in full vector components form as shown in Equation 5.6.

$$\begin{pmatrix} F_x \\ F_y \\ F_z \end{pmatrix} = -\alpha A_i \begin{pmatrix} (\cos\theta)^2 & \cos\theta\sin\theta & 0 \\ \cos\theta\sin\theta & (\sin\theta)^2 & 0 \\ 0 & 0 & 0 \end{pmatrix}\begin{pmatrix} \ddot{u}_x \\ \ddot{u}_y \\ \ddot{u}_z \end{pmatrix} \tag{5.6}$$

The observed mode shapes from the ambient vibration testing are mostly in the downstream-upstream direction. This suggests that the predominant movement in the dam is the upstream-downstream direction. This would then imply that the other two components of the acceleration namely $\ddot{u}_x$ and $\ddot{u}_z$ are insignificant and thus they can be ignored in Equation 5.6. Of the three force components, F_y then becomes the only significant force and it is estimated by Equation 5.7 below.

$$F_y \cong -\alpha A_i\,(\sin\theta)^2\ddot{u}_y \tag{5.7}$$

The angle θ is measured in a given horizontal plane and relative to a plane of Equation y = *b* where *b* is the y-coordinate of the centre of the extrado at the height of the horizontal plane. It is however convenient to measure the angle relative to the reference plane of the dam which in this case corresponds to the y-z plane. This can be achieved by making the substitution θ = γ +90°, from which Equation 5.8 results.

$$F_y \cong -\alpha A_i (\cos\gamma)^2 \ddot{u}_y \quad (5.8)$$

γ is assumed to be negative for the left abutment and positive for the right abutment. Equation 5.8 suggests that the hydrodynamic force of the water at the point on the dam during normal ambient conditions of the dam depends on the position of the point of interest relative to the reference plane. Therefore two points at the same height, one along the crown cantilever and one at an angle to the reference plane will have different added masses associated with them.

The same hydrodynamic force, at a node, when expressed in terms of the original Westergaard method is as follows.

$$F_{y1} = -\alpha A_i \ddot{\boldsymbol{u}}_{\boldsymbol{g}} \quad (5.9)$$

$\ddot{\boldsymbol{u}}_{\boldsymbol{g}}$ is the horizontal ground acceleration in the upstream-downstream direction. In this case even for ambient conditions the horizontal ground acceleration cannot be assumed to be almost zero since the dam is assumed to be rigid. The main differences between Equation 5.8, which relates to ambient behaviour and Equation 5.9, which relates to seismic behaviour are as follows; the presence of the cosine of the angle term in Equation 5.8 and the fact that the acceleration part of Equation 5.8 is likely to be less as it is the acceleration at a point on the dam relative to the base of the dam.

It turns out that the different magnitudes of the acceleration does not really matter as in ambient vibration, the magnitude of the generated hydrodynamic pressures does not depend on the magnitude of the total normal acceleration. In earthquakes, this is however the case. The presence of the factor of the cosine of the angle term in Equation 5.8 has an effect of lowering the added mass associated with a given node for the generalized Westergaard method as compared to the masses to the same node for the original Westergaard method.

Since the hydrodynamic force at any point varies with the angle from the reference plane, this in turn means that the added mass will also depend on the angle from the reference plane. The combined variation of the added mass with the height and with the angle from the reference plane infers that the actual application of this to a curved dam can be complicated especially when is not applied as point masses but rather as increase in density of an underlying structure. It was decided that the original Westergaard masses would be reduced using trial-

and-error until a good correlation is found between the analytical and the experimental results. The results of the trial and error are presented in Table 5.3 and Figure 5.13.

Table 5-3: FEM results of the natural frequencies compared with the field results of December 2008.

Mode number	Field results December 08	Natural frequencies obtained by applying the given % of the original Westergaard masses;					
		100%	90%	80%	60%	40%	20%
1	3.07	2.32	2.39	2.46	2.62	2.80	3.06
2	3.59	2.59	2.66	2.74	2.93	3.13	3.44
3	4.11	3.71	3.80	3.91	4.14	4.41	4.77
4	4.49	4.37	4.48	4.60	4.88	5.20	5.60
5	5.64	5.39	5.54	5.70	6.08	6.19	7.14
6	6.41	5.70	5.84	5.99	6.32	6.72	7.20
7	7.22	6.25	6.40	6.57	6.94	7.16	7.86
8	7.51	7.06	7.24	7.43	7.86	8.29	8.98

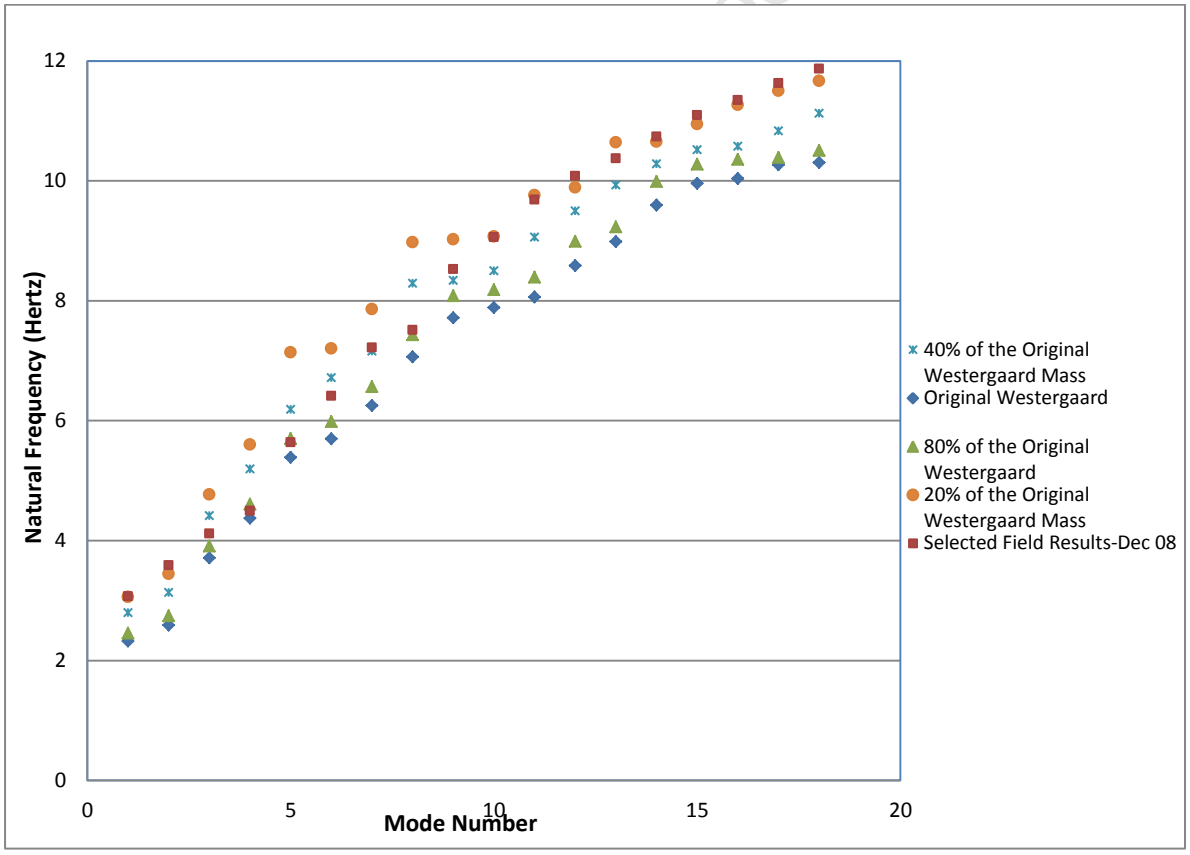

Figure 5.13: Comparisons of the natural frequencies when the different percentages of the Original Westergaard masses are applied.

When the original Westergaard masses for a full dam model are factored by a 0.2, the analytical masses match very well with the results from the field experiments which were

taken in December 2008 when the dam was full. As it was suggested in Section 5.4.1, a factor of 0.8 was applied first to the masses which were calculated using the original Westergaard method to account for diverging reservoir walls of the dam. The 0.2 applied on the same original Westergaard masses is equivalent to 0.25 applied on the resulting masses after the effect of diverging reservoir walls was accounted for.

The higher measured mode shapes were then revisited and it was observed that they did not exactly match with the analytical ones. This was because at times when the ambient vibration testing is done, it is possible that some modes may not be identified. The data in Table 5.4 is for the modified mode numbers in the field results. Table 5.4 and Figure 5.14 show that, there is a better correlation of the field results when a factor of 0.25 is applied on the original Westergaard method masses. This is equivalent to a factor of 0.31 applied on the resulting masses after the effect of diverging reservoir walls was accounted for.

On the study carried by Lemos et al. (2008) on Cabril dam, the Westergaard added masses were reduced to 70% of their theoretical value in order to eventually match the experimental results to measured ones to a reasonable degree. This factor of 0.7 compares well with the 0.75 which was applied in this study or the 0.69 which was applied on the resulting masses after the effect of diverging reservoir walls was accounted for. In the Lemos et al. (2008) study it was not specified what the applied factor accounted for. A small summary of the achieved calibration is presented in Table 5.4 together with the material properties used for the calibration in Table 5.5.

Table 5-4: FEM's natural frequencies for a full dam compared with the field results of December 2008 after the missing modes were identified from the field results.

Mode number	Field results December 2008 (Hertz)	Natural frequencies obtained by applying the given % of the original Westergaard masses (Hertz)				Percentage error between the field results and the best correlated FEM results (%)
		100%	80%	40%	25%	
1	3.07	2.32	2.46	2.80	3.07	0.0
2	3.59	2.59	2.74	3.13	3.46	3.6
3	4.49	3.71	3.91	4.41	4.78	-6.5
4	5.64	4.37	4.60	5.20	5.62	0.4
5	7.22	5.39	5.70	6.19	7.21	0.1
6	7.51	5.70	5.99	6.72	7.86	-4.7
7	8.53	6.25	6.57	7.16	8.99	-5.4
8	Not Identified	7.06	7.43	8.29	9.02	
9	9.06	7.71	8.08	8.34	9.07	-0.1
10	Not Identified	7.89	8.18	8.50	9.76	
11	9.68	8.06	8.39	9.06	9.89	-2.2

Table 5-5: A summary of the final dynamic material properties used in the calibration.

	Dynamic Material Properties		
	Elastic/ deformation Modulus (GPa)	Poisson's ratio	Density (kg/m^3)
Dam Concrete	40	0.22	2400
Foundation (Left Abutment*)	25	0.25	2500
Foundation (Right Abutment*)	20	0.25	2500
Foundation Size	The foundation used to achieve the results extends 1.35*Dam height in all directions.		

*Left and right in dam engineering is determined from a point of view of a particle moving along with the river current from upstream to downstream.

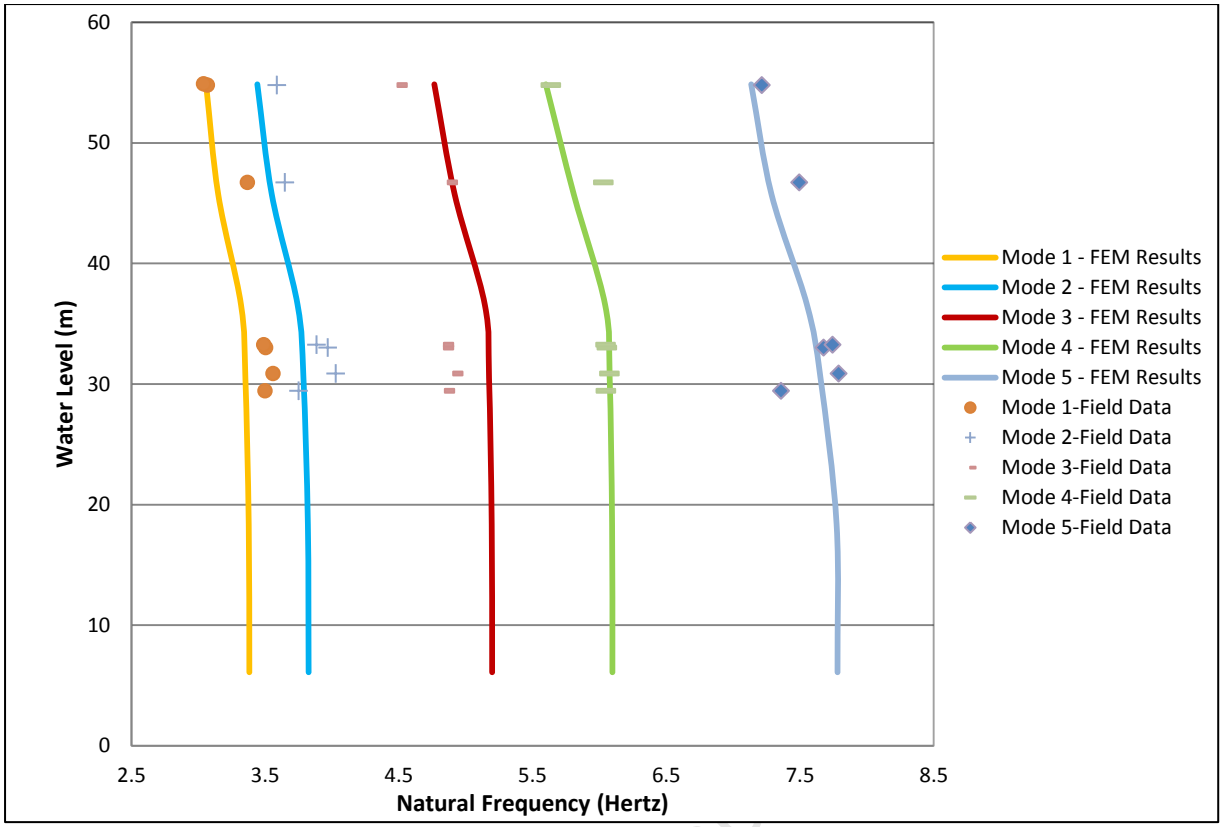

Figure 5.14: The final best calibration achieved between several field results and FEM results at different water levels where 25% of the original calculated Westergaard masses were used.

Figure 5.14 shows that for higher water levels there is a good correlation between the field results and the FEM results. There are discrepancies observed for lower water level frequencies and some higher modes at higher water levels as well. This can be attributed to the effects of temperature which were not considered in the analysis. Temperature can clearly have an effect on the natural frequencies of a system since it affects the stiffness of the system.

5.6 Static analysis

The dam was also calibrated for static displacements using the geodetic survey results which are taken regularly on the dam.

Two sets of geodetic survey data were chosen to be used in the calibration. It was important that these surveys were taken at almost around the same of the year. It was assumed that the average temperatures would have been almost the same in both times. However, the chosen surveys had to have happened when the water levels in the dam were significantly different. This is because the variation of the geodetic displacements with water level is what was

going to be assessed hence other parameters such as temperature had to be kept constant in the analysis.

Hence, the chosen sets of data were the data collected on the 24th August, 2008 and on the 24th August, 2009. The water levels in the dam were 559.86m and 573.09m respectively.

The geodetic surveys data showed the displacements with comparison to the base date displacements. The base date is the 01st August, 1984 and it is supposedly the first date on which the geodetic surveys were first done on the dam. Hence it was important for both the analytical model and survey results that not the actual geodetic surveys displacements are compared but the difference between two set of results/data. An extract from the geodetic surveys data is shown in Figure 5.15.

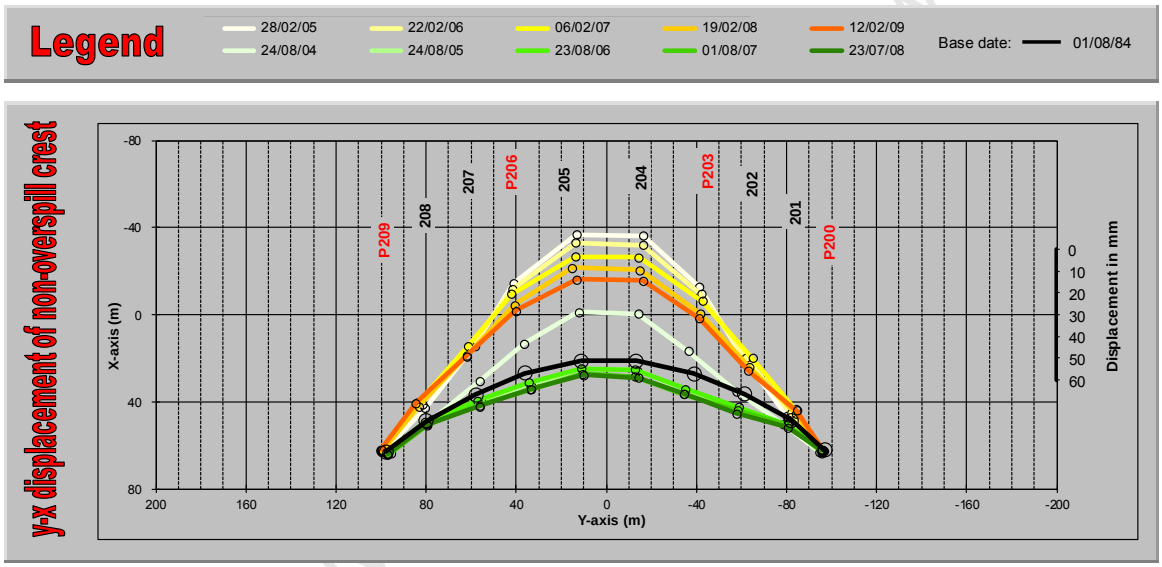

Figure 5.15: Sample of results from the geodetic survey (Source: DWA)

The upstream-downstream displacements or y-displacements at a reduced level of 557m were found in the dam model for a full capacity condition. Then another set of y-displacements at the same level of 557m were found for a dam water level of 560m. The difference of these two displacements were found and they are graphed in Figure 5.16 where they are compared with the geodetic difference of the similar y-displacements at the same reduced level of 557m observed on site for the same water levels in the dam.

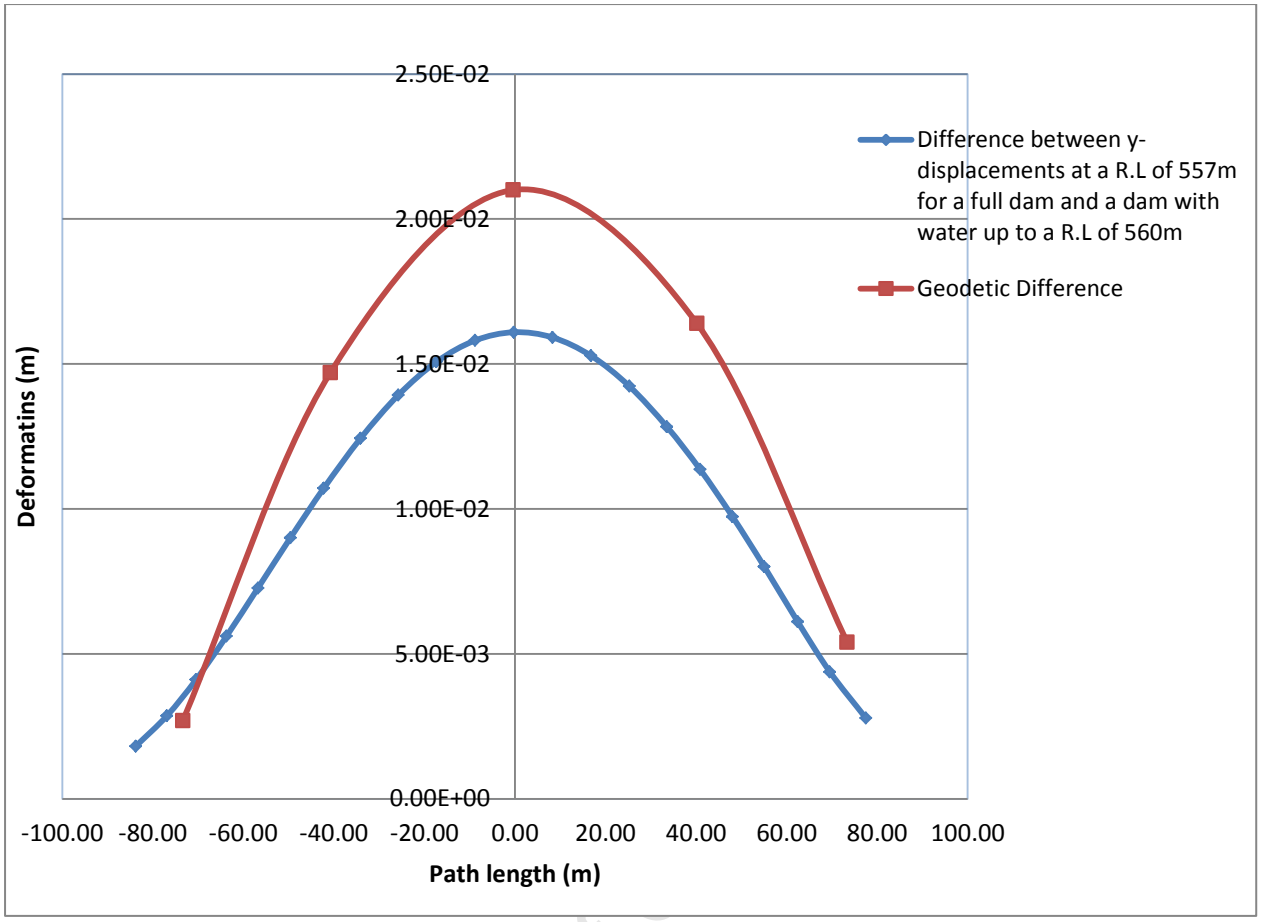

Figure 5.16: The upstream-downstream displacement differences compared for geodetic results and the finite element model results.

The material properties which were used were static properties which are different from the dynamic ones which were being used for the natural frequencies extraction process earlier in this study. Some of the used properties are summarized in Table 5.5.

Table 5-6: Material properties of the dam components used in the static analysis of Roode Elsberg dam.

	Elastic Modulus (GPa)	Density (kg/m^3)	Poisson's ratio
Dam wall and Cushion concrete	25	2400	0.2
Foundation-left abutment	20	2500	0.22
Foundation-right abutment	15	2500	0.22

The observed differences between the results in Figure 5.16 is likely to be due to the ignored effect of boundary conditions related to temperature. It was assumed that the average temperatures in August 2008 were similar as in August 2009 which is not a bad assumption given that the same month in each year was used. The fact that there were different water levels in the dam during these times implies different temperature boundary conditions for the upstream dam wall was ignored. When the dam is not full, the part of the upstream dam wall above the water level is exposed to air coditions while when the dam is full the same part will be in contact with the water and hence a different boundary condition. Despite this, only a maximum difference of about 5cm at the crown cantiliver is observed.

5.7 Chapter summary

The field and experimental results were presented and discussed in this chapter. First the experimental data was presented together with the data collection methods used. Although the data was limited as there was no data captured for lower levels of water in the dam, the collected data proved to be valid on the basis of trends observed on the data and how this compared with other experimental data from other studies. Hence, on the basis of this, it was assumed that, the data could then be used for model calibration purposes.

The original Westergaard added masses were then applied on the developed model. It was then observed than the calculated analytical natural frequencies were considerably less than the measured values while the corresponding mode shapes were similar in both the experimental data and the analytical model. It was at this point that all the assumptions that were made in the derivation of the method were revised with a view of assessing their applicability to the problem at hand. Assumptions related to a prismatic reservoir and an infinite reservoir proved not to hold for Roode Elsberg dam and it was shown that keeping these assumptions leads to an overestimation of the added mass.

Hence modifications had to made to the added mass to allow the analytical frequencies to match the field ones. A factor of 0.8 was decided on to account for the effect of the non-prismatic and diverging reservoir walls in Roode Elsberg dam. The geometry of the dam reservoir and literature guided the choice of this factor. To further account for the curvature and flexibility of the dam wall a factor of 0.69 was applied on the resulting masses on which the effect of diverging reservior walls had just been accounted for. This compares well with a

factor applied on a different dam on a previous study even though it is unclear in the study as to for what effects was the factor applied factor for.

CHAPTER 6

CONCLUSIONS AND RECOMMENDATIONS

6.1 Summary

The work of this thesis involves the development and calibration of a finite element model of an existing arch dam. It is important that such a model allows and enables a user to execute with great ease several analyses which assess the day-to-day behaviour of the dam e.g. thermal analysis, natural frequencies extractions, static stress analysis etc.

In order to achieve this, a thorough understanding of dam behaviour monitoring systems and modelling was needed. Thus, a careful study of the literature on dams and modelling was carried out. Roode Elsberg dam was chosen as a case study for this project. It became apparent that there are already static displacements and temperature monitoring systems on this dam. Therefore, it was decided that a monitoring system which is based on the ambient dynamic behaviour will be installed on-site to complement the existing system.

The concept of using ambient dynamic behaviour to monitor the dam's health has been done before. First dynamic properties, namely, mode shapes, natural frequencies and sometimes damping ratios are extracted from the field experiments. This data is then used as a benchmark for the calibration of the model. Once the model is calibrated, it can then be used in conjunction with long term ambient dynamic monitoring systems installed on-site to predict the behaviour under various loading conditions so that precautions can be taken to avoid disasters, which helps in realistic risk management.

One of the major problems encountered in the building and calibration of dam models for dynamic monitoring purposes, is the modelling of the dam wall-impounded water interaction. This is very important especially for dynamic behaviour where interactions between the different components are crucial to the general behaviour. One of the most attractive methods to be proposed for the representation in computer models of the dam wall-impounded water interaction during earthquakes was the added mass Westergaard method.

The attractiveness of the method is, among others, its ease of applicability as compared to other methods such as a full finite element representation where the dam wall, foundation and water body are modelled by finite elements. This is very relevant in this case as the Westergaard method will be used as part of the model which forms part of a structural health

monitoring and condition assessment of the dam. Ease of application of an assessment tool is very important in dam monitoring as the ambient conditions keep changing all the time, for example, water level, hence the adopted modelling tool has to be versatile as well.

It is very normal in engineering problems that an easier solution to a problem comes with loss of accuracy. This dam wall-water interaction problem is no exception to this. This is mainly observed in the seismic safety analysis of arch dams where the Westergaard method has been shown not to be very accurate since among others it ignores the compressibility of the water body in the dam.

However, the focus of this work, among others, was to assess the applicability of the Westergaard method in the representation of the dam wall-water interaction for monitoring purposes of dams under ambient conditions. Any observed trends; any remarks worth noting following the work of this thesis are outlined in the next sections. These are then followed by recommendation for any further work which can be done in this field.

6.2 Concluding remarks

A finite element model of Roode Elsberg dam was developed in a commercial programme called ABAQUS. It was desirable that such a model can be used for any analysis that assesses the ambient behaviour and operating conditions. This was achieved as the model can be used for each or a combination of any of the following analyses; natural frequencies extraction, temperature and thermal stress distribution, static and dynamic stress analysis, buckling behaviour etc.

The model can still be used for extreme case scenarios such as earthquakes but obviously for such an event some modifications may need to be made on the model. For example, it will certainly be important in this case to represent the dam wall- water interaction using some technique besides the Westergaard method given the method's proven inaccuracies for seismic analysis.

The developed model also attempted to recognise that the foundation properties are very important for the general behaviour of the dam. There is evidence of dissimilar deformation properties between the two abutments of the dam. This however could not be investigated any further due to lack of recent field data of the actual foundation properties.

With regards to the application of the Westergaard's added mass method, it has always been speculated that the method can provide an attractive technique to represent the dynamic interaction of the water body and the dam wall for the monitoring of ambient dynamic behaviour of arch dams. This study hence evaluated whether the method can satisfactorily be used to give comparable results in the monitoring of the ambient dynamic behaviour of arch dams. The assumptions made in the derivation of the Westergaard formulation, which was based on seismic analysis, were looked at with a view of assessing whether the same assumptions still hold for arch dams under ambient conditions.

The evaluations which were made were as follows:

i. Small deformations assumption was made in the derivation of the Westergaard method. In ambient vibrating dams the deformation of both the structure and the water are relatively small. On the basis of this, this assumption hence holds in this case.
ii. All the assumptions about the ground motions of the earthquake can be ignored as in ambient vibrations there are insignificant ground motions.
iii. The assumptions of a 2-dimensional rigid dam and a vertical upstream face which were made in the original Westergaard method are not very realistic for arch dams but these assumptions were essential to the Westergaard's derivation of the added mass concept. The concept threw some light on the problem and later led to derivations which accounted for the more realistic generalized Westergaard method for flexible and curved upstream face by Kuo (1982).
iv. In the derivation of the Westergaard method it was assumed that the reservoir length is infinite in the upstream. This assumption can be accepted to be valid for most arch dams unless it is a very small dam which is rarely a case. In Roode Elsberg dam, this assumption does not hold due to a presence of a kink just upstream of the dam wall. This kink was found to be less than a Westergaard length parameter *b* (as determined for a full dam reservoir) away from the dam wall. Since this parameter *b* is used to estimate the added mass, it was concluded that this added mass of the water is likely to be overestimated for a reservoir at full capacity.
v. The Westergaard method also assumes symmetric prismatic reservoirs while in reality most dams are asymmetric and have diverging reservoir walls. This proved to be the case in Roode Elsberg. The quantitative effect of the over-estimation of the Westergaard's added mass due to diverging reservoir walls has not been explored very much in

literature. Even though it was covered in Kuo (1982), there was no field data to compare with. The method's results were rather compared with the ones from the Galerkin finite element method which uses the incompressible water assumption.

From the review above, it is clear that the assumptions related to an infinite reservoir and a prismatic reservoir are the ones that engineers have to consider very carefully when using the Westergaard added mass formulations to estimate the effect of the dam-water interaction on the dynamic behaviour. They proved to be very important in Roode Elsberg dam arch dam-water interaction modelling using the Westergaard added mass formulation.

Roode Elsberg dam reservoir is highly asymmetrical and has diverging reservoir walls, an effect which, on the basis of literature, can result in the added masses being overestimated by about 25%. This was accounted for by reducing the added original Westergaard method masses. An angle of the diverging reservoir wall to the reference plane was used as a variable that determines how much the overestimation of the added mass due to the diverging reservoir wall is. To the knowledge of the author, the effect that the diverging reservoir walls have on the added masses is rarely specifically accounted for quantitatively in previous studies.

This study also recognises the use of the generalized Westergaard method for flexible dams curved in plan and in elevation. It was shown that the added masses calculated using the generalised Westergaard method are less than the ones for the original Westergaard for the dams of the same height. For Roode Elsberg dam, it was also shown that the added mass also depend on the angle from the reference plane of the dam.

All in all, after the effects of diverging dam reservoir walls, finite reservoir, upstream curvature and flexibility of the dam wall were considered, better correlation was achieved between analytical results and the experimental ones. These mentioned factors were ignored in the derivation of the original Westergaard method. The overall factor of 0.75 was applied on the masses calculated using the original Westergaard method to account for all the above-mentioned factors and hence to an extent, match the analytical results and the experimental ones. This factor compared with a factor of 0.7 which was applied on a different study on a Cabril arch dam where the purpose was still to reproduce the fundamental aspects of the ambient dynamic behaviour of the structure in the model.

Despite all of this, it is worth noting that the Westergaard added mass method was derived for use in the seismic safety analysis of gravity dams where large deformations are expected. However, the small deformations assumption was made which justified the ignoring of the water compressibility. On the other hand, in the ambient dynamic behaviour of dams, deformations are generally small hence water compressibility can be neglected. It is in such cases where it is proposed that the Westergaard method can effectively represent the dam-water interaction provided factors such as diverging reservoir walls effects are accounted for, if applicable.

This study also recognizes that the application of a generalized Westergaard method can be complex unless this is embedded in the program as is the case in many dam safety analysis programs.

6.3 Recommendations

Calibration of the dam model should include all the parameters which influence the day to day behaviour of the dam. Variation of the field results with finite element results even for similar water levels in the dam suggest there are some parameter(s) which influence the ambient dynamic behaviour besides the dam-water interaction which was studied in this work. Seasonal temperature variations is likely to be the main other factor which affects the ambient behaviour. Therefore better calibration results could have been achieved had the temperature effects been included in the analysis. This should be included in the future studies of this kind.

Efforts were made in this project to achieve a good approximation of the properties of the material on-site. Rough estimates done using guidelines without proper field testing can at times be assumed to good enough for the dam concrete but conversely proper field tests are needed to determine the material properties of the foundation rock. Hence, in this study only a rough study into the effects of the differential foundation properties could be done due to lack of field testing.

Incorporation of the nonlinear behaviour in the calibration will provide a better and more realistic behaviour of arch dams. This is important because the general stiffness of the dam wall changes with time due to the opening and closing of the contraction joints. While this behaviour was ignored in this study, it is speculated that it can however be important for

thermal studies, as the expansion and compression of the blocks is directly related to temperature effects. A combined study in which this nonlinear behaviour, seasonal temperature variations, water level changes are studied as a function of time can provide a better understanding into the behaviour of arch dams.

During the ambient vibration testing, it was assumed that the movement of the block at the dam crest reflects the overall motion of the block along the entire length of the block. Hence the measurements were only taken at the dam crest. It is recommended that some measurements be taken at a lower level to assess the movement of the dam at that level. Measurements at a lower level close to a foundation can even give an idea of the movements of the dam wall relative to the foundation. The interaction of the dam wall and the foundation can then be modelled better.

REFERENCES

Alexander, M. & Mindess, S., 2005. *Aggregates in Concrete*. Taylor & Francis.

Atalla, M.J., 1996. *Model updating using neural networks*. PhD Thesis. Virginia: Virginia Polytecnic Institute and State University.

Aznarez, J.J., Maeso, O. & Dominnguez, J., 2006. BE analysis of bottom sediments in dynamic fluid structure interaction problems. *Engineering analysis with Boundary elements*, pp.124-36.

Bathe, K.J., 1996. *Finite Element Procedures*. New Jersey: Prentice-Hall.

Bayraktar, A., Sevim, B. & Altunisik, C.A., 2011. Finite element model updating effects on nonlinear seismic response of arch dam-reservoir-foundation systems. *Finite elements in analysis and design*, pp.85-97.

Bieniawski, Z.T., 1989. *Engineering rock mass classification: a complete manual for engineers and geologists in mining, civil and petroleum engineeering*. John Wiley & Sons.

Bouaanani, N. & Miquel, B., 2010. A new formulation and error analysis for vibrating dam-reservoir systems with upstream transmitting boundary connditions. *Journal of sound and vibration*, pp.1924-53.

Brebbia, C.A. et al., 1975. *Vibrations of Engineering Structures*. Southampton: Computational Mechanics.

Burman, A., Maity, D. & Sreedeep, S., 2010. Iterative analysis of concrete dam-nonlinear foundation interaction. *International Journal of Engineering, Science and Technology*, pp.85-99.

Chopra, K.A., 1967. Hydrodynamic pressure on dams during earthquakes. *ASCE Journal of Mechanical Engineering Division*, pp.205-23.

Chopra, A.K., 2010. *Earthquake Analysis of Arch Dams*. Denver: U.S. Bureau of Reclamation.

Chuhan, Z., Jianwen, P. & Jinting, W., 2009. Influence of seismic input mechanisms and radiation damping on arch dam response. *Soil Dynamics and Earthquake Engineering*, pp.1282-93.

Clough, P.W. & Tocher, J.L., 1964. Analysis of thin arch dams by the finite element method. In *International Symposium*. Southampton, 1964. Pergamon Press.

Daniell, W.E. & Taylor, C.A., 1999. Effective ambient vibration testing for validating numerical models of concrete dams. *Earthquake engineering and structural dynamics*, pp.1327-44.

Darbre, G.R., 2000. *State of practice in earthquake analysis of dams*. Zurich.

Darbre, G.R., de Smet, C.A.M. & Kraemer, C., 2000. Natural frequencies measured from ambient vibration response of the arch dam of Mauvoisin. *Earthquake engineering and structural dynamics*, pp.577-86.

Darbre, G.R. & Proulx, J., 2002. Short communication: Continuous ambient-vibration of the arch dam of Mauvoisin. *Earthquake Engineering and Structural Dynamics*, pp.475-80.

Dassault Systems Simulia Corp., 2010. *Abaqus/CAE User's Manual*. Providence: Dassault Systems.

Davey, R.A., Walker, J. & Ho, K.V., 2006. *Seismic Assessment and Remediation of the Aviemore Dam Spillway and Sluice Gates*.

Dowling, M.J., 1987. Nonliear seismic analysis of arch dams. Pasadena, California, United States of America: California Institute of Technology.

Duron, Z.H., 1987. *Experimental and finite element studies on a large arch dam*. Carlifonia: Earthquake Engineering Research Laboratory.

Du, X., Zhang, Y. & Zhang, B., 2007. Nonlinier seismic response analysis of arch dam-foundation systems-part 1dam-foundation rock interaction. *Bull Earthquake Engineering*, (5), pp.105-19.

DWA, 1971. *Design Drawings; Roode Elsberg Dam*. Pretoria, South Africa: Department of Water Affairs.

Federal Energy Regulatory Committee, 1999. *Engineering guidelines for the evaluation of hydropower projects: Arch Dams*. Washington DC: Division of Dam Safety and Regulations.

Fenves, G. & Chopra, A.K., 1985. Effects of reservoir bottom absorption and dam-water-foundation rock interaction on frequency response functions for concrete gravity dams. *Earthquake engineering and structural dynamics*, pp.13-31.

Fok, K.L. & Chopra, A.K., 1986. Earthquake analysis of arch dams including dam-water interaction,reservoir boundary absorption and foundation flexibility. *Earthquake Engineering and Structural Dynamics*, pp.155-84.

Fok, K.A.M. & Chopra, A.K., 1987. Water compressibility in earthquake response of arch dams. *Journal of Structural Engineering*, pp.958-75.

Ghanaat, Y., 1993. *Theoretical Manual for Analysis of Arch Dams*. Washington DC: U.S. Army Corps of Engineers.

Gogoi, I. & Maity, D., 2010. A novel procedure for determination of hydrodynamic pressure along upstream face of dams due to earthquakes. *Computers and Structures*.

Hall, J.F., 1996. *Efficient nonlinear seismic analysis of arch dams*. Carlifonia: Carlifonia Institute of Technology.

Huang, C.S., 2001. Structural identification from ambient vibration measurement using the multivariable ar model. *Journal of sound and vibration*, pp.337-59.

ICOLD, 2001. *Computational Procedures for Dam Engineering: Reliability and aoolicability*. Paris: ICOLD.

Kennedy, R.C. & Hanna, F.W., 1931. *The Design of dams*. New York: McGraw- Hill.

Kucukarslan, S., Coskun, S.B. & Taskin, 2005. Transient analysis of dam–reservoir interaction including the reservoir bottom effects. *Journal of Fluids and Structures*, pp.1073-84.

Kuo, H., 1982. *Fluid-Structure Interactions: Added Mass Computations for Incompressible Fluids*. Berkerly: University of Carlifonia.

Lemos, J.V., Oliveira, S. & Mendes, P., 2008. Analysis of the dynamic behaviour of Cabril dam considering the influence of contraction joints. In *7th Annual Conference on Structural Dynamics*. Southampton, 2008. Eurodyn 2008.

Leung, A.Y.T., Fok, A.S.L., Dai, H. & Su, R.K.L., 2008. The fractal finite element method for added mass type problems. *Internation Journal for Numerical Methods in Engineering*, pp.1194-213.

Loh, C.-H. & Wu, 1996. Identification of Fei-Tsui arch dam from both ambient and seismic response data. *Soil Dynamics and Earthquake Engineering*, pp.465-83.

Maeso, O. & Diminguez, J., 1993. Earthquake analysis of arch dams 1: Dam-foundation interaction. *Journal of Engineering Mechanics*, pp.496-512.

Maghous, S., Bernaud, D., Freard, J. & Garnier, D., 2008. Elastoplastic behaviour of jointed rock masses as homogenized media and finite element analysis. *International Journal of Rock Mechanics & Mining Sciences*.

Mendes, P., 2006. Development of a monitoring system to Cabril dam with operational modal analysis.

Mendes, P. et al., 2004. Dynamic behaviour of concrete dams: Monitoring and modeling. In *13th World Conference on Earthquake Engineering*. Vancouver, 2004. WCEE.

Modak, S.V., Kundra, T.K. & Nakra, B.C., 2002. Comparative study of modal updating methods using simulated experimental data. *Computers and Structures*, 80, pp.437-47.

Mottershead, J.E. & Friswell, M.I., 1993. Model updating in structural dynamics: A survey. *Journal of sound and vibration*, 167(2), pp.347-75.

Moyo, P. & Oosthuizen, C., 2010. Ambient vibration survey trials of two arch dams in South Africa. In *8th ICOLD European Club Symposium*. Innsbruck, 2010. Grez University of Technology.

Moyo, P. & Oosthuizen, C., 2011. *Structural Health Monitoring of Arch Dams Using Dynamic and Static Measurements*. Water Research Commision.

Noble, C.R., 2002. Seismic Analysis of Morrow Point Dam. In *Non-Linear Structural Analysis of Concrete Dams and Concrete Appurtments to Dams*. Denver, 2002. U.S. Department of Energy.

O'Connor, J.P.F., 1985. Comparison of the observed and predicted behaviour of Roode Elsberg arch dam including the effect of tensile cracking in the concrete. In *Fiftenth Congress on large dams*. Paris, 1985. ICOLD.

Okuma, N., Etou, Y., Kanazawa, K. & Hirata, K., 2008. *Evaluation of Dynamic Properties of an Aged Large Dam*. Chiba: Central Research Institute of Electric Power Industry.

Pani, P.K. & Battacharyya, S.K., 2008. Hydrodynamic pressure on a vertical gate considering fluid-structure interaction. *Finite Elements in Analysis and Design*, pp.759-66.

Proulx, J., Paultre, P., Rheault, J. & Robert, Y., 2001. An experimental investigation of water level effects on the dynamic behaviour of a large arch dam. *Earthquake engineering and Structural Dynamics*, pp.1147-66.

Samii, A. & Lotfi, V., 2007. Comparison of coupled and decoupled modal approaches in seismic analysis of concrete gravity dams in time domain. *Finite Elements in Analysis and Design*, pp.1003-12.

Sani, A.A. & Lofti, V., 2007. Linear dynamic analysis of arch dams utilizing modified efficient fluid hyper-element. *Engineering Structures*, pp.2654-61.

Sani, A.A. & Lotfi, V., 2010. Dynamic analysis of concrete arch dams by ideal-coupled Modal Approach. *Engineering Structures*, pp.1377-83.

Seghir, A., Tahakourt, A. & Bonnet, G., 2009. Coupling FEM and symmetric BEM for dynamic interaction of dam-reservoir systems. *Engineering Analysis with Boundary Elements*, pp.1201-10.

Serafim, J.L. & Pereira, J.R., 1983. *Considerations on the geomechanical classification of Bieniawski*. 2nd ed. Lisbon: International Symposium on Engineering Geology and Underground Construction.

Severn, R.T., Brownjohn, J.M., Dumanoglu, A.A. & Taylor, C.A., 1988. *A review of dynamic testing methods for civil engineering structures (keynote lecture)*. University of Bristol.

Sevim, B., Bayraktar, A. & Altunisik, A.C., 2009. Finite elememnt model caliration of berke arch dam using operational modal testing. *Journal of Vibration and Control*.

Seyedpoor, S.M., Salajegheh, E. & Salajegheh, E., 2010. Shape optimal design of arch dams including dam-water–foundation rock interaction using a grading strategy and approximation concepts. *Applied Mathematical Modelling*, pp.1149-63.

Tan, H. & Chopra, A.K., 1995. Earthquake analysis of arch dams including dam-water-foundation rock interaction. *Earthquake Engineering and Structural Dynamics*, pp.1453-74.

Tan, H. & Chopra, A.K., 1996. Dam-foundation rock interaction effects in earthquake response of arch dams. *Journal of Structural Engineering*.

Tiliouine, B. & Seghir, A., 1998. Fluid-structure models for dynamic studies of dam-water systems. In *Elenth European Conference on Earthquake Engineering*. Paris, 1998.

Toyoda, Y., Shiojiri, H., Ueda, M. & Tsunekawa, K., 2004. Dynamic analysis of an existing arch dam including joint non-linearity and dam-water-foundation rock interaction. In *13th World Conference on Earthquake Engineering*. Vancouver, 2004.

U. S. Corps of Engineers, 1994. *Engineering and Design: Arch dam Design*. Washington DC: Department of the Army.

U.S. Army Corps of Engineers, 1994. *Engineering and Design: Arch dam design*. Washington DC: Department of the Army.

United States Bureau of Reclamation, 1977. *Design of Arch Dams*. Colorado: Water Resource Technical.

USACE, 2003. *Analytical Modeling of Hydraulic Structures*. Washngton D.C.: Engineering and Design.

USACE, 2003. *Time-History Dynamic Analysis of Concrete Hydraulic Structures*. Washington DC: Engineering and Design.

USACE, 2007. *Earthquake design and evaluatin of hydraulic structures*. Washington, DC: Engineering and Design.

Westergaard, H.M., 1933. Water pressure on dams during earthquake. *Transactions,ASCE*, pp.418-33.

Zangar, 1952. *Hydrodynamic pressure on dams due to horizontal earthquake effects*. Colarado: U.S. Bureau of Reclamation.

Zienkiewicz, O.C., Clough, R.W. & Seed, H.B., 1984. *Earthquake Analysis procedures for concrete and earth dams: State of the art*. ICOLD.

Zienkiewicz, C. & Taylor, R.L., 2000. *The finite element method*. London: McCGraw-Hill.

APPENDIX 1: KEY MODELLING ASPECTS IN ABAQUS CAE

Assembling part instances

A part instance in the assembly module can either be created as a dependent or an independent instance. One major difference between these two is that a dependent instance shares the geometry and the mesh of the original part while an independent instance is only a copy of the geometry of the original part. This implies that one needs to mesh the original part of a dependent instance while for an independent instance an original part cannot be meshed but rather the instance itself needs to be meshed (Dassault Systems Simulia Corp., 2010) . For this work, it was a plan to use orphan meshes whose instances can only be dependent, therefore it was decided that all the three parts were to be instanced as dependent in the assembly module.

Meshing

The main commands which were used in this module include seeding, mesh controls, element type selection and the actual meshing command itself. For simple geometries, Abaqus CAE can do the meshing automatically using Top-down meshing technique while for those complicated geometries; the mesh needs to be created with great involvement from the user using predominantly Bottom-up meshing technique. With the help of partitions, top-down meshing can still be executed on some complex geometry. Top-down meshing relies on the geometry of a part to define the outer bonds of the mesh while in bottom-up the part geometry is only used as a guideline for the boundary of the mesh and the mesh does not necessarily conform to the geometry (Dassault Systems Simulia Corp., 2010).

Seeding

Seeding defines the size of the elements the user would want to use in the meshing of the part. It can either be specified as global seeds or local seeds. Abaqus CAE has its own default global seeding value which it uses in case the user does not specify this. This global seeding

depends on the value specified for the approximate part size by the user. This can however still be changed for the convenience of the user in the meshing process.

At times the user might wish that some parts of the model have a different mesh density as compared to others. This is where the local seeds need to be defined and they tend to override the global seeds in the region on which they are specified (Dassault Systems Simulia Corp., 2010). Local seeds were used in the meshing of the three parts used in the model of Roode Elsberg dam.

Meshing Controls

This is a command in the mesh module which allows the user to choose between the different meshing techniques and methods available in Abaqus CAE. Top-down meshes can be generated using the free, structured and swept meshing techniques while bottom-up meshes use the sweep, extrude and revolve methods to create meshes (Dassault Systems Simulia Corp., 2010). The geometry of a part to be meshed determines which of these methods can be used to mesh the part in question as certain methods are only able to mesh the shapes of certain geometries only.

Abaqus CAE uses colour codes on part instances to suggest to the user which method is most suited to mesh the part/instance in question. Partitions can be used to simplify the geometry of the parts and in the process make the parts meshable using methods which produce good meshes but with less involvement from the user. For example, the foundation part shown on the left in Figure 7.1 could only be meshed by bottom-up methods but with the introduction of a cell partition as shown, the part could be meshed using swept meshing top-down technique. Hence, the colour code change, from brown to yellow. The pulvino and the dam-wall arch were also meshed by the swept meshing technique

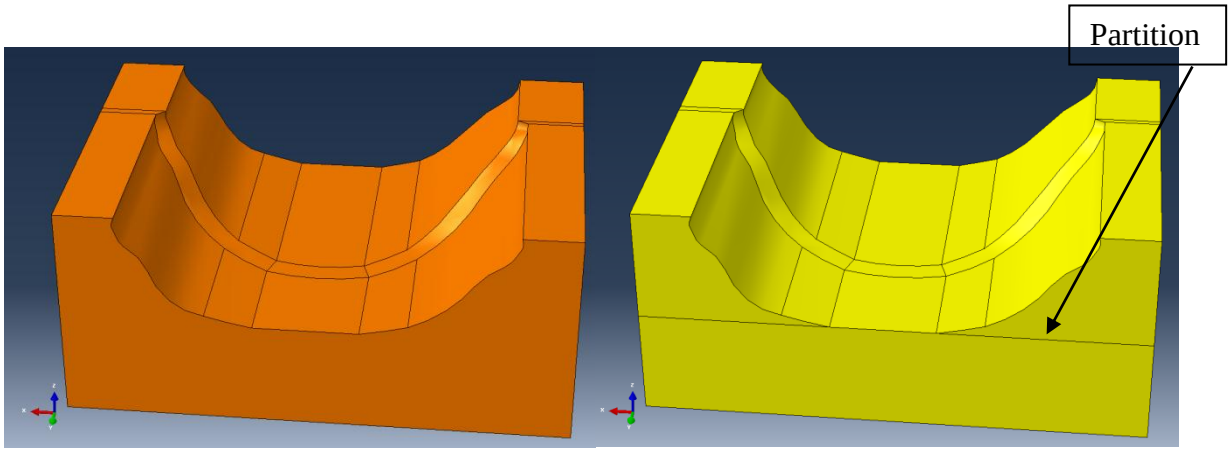

Figure 7.1: The use of partitions to change mesh control techniques in Abaqus CAE. Due to the introduction of a cell partition, the same part which could only be meshed by bottom-up techniques (left) can now be meshed using top-up techniques as well (right).

Element types

With regards to element type selection, firstly the choice of the elements' shape to be used is made in the mesh controls command. A choice of hexahedral elements was made for both the solid foundation and pulvino parts and the dam-wall arch was meshed with a hexahedral dominated mesh with some wedge elements.

Secondly, there was the choice of the order of the elements to be used in the modelling which was to be made. The degrees of freedom such as displacements, rotations and temperature are calculated on the nodes in finite element analysis procedures. At any other point in the element, the degrees of freedom are calculated by interpolating from the nodes. Usually, the interpolating order is determined by the number of nodes in an element (Dassault Systems Simulia Corp., 2010).

The most common hexahedral elements are the 8-noded and the 20-noded elements. The former have the nodes at the vertices only and hence use linear interpolation while the latter have mid-sides nodes as well which allows them to interpolate using quadratic functions. The most common wedge elements are the 6-noded and the 15-noded elements which correspond to the 8-noded and the 20-noded elements respectively in terms of order of interpolation.

Abaqus uses numerical techniques such as Gauss quadrature to integrate various quantities over the volume of each element. Either full or reduced integration can be carried out on an element. Full integration refers to the number of Gauss points required to integrate the polynomial terms in an element's stiffness matrix exactly when the element has a regular

shape. For hexahedral elements, a ‘regular shape’ means that the edges are straight and meet at right angles and that any edge nodes are at the midpoint of the edge. Fully integrated, linear elements use two integration points in each direction while the fully integrated, quadratic elements use three integration points in each direction (Dassault Systems Simulia Corp., 2010).

In bending problems, the fully integrated linear elements tend to shear lock which means that they become too stiff and hence do not predict bending behaviour accurately. Reduced integration elements use one fewer integration point in each direction than the fully integrated elements. Reduced integration elements can be used to solve the problem of shear locking although they can also exhibit the problem of hour-glass/zero energy modes. In coarse meshes this zero-energy mode can propagate through the mesh, producing meaningless results. The Abaqus user manual (2010) states that,

‘In Abaqus a small amount of artificial “hourglass stiffness” is introduced in first-order reduced-integration elements to limit the propagation of hourglass modes. This stiffness is more effective at limiting the hourglass modes when more elements are used in the model, which means that linear reduced-integration elements can give acceptable results as long as a reasonably fine mesh is used.’

In light of this information, the elements which were used in the modelling are the C3D20R elements as named according to the Abaqus naming system. They are the continuum, quadratic interpolation; 3-dimensional hexahedral elements of reduced integration nature as suggested by the R at the end. In total there were 4100 elements with 20263 nodes that were used in the modelling.

APPENDIX 2: CALCULATION OF THE WESTERGAARD MASSES

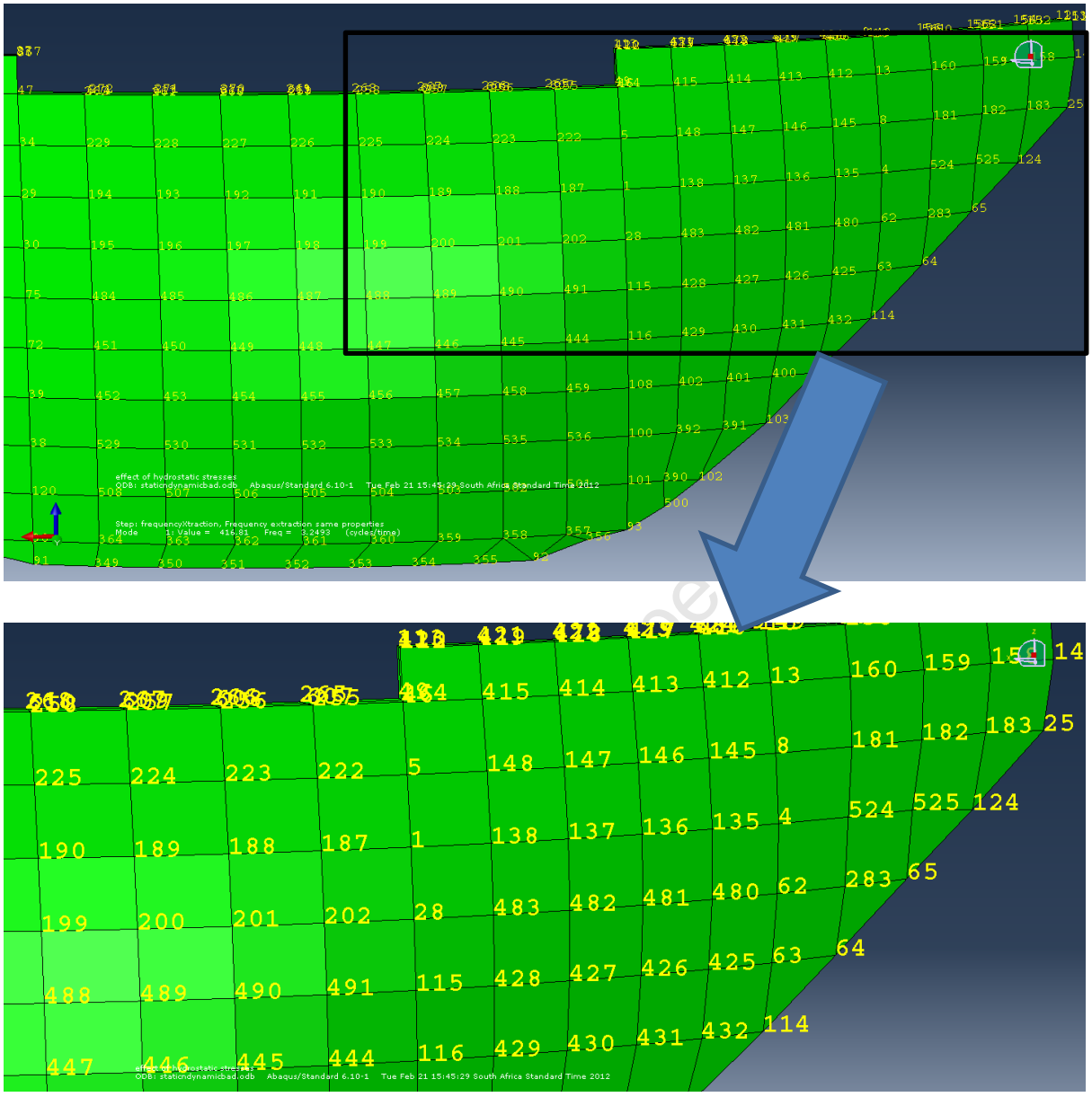

Figure 8.1: The location of nodes 25-229 which are used in Table 8.1 to show the calculation of the added original Westergaard masses.

Table 8-1: Sample calculation of the Westergaard masses for the given nodes.

Node ID	x-coordinate	y-coordinate	z-coordinate	Area	b*density	Masses (Kg)
25	-105.5	102.6	51.53	48.8	0.00	0.00
183	-99.1	109.8	51.81	48.8	3669.05	179049.5
182	-92.3	116.4	51.81	48.8	3811.14	185983.4
181	-85.0	122.6	51.81	48.8	3947.31	192628.6
8	-77.3	128.2	51.81	48.8	4078.02	199007.2
145	-70.7	132.5	51.81	48.8	4205.15	205211.1
146	-63.9	136.3	51.81	48.8	4327.59	211186.3
147	-56.9	139.8	51.81	48.8	4447.20	217023.5
148	-49.6	142.8	51.81	48.8	4562.69	222659.4
5	-42.2	145.5	51.81	48.8	16605.67	810356.4
222	-34.0	147.8	51.81	48.8	16605.93	810369.5
223	-25.6	149.7	51.81	48.8	16606.20	810382.5
224	-17.2	151.0	51.81	48.8	16606.33	810389.0
225	-8.6	151.9	51.81	48.8	16606.47	810395.6
226	-0.1	152.1	51.81	48.8	16606.47	810395.6
227	8.5	151.9	51.81	48.8	16606.47	810395.6
228	17.0	151.1	51.81	48.8	16606.33	810389.0
229	25.5	149.7	51.81	48.8	16606.20	810382.5

APPENDIX 3: MODE SHAPES COMPARISONS

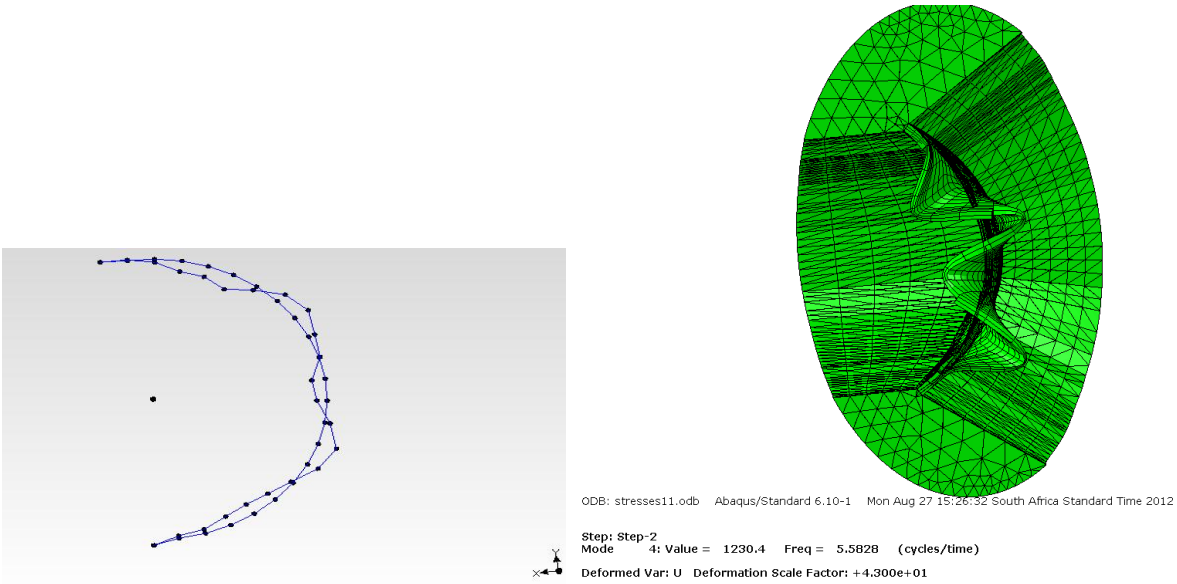

Figure 9.1: The experimental forth mode of Kouga dam compared with the forth mode of the analytical model of Roode Elsberg dam.

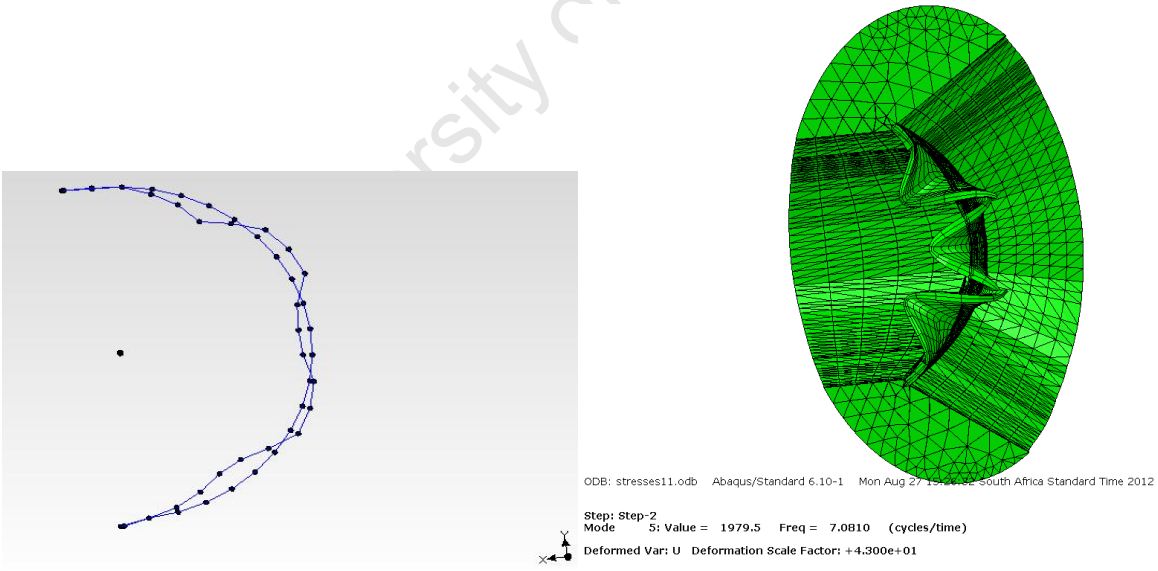

Figure 9.2: The experimental forth mode of Kouga dam compared with the forth mode of the analytical model of Roode Elsberg dam.